Hybridization of Basic Copper Salt Using (2-hydroxypropyl)Cellulose/Titania Nanosheet Composite

I. Bobowska, P. Wojciechowski

Department of Molecular Physics, Technical University of Lodz
Żeromskiego 116, 90-924 Łódź, Poland

The aim of our work is hybridization of a basic copper nitrate using (2-hydroxypropyl)cellulose(HPC)/titania nanosheet composite. Basic copper salt with the formula $Cu_2(OH)_3NO_3$ was obtained by the chemical bath deposition method which is known in the literature [1]. The deposition of basic copper salt proceeds in a water solution of copper nitrate and hexamethylenetetramine at 90°C. Figure 1a illustrates the surface morphology of a basic copper nitrate measured by a scanning electron microscope (SEM). Thin platelets, nearly perpendicular to the surface can be seen. The thickness of platelets is equal to about 0.5 μm, and the lateral dimensions are considerably bigger – about 5–10 μm.
The hybridization proceeds by impregnation of a $Cu_2(OH)_3NO_3$ platelets layer, by a water solution of HPC and titania nanosheets. The titania nanosheets were obtained by a chemical method [2]. The $Cu_2(OH)_3NO_3$/HPC/titania hybrid was calcinated at 550°C. Thermal treatment of these organic-inorganic hybrid leads to a decomposition of the basic salt to a copper oxide and to removal of the organic phase. An X-ray analysis indicates the presence of a CuO phase in the calcinated layer. Figure 1b illustrates the SEM image of the CuO morphology obtained after calcination of the hybrid. A platelet structure characteristic for basic salt is maintained. The platelets

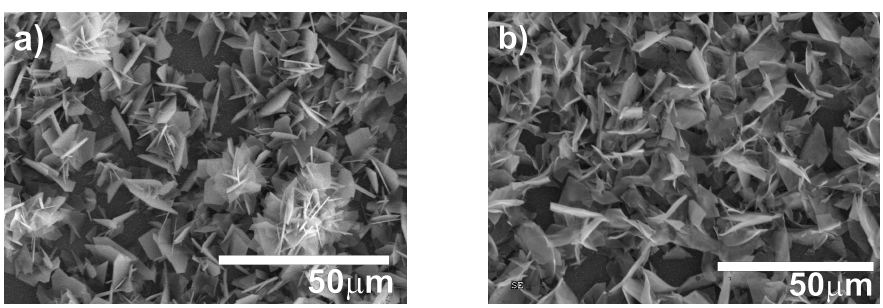

Figure 1: SEM images of: a) basic copper nitrate $Cu_2(OH)_3NO_3$ obtained by the chemical bath deposition method; b) CuO obtained by calcination at 550°C of hybrid composite $Cu_2(OH)_3NO_3$/HPC/titania nanosheets.

are slightly deformed, but the dimensions and perpendicular orientation to the surface are preserved.

Thermal calcination of basic copper nitrate platelets without HPC/titania nanosheets hybridization layer results in destruction of platelet morphology. A copper oxide layer with grain morphology is obtained.

Acknowledgements
This project was financially supported under project nr N N507 279636 and nr N N507 401935 from the Ministry of Science and Higher Education of Poland.

References
[1] Hosono E, Fujihara S, Kimura T, Imai H 2004 *J. Colloid Interface Sci.* **272** 391
[2] Wojciechowski P, Halamus T, Sadowska M, Bobowska I 2009 *Polym. Adv. Technol.* DOI: 10.1002/pat.1396

Energetics of the Reactions of Reduction of Metal Salts by Biradical Di-para-xylylens

M. Bobrowski[1,2]

[1] *Department of Solid State Physics, Gdansk University of Technology Narutowicza 11/12, 80-233 Gdansk, Poland*

[2] *TASK Computer Center, Gdansk University of Technology Narutowicza 11/12, 80-233 Gdansk, Poland*

Recently it was found that some metals and some metal salts can quenche the polymerisation of poly-para-xylylenes (also known as parylenes) [1] which in turn indicate that some kind of interaction between metals and metal salts occur during quenching of the polymerisation. Moreover, it was found that there is a strong dependence on the metal type in this type of interaction. On the other hand it is already well known that the polymerisation mechanism of parylenes is of radical type [2,3]. and the radicals are formed during the polymerisation process which takes place in vacuo without any catalyst. In this work, we propose a stechiometric reaction mechanism of radical poly-para-xylylens and metal salts and calculate eneregetical relations between appropriate substrates and products by means of *ab initio* open-shell Hartree-Fock and complete active space self-consistent field (CASSCF) methods. Dynamic electron correlation was estimated by the second-order Møller-Plesset (MP2) or multiple reference Møller-Plesset (MRMP), respectively. It turned out that in the case of metal salts where an appropriate reduction of metal characterises by sufficiently high positive value of normal redox potential, the energy of the reaction is lower then zero which in turn is in agreement with the experimental value of measuring of inhibition of polymer growth [1].

Acknowledgements
The investigations were supported by STREP No. 033201 (NMP3-CT-2006-033201) from the EC as well as by the Polish State Committee for Scientific Research. Calculations were carried out with the use of the resources and software at the Informatics Center of the Metropolitan Academic Network (IC MAN) at the Technical University of Gdansk and at the Department of Solid State Physics at the Technical University of Gdansk, Poland.

References

[1] K. M. Vaeth and K. F. Jensen *Chem. Mater.* 2000 **12** 1305-1313
[2] K. Smalara, A. Gie3don, M. Bobrowski, J. Rybicki, C. Czaplewski. paper sent for publication to *J. Phys. Chem.*
[3] L. A. Errede and M. Szwarc *Q. Rev. Chem. Soc.* 1958 **12** 301

Magnetic Properties of $LiNbO_3$: Er, Tm Single Crystal

T. Bodziony[a], S. M. Kaczmarek

Institute of Physics, West Pomeranian University of Technology
70-310 Szczecin, Al. Piastów 17, Poland

[a] *tbodziony@ps.pl*

The results of magnetic susceptibility (MS) measurements of a weakly doped lithium niobate (LN) $LiNbO_3$: Er (0.2 wt. %), Tm (0.3 wt. %) single crystal are presented. They are explained by the presence of interacting Er^{3+} and Tm^{3+} ions. The exchange interaction energies are established for both magnetic impurities. The dependence of the magnetic susceptibility versus temperature fulfils the Curie-Weiss law. The estimated Curie-Weiss temperature for an $LiNbO_3$: Er, Tm single crystal is equal to $\Theta = 0.37 \pm 0.13$ K. The results are compared to those obtained from the electron paramagnetic (EPR) measurements performed for $LiNbO_3$: Er, Tm and MS and EPR measurements of an $LiNbO_3$: Yb, Pr crystal. A model of substituting Er^{3+} and Tm^{3+} ions in a weakly doped $LiNbO_3$: Er, Tm single crystal is proposed. A crystallographic analysis of the surrounding of impurity ions in the $LiNbO_3$: Er (0.2 wt. %), Tm (0.3 wt. %) host suggests that Er^{3+} ions, Tm^{3+} ions and mixed Er^{3+}, Tm^{3+} ions clusters may appear.

Color-center Photoluminescent Nano-patterns Induced in Lithium Fluoride by Soft X-ray Laser Beam

F. Bonfigli[1], S. Almaviva[1], F. Flora[1], R. M. Montereali[1], A. Reale[2], A. Ritucci[2], P. Zuppella[2]

[1] *ENEA, Physical Technologies and New Materials Department, C.R. Frascati Via E. Fermi 45, 00044, Frascati, Rome, Italy*

[2] *Physics Department of University of L'Aquila, gc-LNGS INFN Via Vetoio, 67010 Coppito, L'Aquila, Italy*

We present the realization and characterization of photoluminescent sub-micrometric periodic patterns based on color centers (CCs) [1] in lithium fluoride (LiF) obtained by using an interferometric method based on a soft X-ray (SXR) laser beam. Among broad-band light-emitting materials, LiF, in form of crystals and thin films, is a radiation-sensitive material well known in dosimetry and as active medium in optically pumped photonic devices. Primary and aggregate electronic defects, known as CCs, can be produced in LiF by low-penetrating electromagnetic radiation, such as SXR from several sources [2–4]. Among them, F_2 and F_3^+ aggregate centers present a broad photoemission in the red and green spectral range, respectively. The high brightness and spatial coherence of a capillary discharge laser, with the emission wavelength of 46.9 nm, permitted to write stable periodic lines of F_2 and F_3^+ CCs at a nanometric scale emitting visible light under optical pumping in the blue spectral interval. The fringes encoding in LiF was obtained using a Loyd mirror interferometer where the pitch could be easily adjusted by varying the grazing angle. Laser scanning confocal fluorescence microscope permitted to characterize the LiF-based luminescent structures down to about 220 nm. Interferometric encoding of luminescent nanostructures in LiF represent a powerful tool for producing low dimensionality optical devices for photonic applications.

References

[1] Beall Fowler, W. (Ed.) (1968) *Physics of Color Centers*, Chap. 2. New York and London, p. 72

[2] R. Larciprete, L. Gregoratti, M. Danailov, R.M. Montereali, F. Bonfigli, M. Kiskinova., *Appl. Phys. Lett.* 80 (2002) 3862

[3] G. Baldacchini, F. Bonfigli, F. Flora, R.M. Montereali, D. Murra, E. Nichelatti, A. Faenov, T. Pikuz, *Appl. Phys. Lett.* 80 (2002) 4810-4812

[4] G. Tomassetti, A. Ritucci, A. Reale, L. Arizza, F. Flora, R.M. Montereali, A. Faenov, T. Pikuz, *Appl. Phys. Lett.* 85 (2004) 4163

Carbon Nanotubes Synthesis from Germanium Nano-particles

A. Capasso[1], E. R. Waclawik[2], J. M. Bell[1], S. Ruffel[3], M. Scarselli[4], A. Sgarlata[4], N. Motta[1]

[1] *School of Engineering Systems, Queensland University of Technology George St., Brisbane 4001, Australia*

[2] *School of Physical and Chemical Sciences, Queensland University of Technology 2 George St., Brisbane 4001, Australia*

[3] *Research School of Physical Sciences and Engineering, Australian National University Canberra 0200, Australia*

[4] *Dipartimento di Fisica, Unità CNISM, Università di Roma "Tor Vergata" 00133 Roma, Italy*

Controlled synthesis of carbon nanotubes (CNTs) is desirable for nanoelectronics application. Several CNTs-based devices have been already demonstrated, while many future applications for this promising material are attracting a growing interest. Up to date, fine metallic catalyst particles have been deemed unavoidable for the nucleation and growth of any kind of CNTs. Such metal particles can be deposited and assembled on various substrates with a high degree of control, leading to highly-ordered growths of CNTs, as carpets and geometric architectures [1].

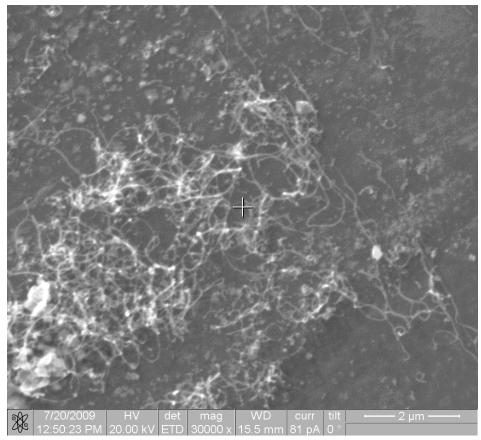

Figure 1: SEM image of a bundle of multi walled CNTs grown on a Si(001) non-patterned area

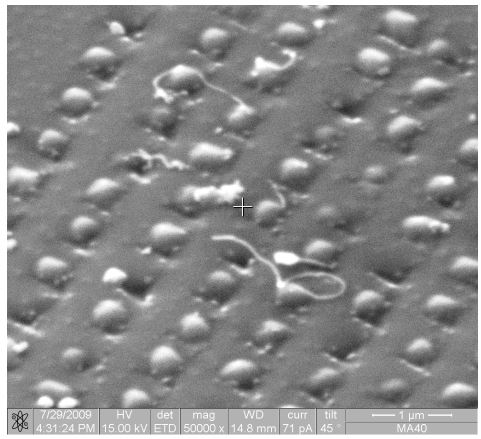

Figure 2: SEM image of a Si(001) patterned area after evaporation of Ge and CVD of acetylene. A few CNTs sprout from Ge nano-particles located at the edge of the indents

However, the presence of metal species mixed with the CNTs represents a shortcoming for most electronic applications, as metal particles are often incompatible with silicon semiconductor technology. Despite sustained efforts, it is still impossible to remove metal catalysts completely from CNT samples without introducing defects and contamination. Remarkably, recent studies claim that only a nano-scale curvature would be necessary to grow CNTs by hydrocarbon decomposition, thus opening the way for a wide range of materials to act as catalyst. In particular, it has been demonstrated that it is possible to obtain CNT formation on semiconductor substrates as SiC, Ge, and Si from semiconductors nano-particles of the same materials [2]. This method still suffers from low yields and poor quality of the samples and needs to be further improved, given the relevance of the implications.

In the present paper we report on a metal-catalyst-free synthesis of CNTs, obtained through Ge nano-particles on a Si(001). A few monolayers of Ge are deposited by Physical Vapour Deposition at 600°C on the silicon substrate. The surface has been previously patterned in specific sites by nanoindentation, in order to create a set of holes with defined size (300 nm) and pitch (1 um). Ge evaporation at high temperature results in the formation of islands and dots with random and ordered arrangements, respectively on pristine and patterned areas. CNTs growth is obtained by low-pressure Chemical Vapour Deposition (CVD) of acetylene, at a temperature of about 800°. A wide growth of entangled CNTs occurs on random deposited Ge dots, (Figure 1) while a narrower but more ordered growth arises from arrays of Ge nano-particles (Figure 2) in the patterned areas. The grown CNTs and the Ge three-dimensional structures are analysed by SEM, TEM, and AFM, in order to assess their features and properties.

References

[1] Avouris, P. et al 2007 *Nature Nanotechnology* **2** (10) 605-615
[2] Takagi, D. et al. 2007 *Nano Letters* **7** (8) 2272-2275

Avalanche Noise in Granular Disordered High-T_c Superconductors

L. Ponta[1], A. Carbone[1], M. Gilli[2], P. Mazzetti[1]

[1] *Physics Department, Politecnico di Torino*
Corso Duca degli Abruzzi 24, 10129 Torino, Italy

[2] *Electronic Department, Politecnico di Torino*
Corso Duca degli Abruzzi 24, 10129 Torino, Italy

The resistive transition of granular high-T_c superconductors, characterized by either weak (YBCO-like) or strong (MgB_2-like) links, occurs through a series of avalanche-type current-density rearrangements. These rearrangements correspond to the creation of resistive layers, crossing the whole specimen approximately orthogonal to the current-density direction, due to the simultaneous transition of a large number of weak links or grains. The solution of the Kirchhoff equations for strongly and weakly linked networks of nonlinear resistors, with the Josephson-junction characteristics, yields a subsequent formation of resistive layers within a superconductive matrix as the temperature increases. The voltage noise observed at the transition is related to the resistive layer formation process. The noise intensity is estimated from the superposition of voltage drop elementary events related to the subsequent resistive layers. At the end of the transition, the layers mix up, the step amplitude decreases, and the resistance curve smoothes. This results in the suppression of noise, as found experimentally. Remarkably, a scaling law for the noise intensity with the network size is argued. It allows us to extend the results to networks with an arbitrary size and, thus, to real specimens. The superconducting material is modeled as a network of nonlinear resistors having the Josephson junction current-voltage (I-V) characteristics with a Gaussian distribution of critical currents. The nonlinear resistors represent either weak links between grains (YBCO-like) or grains with strong links (MgB_2-like). In the strong-link case, a couple or triple of resistors is used to represent two or three current components flowing through each grain, respectively, for two-dimensional (2D) and three-dimensional (3D) networks.

The solutions of the Kirchhoff equations for these networks are found by an iterative routine.

The main results of this analysis are the following:

1. The resistive transition undergoes discrete step-like increments both in weak- and strong-link materials. The steps correspond to the creation of resistive layers constituted by grains or weak links in the normal or in the intermediate state. As the temperature increases, grains or weak links in the intermediate state gradually switch to the normal state. The trailing edge of the resistive transition grows more smoothly in MgB_2-like than in YBCO-like networks. This fact is

related to a higher correlation when the elementary transition events occur in triplets rather than in independent nonlinear resistors.

2. The abrupt formation of resistive layers causes large voltage noise observed at the transition in these materials. At the end of the transition, the resistive layers mix up. The resistance steps become smaller and the transition curve becomes smoother. This smoothing results in a noise suppression. A scaling law for the noise intensity is proposed in order to extend the results to larger networks, representing real materials. Here it is shown that the transition noise can be estimated once the grain size and the critical current distribution are defined.

References

[1] L. Ponta, A. Carbone, M. Gilli, and P. Mazzetti, Phys. Rev. B **79**, 134513 (2009)
[2] P. Mazzetti, C. Gandini, A. Masoero, M. Rajteri, and C. Portesi, Phys. Rev. B **77**, 064516 (2008)

Study of Dynamical Relaxation in MWCNs Films by Optical Pump-probe Technique

A. Ambrosio[1], M. Ambrosio[2], G. Cerulo[1], C. de Lisio[1], S. Lettieri[1], P. Maddalena[1], P. Castrucci[3], M. Scarselli[3], M. De Crescenzi[3]

[1] *CNR-INFM CRS-COHERENTIA and Dipartimento di Scienze Fisiche Università di Napoli Federico II, Complesso Universitario di Monte Sant'Angelo Via Cintia, I-80126 Napoli, Italy*

[2] *INFN Sezione di Napoli, Complesso Universitario di Monte Sant'Angelo Via Cintia, I-80126 Napoli, Italy*

[3] *Dipartimento di Fisica and Unità CNISM Università di Roma Tor Vergata, I-00133 Roma, Italy*

Single Walled Carbon Nanotubes (SWCNs) and Multi Walled Carbon Nanotubes (MWCNs) raised great interest because of their photoconductive properties that make them good candidates as active materials to realize photodetectors with a fast response in a large wavelength band.

Despite these interesting properties little or nothing is reported about the underlying mechanisms that lead to the photoresponse. We propose in this work an optical characterization of MWCNs films through a Pump & Probe technique [1,2].

The samples are MWCNs thin films ($\sim$ 10 micron), grown on two different substrates: the first is a sapphire substrate that allows analyzing both transmitted and reflected signals; the other is a silicon substrate that allows only an analysis in reflection.

The idea at the basis of the Pump & Probe technique is to excite the electrons of the sample through an intense pulse (Pump, time duration $\sim$ 100 fs) from a mode-locked Ti:sapphire laser operating at 800 nm wavelength, to obtain a modification of the optical properties of the sample. The second weaker pulse (Probe) has the role of analysing the modified optical properties of the sample.

The carbon nanotubes grown on the sapphire substrate showed a very symmetrical (quasi-Gaussian) and sharp signal ($\sim$ 800 fs) both in the reflection and transmission mode. The levels of symmetry and sharpness are, however, far from the features of an eventual cross correlation signal between Pump & Probe pulses (both Gaussian with a $\sim$ 300 fs width). The experimental results also show a linear dependence of the peak signal amplitude (both in reflection and transmission) on the Pump power at a fixed value of the Probe power.

On the basis of these preliminary results, a double exponential behaviour can be argued with a fast (hundreds of fs) and a slow (tens of ps) decay times related to carrier-carrier and carrier-lattice relaxation, respectively.

References

[1] Parlato L, Pepe GP, Latempa R, De Lisio C, Altucci C, D'Acunto P, Peluso G, Barone A,

Taneda T, Sobolewski R, "Time-resolved photoresponse of nanometer-thick Nb/NiCu bilayers", *Appl. Surf. Sc.*, 248, 177–180 (2005)

[2] S. Reich, M. Dworzak, A. Hoffmann, C. Thomsen, M. S. Strano, "Exited-state carrier lifetime in single-walled carbon nanotubes", *Phys. Rev. B* 71, 033402 (2005)

Influence of Dielectric Coverage on Epitaxial Thin Films and Photovoltaic Conversion in Solar Cells Obtained by Epitaxial Lateral Overgrowth

K. Cieślak[a], S. Gułkowski, J. M. Olchowik

Institute of Physics, Lublin University of Technology
Nadbystrzycka 38, 20-618 Lublin, Poland

[a] *k.cieslak@pollub.pl*

The main subject of this paper are thin film technologies are based on silicon epitaxial lateral overgrowth (ELO) made by liquid phase epitaxy (LPE). This way of obtaining silicon layers can be easily used in photovoltaic applications. The main advantage of this method is the possibility of applying a poor quality silicon growing substrate which decreases the costs of production, moreover, liquid phase epitaxy apparatus does not require complicated systems, which is also economical. All of these arguments lead to lowering the price of solar cells production.

We made a special design of silicon epitaxial layers placed between two dielectric films – an SiO_2 mask and an anti-reflection coating what causes a multi reflection of the light beam from the SiO_2–Si and SiN_x–Si surfaces and increases the optical way of light inside the active layer (see figure). This makes the probability of light absorption higher.

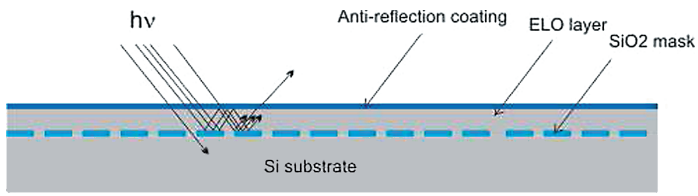

This work contains an analysis of the SiO_2 dielectric geometry influence on the ELO thin films and solar photo-conversion efficiency. The layers used in our experiment were obtained in an LPE process in the same thermodynamical conditions: the starting temperature of growth: 920°C, temperature difference $\Delta T = 60$°C, ambient gas: Ar, metallic solvent: Sn+Al and at different cooling rates: 0.5°C/min, 1°C/min, 0.75°C/min. We also used 4 dielectric masks with a different geometry: a grid opened in a SiO_2 along $\langle 110 \rangle$ and $\langle 112 \rangle$ directions on a p^+ boron doped (111) silicon substrate where the silicon dioxide covered 65%, 68%, 75%, 80% of the silicon surface.

The results of our analyzes show a correlation between the efficiency and the percentage of the SiO_2 coverage on the obtained solar cells.

Study on Structural and Optical Properties of Nanostructured Silicon Carbon Films

G. Ambrosone[1,2], D. K. Basa[3], U. Coscia[2,4]

[1] *INFM-CNR, CRS-Coherentia, Complesso Universitario MSA via Cintia, I-80126, Napoli, Italy*

[2] *Dipartimento di Scienze Fisiche, Complesso Universitario MSA via Cintia, I-80126, Napoli, Italy*

[3] *Department of Physics, Utkal University Bhubaneswar-751004, India*

[4] *CNISM Unità di Napoli, Complesso Universitario MSA via Cintia, I-80126, Napoli, Italy*

Ever since the discovery of photoluminescence in porous silicon, there has been a flood of activity on nanostructured silicon materials. Nanostructured silicon embedded in an amorphous matrix of different kinds has generated considerable interest because of the possible applications in future optoelectronic and microelectronic devices. Nanostructured silicon carbon films were prepared by varying the RF power in a PECVD system using a silane and methane gas mixture highly diluted in hydrogen. The evolution of the structural and optical properties of the films with the RF power was investigated using XRD, Raman, FTIR and photoluminescence spectroscopy. The study demonstrated not only that FTIR could be a sensitive probe to investigate the nanostructured materials but also established that the RF power variation in high hydrogen dilution conditions in a PECVD system could be an effective way to tailor-make the photoluminescence and other properties of these materials.

Structural and Optical Characterizations of 6,13 Pentacenequinone Thin Film on Different Substrates

P. De Marco[1], F. Fioriti[3], P. Parisse[1,4], D. Luciani[2], S. Santucci[1], P. Zuppella[2,5], P. Tucceri[2], A. Reale[2], L. Ottaviano[1]

[1] *CASTI CNR-INFM and Dipartimento di Fisica, Universita dell'Aquila Via Vetoio, 67010 Coppito (AQ), Italy*

[2] *Dipartimento di Fisica, Universita dell'Aquila, gc-LNGS INFN Via Vetoio, 67010 Coppito (AQ), Italy*

[3] *Dipartimento di Fisica, Universita dell'Aquila Via Vetoio, 67010 Coppito (AQ), Italy*

[4] *Sissa/Elettra NanoInnovation Lab Sincrotrone Trieste S.C.p.A 34149 Trieste, Italy*

[5] *CNR – INFM Luxor Laboratory, University of Padova 35131 Padova, Italy*

Recently pentacenequinone (PQ) has shown very appealing properties in view of the fabrication of photonic devices [1]: 6,13 pentacenequinone thin films, evaporated in ultra high vacuum on a pre-patterned PMMA/Si(100) substrate, show, under UV

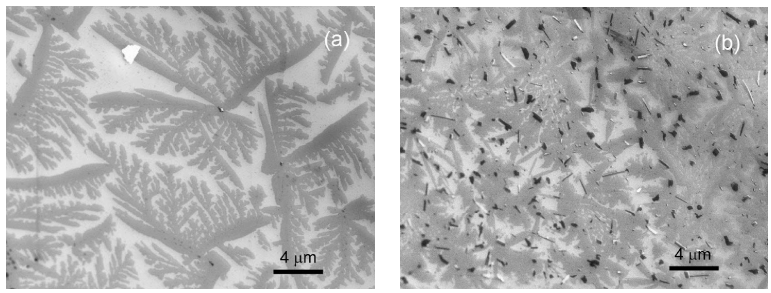

Figure 1: (a) SEM image (10000 × magnifications) of PQ evaporated on thermal silicon oxide. The dendritic growth of the molecules onto the substrate is clearly visible. (b) SEM image (10000 × magnifications) of nominal 5 nm PQ evaporated on thermal silicon oxide. The wetting layer is still visible, but this is evidence of the formation of crystallites with different shapes. Moreover, the PQ islands are mostly visible in the region covered by the dendritic structures.

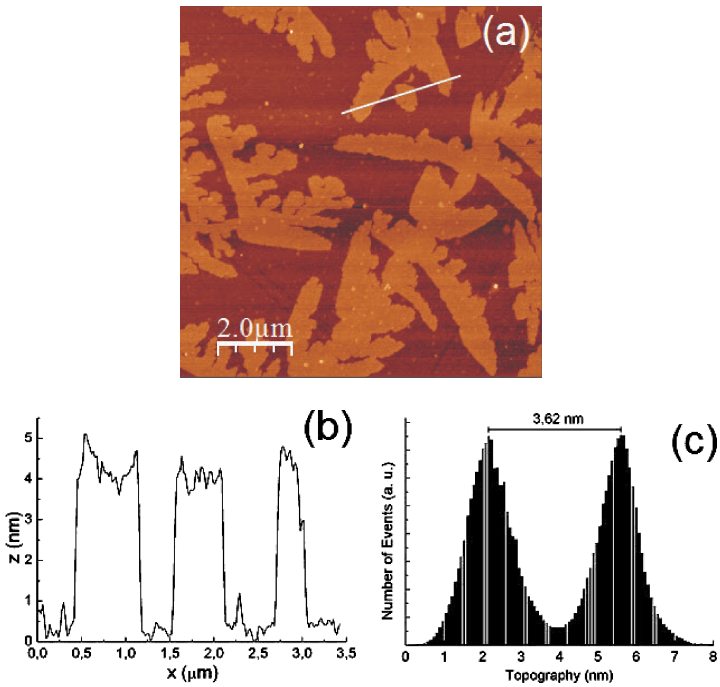

Figure 2: (a) AFM image of the sample shown in Figure 1. This result confirms that the first growth step is the formation of dendritic structures. (b) Line profile of the heights from the AFM picture. (c) Height distribution of the molecule. The molecular layer thickness is 3.62 nm.

illumination, a yellow photoluminescence (PL) response with strong spatial modulation (Figure 3). In particular, the intensity of the emitted light is enhanced in regions where the PQ is lying on the PMMA substrate. This behavior led us to study quantitatively the PL efficiency as a function of the substrate and film thickness. To this aim, the PQ was co-evaporated on PMMA/Si(100) (PMMA thickness is 20–30 nm), on SiO_2/Si(100) (100 nm oxide thickness) and on a Si(100) substrate. Samples of different thickness were prepared to check the volume impact on the PL response.

As in the SEM and AFM analyses (Figures 1 and 2), the PQ have crystalline and irregular morphology and their shape and dimension are comparable to those observed in [2,3]. The fraction of the surface area covered by PQ shows that the molecule grows on SiO_2 in the Volmer-Weber mode (strong interaction between the molecule and the substrate and weak interaction between molecules) while the PQ lying on Si grows in the Stransky-Krastanov mode (with the formation of a molecular "wetting" monolayer). The PQ wetting layer on the Si minimizes the Si–PQ interaction, enhancing the PQ-PQ interaction. The microscopic investigation shows also that, contrary to pentacene, the PQ growth is not dendritic, meaning that the "Capture Zone" aggregation model [4] is not valid. A "Generalized Wigner Gurmise" model [5] is working, instead. The distribution of the characteristic island size is bimodal, corresponding to two different crystalline phases of PQ (namely bulk and thin

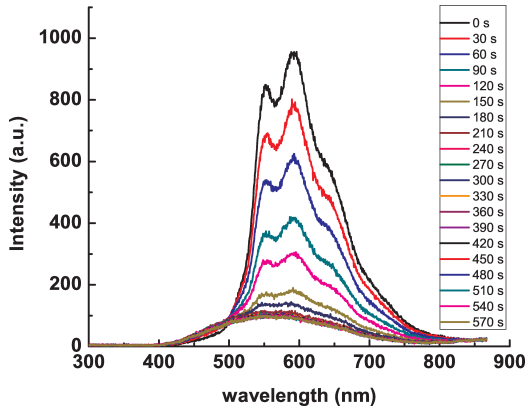

Figure 3: Time evolution of the photoluminescence spectra of the PQ (20 nm nominal thickness) evaporated on silicon oxide.

film phases), as confirmed by XRD measurements. Photoluminescence response data as a function of substrate and PQ thickness will also be shown.

References

[1] Parisse P, Luciani D, Santucci S, Zuppella P, Tucceri P, Reale A and Ottaviano L 2008 *J. Phys. D: Appl. Phys.* 41 112003
[2] Hwang D K, Kim K, Kim J H, Im S, Jung D Y and Kim E 2004 *Appl. Phys. Lett.* 85 5568
[3] Parisse P, Picozzi S and Ottaviano L 2007 *Org. Electr.* 8 498
[4] Mulheran P A and Blackman J A 2006 *Physical Review B* 53 10261
[5] Pimpinelli A and Einstein T A 2007 *Physical Review Letters* 99 226102

Rapid Identification of Graphene Sheets: Alumina Does It Better

P. De Marco[1], M. Nardone[2], S. Santucci[1,2], A. Del Vitto[3], M. Alessandri[3], L. Ottaviano[1,2]

[1] *CASTI CNR-INFM and Dipartimento di Fisica, Università dell'Aquila Via Vetoio, 67100 Coppito (AQ), Italy*

[2] *Dipartimento di Fisica, Università dell'Aquila Via Vetoio, 67100 Coppito (AQ), Italy*

[3] *NUMONIX Via C. Olivetti 2, Agrate Brianza (Mi), Italy*

Even if the 300 nm silicon oxide is widely recognized as a good substrate to locate exfoliated graphene flakes [1,2], 72 nm alumina dielectric films were proposed [3] as better substrates suitable to rapidly identify single and multi layers of graphene using an optical microscope. In Figure 1, we show the optical images of HOPG exfoliated onto (a) 300 nm silicon oxide, turquoise green color, and onto (b) 72 nm alumina, black colored. In both panels of this figure, the red box indicates the region in which a graphene three-layer is located as determined by the RAMAN signature in the micro RAMAN spectra of the samples [4], (Figure 2).

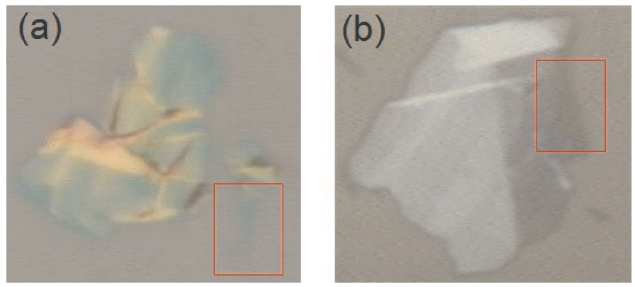

Figure 1: Images by a confocal optical microscope (magnification 100×, numerical aperture 0.9) of exfoliated HOPG on (a) 300 nm thick silicon substrate and (b) 72 nm thick alumina substrate. In both images, the red box outlines the thinner region where a trilayer graphene is identified by Raman (see Figure 2)

The different image contrast in visible light is a result of the optical reflection and transmission for a layered thin-film substrate. The system has three interfaces involved, and because a portion of the beam is reflected from each interface and the rest is transmitted, there exist more than one optical path. The amplitude of the reflected beam results from the interference between all the optical paths and depends on the wavelenght of the incident light, the incidence angles, the refractive

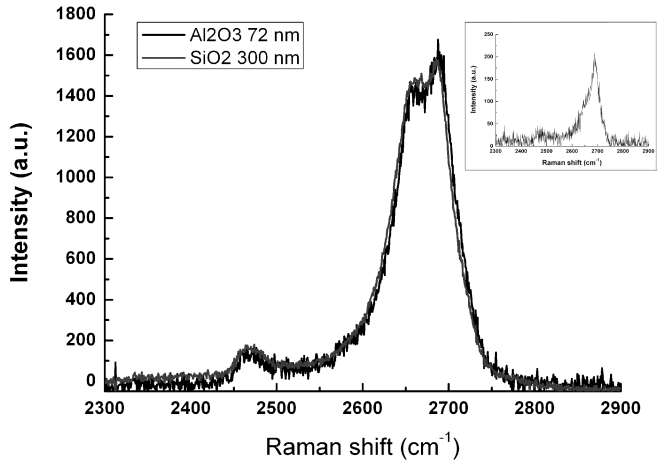

Figure 2: Comparison of the 2D band of the Raman spectra at 633 nm for trilayer graphene on silicon oxide (gray curve) and alumina (black curve). A 2D band of the Raman spectrum of HOPG is reported in the inset

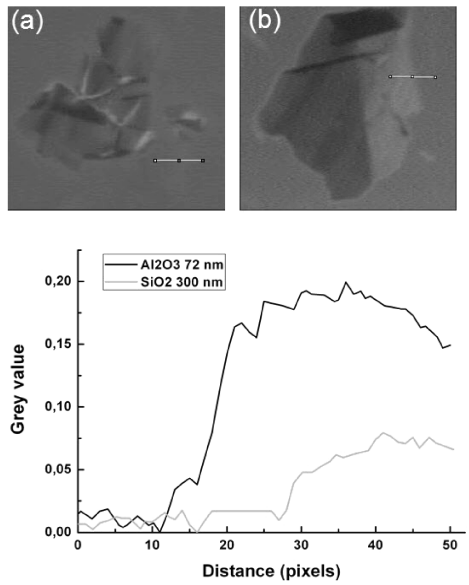

Figure 3: (a) and (b): gray tones of Figures 1 (a) and (b) images. The gray scale contrast graphs reported in the lower side of the figure are taken along the straight light lines. The measurements were performed from the substrate to the flake. In the lower side of the panel we report the gray profiles on silicon oxide (gray curve) and on alumina (black curve)

indices of all layers and their thickness [3]. To compare the contribution of each of the fundamental color components to the real color seen with an optical microscope, we broke up the color into the three fundamental components, namely Red (R), Green(G)

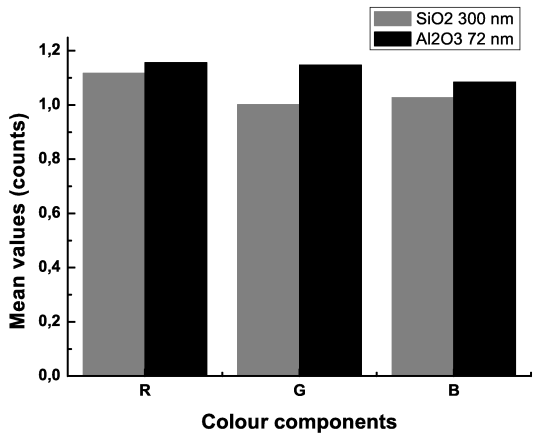

Figure 4: Histogram of the red (R), green (G) and blue (B) components, normalized with respect the substrate, for the images showed in Figure 1. All components are more intense for the graphene flake on alumina

and Blue (B) and we report an RGB component histogram (Figure 4). The yellow lines in Figure 3 (a) and (b) (upper panel) indicate the path used to the gray profile (lower panel), from the substrate to the graphene layer. The ratio between the gray value of the graphene on alumina and the graphene on silicon oxide in the region 30–50 pixel distance (x-axis in Figure 4) is 3, defining the Optical Contrast (OC) calculated by

$$\mathrm{OC} = \frac{(R_g - R_s)^2 + (G_g - G_s)^2 + (B_g - B_s)^2}{3}, \tag{1}$$

where R_g, G_g and B_g are referred to the RGB components of the graphene color and R_s, G_s and B_s to the RGB components of the substrate color. The result is that $\mathrm{OC} = 94$ for the silicon oxide film and $\mathrm{OC} = 307$ for the alumina film.

All the three fundamental components of the color contrast of the graphene flake on the alumina film are more intense with a mean factor 1.1, with respect to the RGB components of the graphene on the silicon oxide film.

The naked eye indicates that the best substrate to rapidly identify the graphene is the 72 nm alumina film. But to strengthen the optical observation, we calculated the gray profile and we quantified the optical contrast between the substrate and the graphene layer, finding that the graphene visibility onto the 72 nm alumina dielectric film was amplified by 3 times with respect to the 300 nm silicon oxide film.

References

[1] Novoselov K S, Geim A K, Morozov S V, Jiang D, Zhang Y, Dubonos S V, Grigorieva I V and Firsov A A 2004 *Science* **306** 666
[2] Novoselov K S, Geim A K, Jiang D, Schedin F, Booth T J, Khotkevich S V, Morozov S V and Geim A K 2005 *Proc. Natl. Acad. Sci. USA* **102** 10451
[3] Gao L, Ren W, Li F and Cheng H M 2008 *ACSNANO* **2** 8 1625
[4] Ferrari A C, Meyer J C, Scardaci V, Casiraghi C, Lazzeri M, Mauri F, Piscanec S, Jiang D, Novoselov K S, Roth S and Geim A K 2006 *Physical Review Letters* **97** 187401

Cytogenetic Stability of Chicken T-cell Line Transformed with Marek's Disease Virus: Atomic Force Microscope, a New Tool for Investigation

S. Di Bucchianico[1], M. F. Giardi[1], P. De Marco[2], L. Ottaviano[2], D. Botti[1]

[1] *Department of Basic and Applied Biology, University L'Aquila L'Aquila, Italy*

[2] *Department of Physics, University of L'Aquila L'Aquila, Italy*

The Marek's Disease Virus (MDV) integration may induce a novel organization of chromatin architecture with a modified genic expression. In our opinion it is worthwhile trying to relate the cytogenetic stability to the functional modifications due to an MDV genome insertion. Recently, the Atomic Force Microscopy technique has been applied to study the structure of chromosomes at a nanoscale level. A structural analysis with a high resolution provides detailed information on such high molecular complexes as 3-dimensional topological data, mechanical behaviour, dynamic processes and molecular interactions. When scanning soft biological surfaces, the AFM can achieve a resolution of about 1 nm. The vertical resolution is mostly determined by the AFM scanner sensitivity, and typically is 0.01 nm. These features allow different structures of chromatin to be investigated in order to study the cytogenetic stability and chromosome aberrations due to an MDV insertion in a chicken lymphoblastoid cell line MDCC-MSB1. Data indicating 78,WZ,dup(1p)(p22-p23) and 78,WZ cht del(3)(q2.10) are presented in our paper. The relationship between GTG bands (the staining techniques of chromosomes highlight a pattern of light and dark bands which differ in terms of gene density, base content, repetitive sequences and replication time) and the topography of chromosomes is discussed: it is possible to talk about Topographic Banding today. Thicker and thinner bands could be associated with GTG+ (dark bands) and GTG- bands. These characteristics may be a new cytogenetic diagnostic tool.

Optical Spectrophotometric Characterization of Organic TPB Films for Dark Matter Particle Detectors

F. Di Pompeo[1,2], R. M. Montereali[3], E. Nichelatti[4], M. A. Vincenti[3]

[1] *INFN, Gran Sasso National Laboratory*
SS 17-bis km 18+910, 67100, Assergi, L'Aquila, Italy

[2] *Department of Physics, University of L'Aquila*
Via Vetoio, 67010, Coppito, L'Aquila, Italy

[3] *ENEA, Physical Technologies and New Materials Department*
C. R. Frascati, Via E. Fermi 45, 00044, Frascati, Rome, Italy

[4] *ENEA, Physical Technologies and New Materials Department*
C. R. Casaccia, Via Anguillarese 301, 00123 Rome, Italy

Tetraphenyl-butadiene (TPB) is the preferred material used as the fluorescent converter for the detection of ultraviolet (UV) radiation in modern particle detectors based on Liquid Argon, especially for direct Dark Matter search [1,3]. Like other organic substances [2], it exhibits an intense broad emission band in the visible spectral interval, peaked at around 440 nm, under light excitation at smaller wavelength. Although some measurements in the Vacuum UV (VUV) range were performed in the past, in order to establish its conversion efficiency under excitation in the wavelength range 100–300 nm [3], a complete and systematic characterization in the optical spectral range is still missed.

In this work, TPB based films, grown on glass as well as reflective substrates, used in the light collection system of particle physics experiments were characterized through careful spectrophotometric measurements in the visible and NUV (Near UV) spectral range. Hemispheric transmittance (T) and reflectance (R) and direct transmittance spectra were successfully obtained at room temperature together with emission and photo-excitation spectra. This approach allowed us to individuate the main spectral features of the TPB films photoluminescence and to directly decouple its significant light contribution in the hemispheric T and R measurements.

Acknowledgements
We are grateful to the WArP collaboration for the scientific and technical support. We wish to thank the Gran Sasso National Laboratory (INFN) for the support of this initiative.

References

[1] P. Benetti *et. al*, *Astropart. Phys.* **28**, (2008) 495
[2] G. Baldacchini, S. Gagliardi, R.M. Montereali, A. Pace and R.B. Pode, *Phylosophical Magazine B* **82**, 6 (2002) 669
[3] W. M. Burton and B. A. Powell, *Applied Optic* **12**, 1 (1973) 87

Effective Elastic Properties of Polycrystalline Samples of Anisotropic Auxetic Materials

A. Duda[1], K. W. Wojciechowski[2a]

[1] *Institute of Theoretical Physics, University of Wroclaw*
Pl. Maxa Borna 9, 50-204 Wroclaw

[2] *Institute of Molecular Physics, Polish Academy of Sciences*
M. Smoluchowskiego 17, 60-179 Poznan, Poland

[a] *kww@man.poznan.pl*

Poisson's ratio characterizes the relative change of lateral to axial dimensions of materials under uniaxial load. For anisotropic materials it depends both on the direction of load and the transverse direction in which the deformation is measured. Common materials exhibit a positive Poisson's ratio. The stability allows, however, for negative values of this quantity. Materials with a negative Poisson's ratio, called auxetics, have been the subject of increasing interest [1].

Effective elastic properties of polycrystalline samples of completely random orientations (no texture) can be computed in various ways, e.g. by averaging the elastic moduli, elastic compliances and by other methods. In this work these approximate methods are used to compute effective elastic properties of polycrystalline samples consisting of auxetics of various symmetries. Regions in which the effective Poisson's ratio is negative are determined for various methods.

References

[1] J. N. Grima, K. W. Wojciechowski, Preface, Physica Status Solidi B245, 2369-2372 (2008); see also papers and references in that issue

Structure of Liquid Cu by a Novel Quantum-Classical Approach

J. Dziedzic[1], J. Rybicki[1,2]

[1] *Faculty of Technical Physics and Applied Mathematics*
Gdansk University of Technology
Narutowicza 11/12, 80-233 Gdansk, Poland
[2] *TASK Computer Centre*
Gdansk University of Technology
Narutowicza 11/12, 80-233 Gdansk, Poland

Molecular-dynamics (MD) calculations can provide a useful insight into the structure of liquid metallic systems. However, the empirical nature of the potentials employed and the neglect of the electronic structure may render the obtained results dubious. Employing first-principles calculations to explicitly take the electronic effects into the picture and using thus obtained forces to drive the atoms within an MD simulation is feasible, yet the computational effort associated with *ab-initio* computations drastically reduces the timescales that may be studied (say, from 100 ns to 100 ps for a periodic supercell of about 1000 atoms).

Learn-on-the-Fly [1] is a recently proposed hybrid approach which allows for hybrid quantum-classical calculations in which the computational cost of the quantum-based computation is reduced by about an order of magnitude, thus allowing for the study of longer timescales or larger systems. The method has been shown to work well for semiconductor systems.

Here we present an extension of the formalism to metallic systems, dubbed Divide-and-Conquer Learn-on-the-Fly [2] and show how it can be utilized to obtain the structure of liquid copper. Apart from the introduction of the proposed technique and its implementation, the structure of the obtained liquid is briefly discussed and compared with the available empirical data and results of other simulations, in terms of pair correlation functions, angular distribution functions and the diffusion coefficient. The advantages and deficiencies of the proposed technique are also highlighted.

References

[1] Csányi G, Albaret T, Payne M C and De Vita A 2004 *Phys. Rev. Lett* **93** 175503
[2] Dziedzic J 2009 *Quantum-Classical Computations of the Nanomechanical Properties of Metals*, PhD thesis, Gdansk University of Technology

Preparation and Magnetic Properties of Magnetite Dispersed in a Carbon Matrix

W. Arabczyk[1], E. Ekiert[1], M. Bałanda[2]

[1] *Institute of Chemical and Environment Engineering*
West Pomeranian University of Technology
ul. Pułaskiego 10, 70-322 Szczecin

[2] *The Henryk Niewodniczański Institute*
of Nuclear Physics Polish Academy of Sciences
ul. Radzikowskiego 152, 31-342 Cracow

A procedure for preparation of nanocrystalline particles of magnetite dispersed in a carbon matrix is described. The carburization of a nanocrystalline iron catalyst with methane led to the formation of iron carbide in a carbon matrix. Next, the iron carbide was oxidized with carbon dioxide to obtain magnetite. The process conditions were matched to prevent loss of the carbon matrix. In this way, specific composites were produced with magnetite superfine particles dispersed in the carbon matrix with different carbon content ranging from 0.5 to 1.3 gC/gFe. A composite with iron nanoparticles in the carbon matrix was formed, as well. The prepared samples of iron and magnetite, but also of iron carbide as the raw material were characterized by scanning electron microscopy and X-ray diffraction. The average crystallite size of Fe_3O_4, Fe, Fe_3C and C was 40, 20, 30 and 10 nm, respectively. The carbon products were present in the samples in form of amorphous carbon, wires and small crystallites of graphite. The magnetization curves and hysteresis loops were obtained at liquid helium temperature. The higher carbon content in the samples caused a decrease in the saturation moment at $T = 4.2$ K.

Artificial Molecular Machines: Stimuli Induced Motion from Solution to Surface

G. Fioravanti

University of Aquila, Dept. of Chemistry, Chemical Engineering and Materials
Piazzale Pontieri 1, Monteluco di Roio (AQ), 67040 L'Aquila, Italy

Synthetic systems in which submolecular motions can be controlled by the application of external stimuli have been vigorously pursued in recent years [1].

Such "mechanical" molecular devices are viewed both as putative components for future functional nanotechnologies and as much simplified models of complex biological machines.

One of the most versatile designs for a simple switch-like molecular machine is the stimuli-responsive molecular shuttle [1]. A molecular shuttle is a rotaxane that consists of a "dumbbell molecule" threaded through a "macrocycle" (see figure).

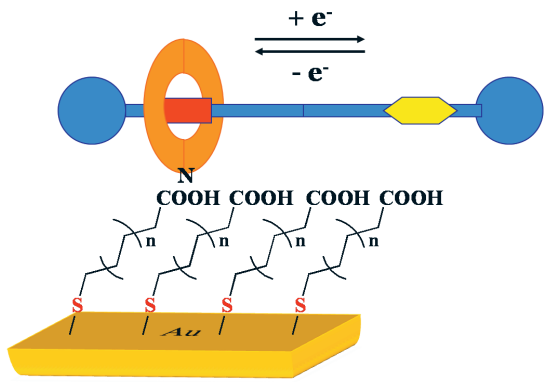

The two components of a rotaxane are kinetically trapped since the ends of the dumbbell (called stoppers) are larger than the internal diameter of the ring and prevent disassociation (unthreading) of the components.

The thread contains two (or more) macrocycle-binding sites ("stations") connected by a traversable pathway. Provided sufficient thermal energy is available to break the intercomponent interactions at each site, the ring moves randomly between the two stations.

Because of their ability to flip between two or more states when external stimuli induce relative movements of their noncovalently interacting components, mechanically interlocked molecules are promising candidates for the fabrication of actuators, amplifiers, motors, sensors, and switches of nanoscale dimensions [1].

Switchable, mechanically interlocked molecules have attracted much interest on account of their ability to alter the relative positions of their ring and dumbbell

components in response to external stimuli (such as a redox process, pH change, ion exchange, polarity, light, temperature, or covalent bond-formation) [2].

One particularly attractive stimulus for the operation of such devices is electrochemistry, as it permits remote, reagent-free, and waste-free control, while providing the opportunity to interface the molecular devices with the existing electronic technologies [3].

Clearly, a key step in the development of electronic (and many other) applications of synthetic molecular machines will be transposing the working systems from a solution phase onto surfaces and into the solid state.

The creation of a rotaxane-based device requires the molecule immobilization onto a surface, keeping the dynamic properties of the interlocked system preserved (like in a solution, where the ample freedom of movements is allowed).

Transposing working systems from a solution phase onto surfaces and into the solid state [4] is fundamental for their technological applications. Molecular shuttles have already been used to construct solid-state and surface-based devices that exhibit switchable conductance, optical properties, wettability, porosity, and shape [5].

Stimuli-induced shuttling is strongly implicated in the operation of each of these systems, but developing reliable methods for anchoring shuttles to solid supports and strategies for directly observing and fully characterizing their stimuli-induced motions have proven challenging.

The system studied is a [2]rotaxane which features succinamide and naphthalene diimide hydrogen-bonding stations for a benzylic amide macrocycle that can shuttle and switch its net position both in a solution and in a monolayer [6].

Three oxidation states of the naphthalene diimide unit can be accessed electrochemically in a solution, each one with a different binding affinity for the macrocycle and, hence, corresponding to a different distribution of the rings between the two stations in the molecular shuttle.

Cyclic voltammetry experiments show the switching to be both reversible and cyclable and allow quantification of the translational isomer ratios (thermodynamics) and shuttling dynamics (kinetics) for their interconversion in each state.

The switching conditions are sufficiently mild to allow access to two of the states when the rotaxanes are confined to an alkanethiol-based self-assembled monolayer (SAM) on gold.

References

[1] a) Molecular Switches Feringa B. L. Ed.: Wiley-VCH, 2001;
b) Tian, H.; Wang, Q.-C. Chem. Soc. ReV. 2006, 35, 361–374;
c) Kay, E. R. et al Angew. Chem., Int. Ed. 2007, 46, 72–191;
d) Molecular Devices and Machines: Concepts and Perspectives for the Nanoworld Balzani V. et al Ed.: Wiley-VCH, 2008
[2] a) Brouwer A. M. et al Science 2001, 291, 2124;
b) Bottari G. et al F Angew. Chem., Int. Ed. 2003, 42, 5886;
c) Marlin D. S. et al Angew. Chem., Int. Ed. 2006, 45, 1385;
d) Kawai H. et al Angew. Chem., Int. Ed. 2006, 45, 4281;
e) Green J. E. et al Nature 2007, 445, 414;
f) Serreli V. et al Nature 2007, 445, 523;
g) Mateo-Alonso A. et al Angew. Chem., Int. Ed. 2007, 46, 3521;
h) Durola F., Sauvage J. P. Angew. Chem., Int. Ed. 2007, 46, 3537;

i) Kay E. R. et al Angew. Chem. Int. Ed. 2007, 46, 72;
j) Hirose K. et al Chem.-Eur. J. 2008, 14, 5803
[3] a) Mendes, P. M. et al Appl. Phys. A 2005, 80, 1197–1209;
b) Green, J. E. et al Nature 2007, 445, 414–417
[4] a) J. Phys. Chem. A 2003, 107, 9634;
b) J. Phys Chem. A 2006, 110, 12963;
c) ChemPhys 2008, 343, 186;
d) Principles and Methods in Supramolecular Chemistry, John Wiley and Sons 2000
[5] a) Willner I. et al J. Electroanal. Chem. 2001, 497, 172;
b) Katz E. et al Angew. Chem., Int. Ed. 2004, 43, 3292;
c) Huang T. J. et al Appl. Phys. Lett. 2004, 85, 5391;
d) Steuerman D. W. et al Angew. Chem., Int. Ed. 2004, 43, 6486;
e) Leigh D.A et al Angew. Chem., Int. Ed. 2005, 44, 3062;
f) Feng M. et al J. Am. Chem. Soc. 2007, 129, 2204;
g) Guo X. F. et al Adv. Funct. Mater. 2007, 17, 763
[6] Fioravanti G. et al J. Am. Chem. Soc. 2008 130, 2593

The First Italian Micro-exposure Tool for EUV Nanolithography

F. Flora[1], S. Bollanti[1], F. Bonfigli[1], A. Gerardino[2], P. Di Lazzaro[1], L. Mezi[1], R. M. Montereali[1], D. Murra[1], A. Reale[3,4], A. Torre[1], P. A. Vincenti[1]

[1] *ENEA, Physical Technologies and New Materials Dept. C.R. Frascati, Via E. Fermi 45, 00044, Frascati, Rome, Italy*

[2] *CNR-IFN, via Cineto Romano 42, 00156 Roma, Italy*

[3] *University of L'Aquila, Dept. of Physics via Vetoio, 67010 Coppito, L'Aquila, Italy*

[4] *g.c. INFN-LNGS, Italy*

Extreme Ultraviolet (EUV) nanolithography is still the main candidate among the next-generation lithographic technologies for the achievement of a sub-32-nm resolution in microelectronic manufacturing. Many research projects on EUV Lithography (EUVL) are in progress in Europe and in the world in order to reach the first high-volume manufacturing tool in a few years.

In Italy the research and the know-how in this field has received a strong acceleration during the past 4 years during a national FIRB project on EUVL coordinated by the Physics Department of L'Aquila University. During this project, the first Italian EUVL tool with a resolution ≤ 100 nm has been developed at the ENEA Laboratories in Frascati [1,2].

We present here the main characteristics of the tool and the results obtained on both PMMA coated silicon wafers and on a photoluminescent material (LiF).

References

[1] S. Bollanti, P. Di Lazzaro, F. Flora, L. Mezi, D. Murra and A. Torre: "First results of high-resolution patterning by laboratory-scale EUV projection lithography", *European Physics Letters*, Vol. 84, p. 58003 (2008)

[2] P. Di Lazzaro, S. Bollanti, F. Flora, L. Mezi, D. Murra and A. Torre: "Excimer-laser-driven EUV plasma source for single-shot projection lithography", *IEEE Transactions on Plasma Science*, Vol. 37, No. 4, April 2009

Metal Voids in 110 nm Lines Due to Thermal Diffusion of Aluminum in Large Metal Plate

F. Galanello, S. Guerrieri, A. D'Anna

Micron Technology Italia – R&D Technology and Pixel Development Group
via A. Pacinotti, 5/7, 67051 Avezzano (AQ), Italy

Aluminum metal voids were observed in a multistack aluminum interconnection on 110 nm technology node CMOS Image devices. By means of SEM analysis and a process flow study it was found that a 400°C thermal treatment was the cause of the formation of aluminum voids. By means of device metallization layout analysis and a correlation with the voids positions it was argued that the metal diffusion mechanism is also at the basis of the void formation. The failure mechanism was proved by a checkboard isolation of large metal plates from aluminum lines where voids were observed. The technological strategy adopted to hamper the void formation was the introduction of a tantalum based barrier to separate the Al layers.

Polymer Material Integration in Light Pipes Module of CMOS Imager Devices

F. Galanello, G. De Amicis, M. Cichocki, A. D'Anna

Micron Technology Italia – R&D Technology and Pixel Development Group
via A. Pacinotti, 5/7, 67051 Avezzano (AQ), Italy

One of most recent innovations in CMOS image sensor applications is the introduction of a polymer material using a refractive index higher than 1.6 in order to guide light on each photodiode. The polymer is spun into pipes obtained by a dry etching cylindrical oxide portion of multistack metallization. Integrating this new module into IC devices is a challenge from the polymer filling and polymer-oxide adhesion point of view. The process of integration of the polymer material was investigated and improved to increase the image quality. The defect effects were also simulated by FDTD (Finite Difference Time Domain) and correlated to the image quality.

Domain Wall Formation and Electron–Phonon Interaction of Bi Reconstructed Phases on Cu(100)

P. Gargiani[1], S. Achilli[2], M. I. Trioni[2], F. Bussolotti[1], M. G. Betti[1]

[1] *Dipartimento di Fisica, Università di Roma "La Sapienza" Piazzale Aldo Moro 5, 00185 Roma*

[2] *CNISM Università Milano-Bicocca, Via Cozzi 53, I-20125 Milano, Italy*

The adsorption of a single layer of bismuth on a Cu(100) surface gives rise to a large variety of structural phases characterized by a $c\,(2 \times 2)$ phase evolving in larger domains with a $p\,(10 \times 10)$ symmetry [1]. These phases can be stabilized by the coupling with an underlying metallic charge and electron phonon (e-ph) interaction with the competing/concomitant effect of the confinement induced by the domain wall formation [2]. We present a combined experimental and theoretical study of the electronic properties of the Bi 2D structural phases investigated by angle resolved photoemission experiments (ARPES) and an *ab initio* calculation performed within the embedding method applied to a realistic semi-infinite system [3]. In particular, the spectral density and the Bi electronic states dispersion of the $c\,(2 \times 2)$ structural phase have been compared with the results obtained by theoretical prediction.

Although a good agreement is observed, the photoemission data do not show any spectral density at the Fermi edge even at low temperature ($T = 40$ K). As e-ph coupling seems to be favored in low dimensional semimetallic systems, suggesting phenomena such as charge density wave (CDW), a detailed analysis of the electronic states dependence on the temperature was performed, giving information about the strength of the electron-phonon coupling on the 2D Bi structural phases. Similar systems have been described as good candidates for 2D-CDW [4], but for the Bi/Cu(100) system the presence of domain wall potential at surface and/or large spin orbit splitting effects seems to overshadow the charge density wave formation [5].

References

[1] Wynblatt P. et al., *Surf. Sci* **601**, 1623 (2007)
[2] Nakagawa T. et al., *Phys. Rev. B* **72**, 165405 (2005)
[3] Achilli S., Caravati S., Trioni M.I., *J. of Phys., Cond. Matt.* **19**, 305021 (2007)
[4] Aruga T. , *Surface Science Reports* **61**, 283 (2006)
[5] Hofmann P., *Progress in surface Science* **81**, 191-245 (2006)

3*d*-metal Phthalocyanines Chains on Au(110): Electronic Structure Dependence on 3*d* Metal Occupancy

P. Gargiani, C. Mariani, M. G. Betti

Dipartimento di Fisica, Università di Roma "La Sapienza"
Piazzale Aldo Moro 5, 00185 Roma

Metal-phthalocyanine (MPc) molecules, identified as promising active elements for many optical, electronic and magnetic applications, have a twofold interest: (i) the π-conjugation guarantees charge delocalization and electron mobility, and (ii) the central metal atom can play a crucial role in establishing the electronic/magnetic properties of the interface.

We study the electronic properties of *long-range ordered* chains of MPc's deposited on the Au(110)-(1×2) surface, changing the metal 3*d* orbital occupancy (M = Fe, Co, Ni, Zn and Cu). The molecular chains arrange along the "channels" of the Au(110) reconstructed surface, giving rise to a highly ordered (5×3) superstructure, as can be observed by the low-energy electron-diffraction [1].

The electronic structure of the MPc chains was studied by means of high resolution angle-resolved photoemission spectroscopy. All the MPc chains presented similar interface electronic states different from pure molecular states, localised at higher binding energy with respect to the HOMO state. CoPc and FePc chains presented also non dispersive interface electronic states close to the Fermi level. In particular, FePc quasi 1D chains induced a localised state close to the Fermi level, whose intensity was enhanced by increasing the 3*d*-metal cross section (from 21.2 to 40.8 eV excitation energy) suggesting its metallic character. Its intensity, strongly dependent on temperature, almost vanished at room temperature. Although the contribution of electron-phonon interaction could not be excluded, the localization of this electronic state in the k-space and its temperature dependence suggested a hypothesis of a Kondo-like peak due to the interaction of the spin of the Fe central atoms with the underlying free electron gas, as previously observed [2].

References

[1] Evangelista et al. *Surf. Sci.* **531**, 123 (2001)
[2] L. Gao, et al. *Physical Review Letters* **99**, 106402 (2007)

Structure and Electrical Properties of Ceramic Proton Conductors Obtained with Solid-state and Molten-salt Synthesis Methods

A. Mielewczyk[1], K. Gdula[1], S. Molin[2], P. Jasiński[1], B. Kusz[1], M. Gazda[1]

[1] *Faculty of Applied Physics and Mathematics*
Gdansk University of Technology
Narutowicza 11/12, 80-233 Gdansk, Poland

[2] *Faculty of Electronics, Telecommunication and Informatics*
Gdansk University of Technology
Narutowicza 11/12, 80-233 Gdansk, Poland

Proton conducting materials which belong to the group of acceptor-doped Ba-Ce-O and La-Nb-O are considered as possible ceramic electrolytes for intermediate temperature solid oxide fuel cells (IT-SOFC). The main advantage of proton conductors in comparison to oxide ions conductors as electrolytes in SOFCs is that the generation of water occurs at the cathode side, thus the fuel which is at the anode side is not diluted [1]. On the other hand, the drawback is the high intergrain resistivity and the too low chemical stability. Therefore, further research is necessary to successfully apply proton conductors in SOFCs.

Several acceptor-doped Ba-Ce-O and La-Nb-O electrolytes with different stoichiometries were synthesized and investigated in this work. Three different elements were used as dopants (calcium, strontium and magnesium). The studied materials were synthesised both by solid state (SS) and molten salt synthesis (MSS) methods. All samples were investigated by X-ray diffraction (XRD). The XRD data were analysed with the Rietveld method. The electrical properties were studied in dry and humid air with impedance spectroscopy (IS).

The synthesis method and the composition of samples had a significant influence on the microstructure of the ceramics. For example, in case of the La-Nb-O samples the crystallite size decreased with an increase in the dopant content. Also the electrical properties of the samples depended on the sample stoichiometry and the dopant element.

The properties of the samples obtained with the molten salt synthesis method seem to be promising in relation to future applications.

References

[1] H. Iwahara, Y. Asakura, K. Katahira, M. Tanaka *Solid State Ionics* 168 (2004) 299

Microscopic and Spectroscopic Study of Poly(3-hexylthiophene)/Carbon Nanotube Composites for Solar Cells Applications

M. Giulianini[1], E. R. Waclawik[2], J. M. Bell[1], M. Scarselli[3], P. Castrucci[3], M. De Crescenzi[3], N. Motta[1]

[1] *School of Engineering Systems, Queensland University of Technology 2 George St., Brisbane (QLD), 4001 Australia*

[2] *School of Physical and Chemical Sciences, Queensland University of Technology, 2 George St., Brisbane (QLD), 4001 Australia*

[3] *Dipartimento di Fisica, Unità CNISM, Università di Roma "Tor Vergata" 00133 Roma, Italy*

Polythiophenes and carbon nanotubes composites have been proposed for solar cells application. Mixtures of Regioregular Poly(3-hexyl-thiophene) (rrP3HT) and multi wall carbon nanotubes have been investigated by Scanning Tunneling Microscopy and Spectroscopy in Ultra High Vacuum to analyse the interaction between

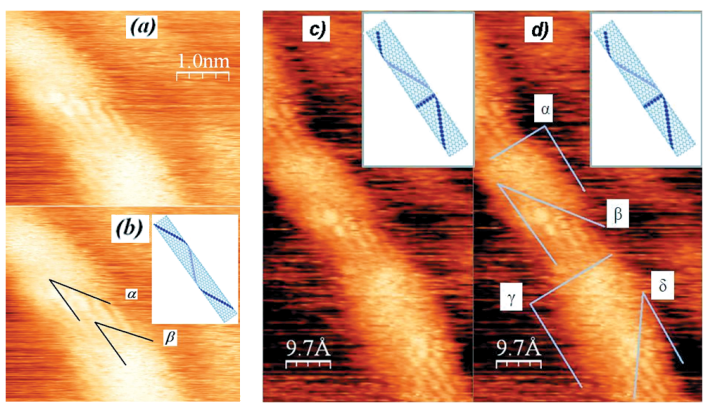

Figure 1: Comparison between unfiltered images of the polymer covered carbon nanotube to show the angles formed between the polymer strands and the nanotube. Image acquired using a bias voltage $V = -500$ mV and a current $I = 350$ pA. The angles indicated with α, β, γ and δ are used to evidence the preferred direction on which the polymer is aligned on the nanotube surface. In Figures a–b the angles α, β amount to 33° and 34°, respectively. In Figures c–d the angles α, β, γ and δ amount to 90°, 33°, 90° and 34°, respectively (insets); (15,0) zigzag nanotubes with 30° and 90° hexagonal cells alignments, reported for comparison, are highlighted

nanotubes and polymer. Carbon nanotubes coiled by rrP3HT have been imaged and analyzed, providing a clear evidence that this polymer self assembles on the nanotube surface following geometrical constraints and adapting consequently its equilibrium chain-to-chain distance. An accurate morphology analysis evidenced the nature of the non covalent bonding of the two materials and the central role played by chirality on the final assembly. On a nanotube with largely spaced polymer covered sections, it has been possible to identify the nanotube chirality and hence the electronic properties. Scanning Tunneling Spectroscopy was performed on the (15,0) single wall carbon nanotube identified partially wrapped by Poly(3-hexyl-thiophene). On the bare nanotube sections, the local density of states resulted in good agreement with the theoretical model based on local density approximation and remarkably results not perturbed by the adjacent polymer wrapping. On the P3HT coiled sections, a rectifying current-voltage characteristic has been observed. Further analysis proved that a consistent charge transfer occured from the sulphur atoms of the thiophene rings of the polymer to the single wall nanotube. The electron transfer from Poly(3-hexyl-thiophene) to metallic nanotubes was previously theoretically proposed and results in good agreement with the energetic band diagram of the two materials. It directly contributes to the presence of the Schottky barrier at the interface responsible for the rectifying behavior. According to our analysis, the heterojunction between P3HT and metallic single wall nanotube should act inefficiently in the photovoltaic conversion.

Four-Level Model for EIT of Cold ^{85}Rb

B. Brzostowski, V. Cao Long, B. Grabiec

Institute of Physics, University of Zielona Góra
ul. Prof. Szafrana 4a, 65-516 Zielona Góra, Poland

It is shown by a theoretical model describing the interaction of a strong electromagnetic field with a four-level atomic system of cold ^{85}Rb that multiple windows of electromagnetically induced transparency (EIT) occur in the spectral profile of the probe absorption in the transition $5S_{1/2} \longleftrightarrow 5P_{3/2}(F = 2, 3)$.

Our results are in good agreement with previous theoretical investigations.

The theoretical predictions will be compared with the experimental observations of the Warsaw group.

Our paper is a continuation of the paper presented a year ago on FNMA'08 and published soon afterwards in the *Journal of Non-Crystalline Solids*.

Atomic Structure Stability of PtCo Electrocatalysts in Proton Exchange Membrane Fuel Cell Subjected to Ageing Process

G. Greco[1], A. Witkowska[2], S. Dsoke[3], A. Di Cicco[1], A. Cognigni[4], N. Menguy[5], J-M. Guigner[5]

[1] *Department of Physics, University of Camerino via Madonna delle Carceri, 9, Camerino (MC), Italy*

[2] *Department of Solid State Physics, Gdansk University of Technology Narutowicza 11/12, 80-233 Gdansk, Poland*

[3] *Chemistry Department, University of Camerino via S. Agostino, 1, Camerino (MC), Italy*

[4] *ELETTRA Sincrotrone Trieste S.C.p.A., AREA Science Park 34149 Basovizza, Trieste, Italy*

[5] *IMPMC, Université P. et M. Curie, CNRS 140 rue De Lourmel, 75015 Paris, France*

Nano-particles of platinum alloys are an interesting class of binary compounds due to their significantly higher electrocatalytic activities and stability towards the oxygen reduction reaction (ORR) than the platinum alone in a low temperature fuel cell. To understand why the alloy structure ensures an increase in the catalyst's activity, stability and durability is fundamental for Proton Exchange Membrane Fuel Cell (PEMFC) commercialization.

Therefore, carbon supported PtCo (E-TEK) electrocatalysts were subjected to an ageing process and, after that, to a structural analysis using the X-ray absorption spectroscopy (XAS), the transmission electron microscopy (TEM) and the X-ray diffraction (XRD) technique. Repetitive step-like potential cycling (between OCV and 0.6 V) by 50, 100, 150 and 300 hours was performed with the considered catalyst working on the oxygen side. XRD and TEM investigations showed that the mean nano-grains dimension increased after 50 hours of ageing and after this period further nano-crystal aggregation was rather not observed. It should be underlined that for pure Pt catalyst aged in the same way continuous agglomeration occurs. Detailed results of a multiple-scattering (MS) XAFS double-edge (Co K and Pt L_3) data analysis were used to obtained a robust model of a local structure in a PtCo nano-alloy as a function of working time. XAFS spectra analysis have been realized accounting for the degeneracy of two and three-body configurations, resulting from both the measured size distribution, i.e. expected surface atom contributions, and the chemical disorder. The role of ligand oxygens on Co and Pt are also discussed.

XPS and SEM Studies of Oxide Reduction of Germanium Nanowires

V. Grossi, L. Ottaviano, S. Santucci, M. Passacantando

Dipartimento di Fisica, Università degli Studi dell'Aquila
Via Vetoio 10, I-67010 Coppito, L'Aquila, Italy

Germanium nanowires (GeNWs) are materials attracting much interest for future computing owing to their higher carrier mobility than silicon nanowires (SiNWs) [1] and a larger exciton radius of 24.3 nm than Si (4.9 nm) with prominent quantum confinement effects [2]. Thus, they offer an appealing potential as candidates for future nanoelectronics. The chemical and electronic stability of nanowire surfaces is important for applications [3].

We grew single crystal germanium nanowires (GeNWs) by vapour-liquid-solid deposition onto silicon oxide substrates with Au catalyst nanoparticles. The surface and morphology of the GeNWs was studied by means of X-ray photoelectron spectroscopy (XPS) and scanning electron microscopy (SEM), respectively. A complete oxidation of the outer shells of the GeNWs was evidenced by an XPS analysis. Most of the surface oxide could be removed by aqueous HF, aqueous HCl, and by pure H_2O. A complete reduction of the oxide was evidenced after chemical treatments by XPS measurements. Furthermore, due to an SEM analysis it could be observed that the chemical etching produced a reduction the diameter of the GeNWs, in agreement with the effective removal of the surface oxide. In addition, the oxidation process of the GeNWs was controlled after various exposure times in ambient atmosphere.

Acknowledgements
V.G. thanks Alessandro Urbani (Dipartimento di Fisica, Università dell'Aquila) for his support during the XPS measurements.

References

[1] Sze S M 1981 *Physics of Semiconductor Devices*, New York: Wiley
[2] Maeda Y, Tsukamoto N, Yazawa Y, Kanemitsu Y and Masumoto Y 1991 *Appl. Phys. Lett.* **59** 3168
[3] Wang D W, Wang Q, Javey A, Tu R, Dai H, Kim H, McIntyre P C, Krishnamohan T and Saraswat K C 2003 *Appl. Phys. Lett.* **83** 2432

Novel Photosensor Made of MWCNTs Grown on Silicon Substrate

V. Grossi[1], A. Urbani[1], M. Ambrosio[2], A. Ambrosio[3], P. Maddalena[3], S. Santucci[1], M. Passacantando[1]

[1] *Dipartimento di Fisica and INFN, Università degli Studi dell'Aquila Via Vetoio 10, I-67100 Coppito, L'Aquila, Italy*

[2] *INFN Sezione di Napoli, Complesso Universitario di Monte Sant'Angelo Via Cintia, I-80126 Napoli, Italy*

[3] *CNR-INFM CRS-COHERENTIA and Dipartimento di Scienze Fisiche Università di Napoli Federico II, Complesso Universitario di Monte Sant'Angelo Via Cintia, I-80126 Napoli, Italy*

Photocurrent measurements derived by light excitation have been reported in different configurations exploiting Carbon Nanotubes (CNTs) [1]. Photoresponse in macro-bundles of Multi-Walled Carbon Nanotubes (MWCNTs) has been recently observed [2], and a technologically promising high photon-to-current conversion has been demonstrated for MWCNTs by means of an electrochemical method [3]. Studies on large area sheets of MWCNTs grown on a sapphire substrate [4] using also pulsed laser beams [5] may provide us opportunities for constructing smart structures with multiple functionalities.

We grew MWCNTs at 500°C by thermal Chemical Vapour Deposition (CVD) of acetylene (C_2H_2) gas, in the ammonia (NH_3) atmosphere, around a platinum (Pt) electrode deposited on a silicon (Si) substrate sandwiched between two insulator silicon nitride (Si_3N_4) layers. This device was used in order to investigate the photoconductivity properties of MWCNTs under white light and different radiation produced by LEDs in the visible region. The CNT sheet was illuminated far from the Pt electrode by a standard optical fiber. The photocurrent signal was captured from the Pt electrodes placed on the top and on the bottom of the device. We illuminated the area without the CNTs and the area with the CNTs, to obtain a zero photocurrent and a photoconductance of about 10^{-21} $s\Omega^{-1}$, respectively.

The photoconductivity properties of these materials are favorable for the potential development of large area light sensors as well as optoelectronic nanodevices.

Acknowledgements

The authors are grateful to the European Collaborative Project "S-five" and to the INFN National Collaborative Project SinPhoNIA for financial support.

References

[1] Balasubramanian K, Fan Y, Burghard M, Kern K, Friedrich M, Wannek U, and Mews A 2004 *Appl. Phys. Lett.* **84** 2400

[2] Wei J, Sun J, Zhu J, Wang K, Wang Z, Luo J, Wu D, and Cao A 2006 *Small* **2** 988

[3] Castrucci P, Tombolini F, Scarselli M, Speiser E, Del Gobbo S, Richter W, De Crescenzi M, Diociaiuti M, Gatto E, and Venanzi M 2006 *Appl. Phys. Lett.* **89** 253107

[4] Passacantando M, Bussolotti F, Grossi V, Santucci S, Ambrosio A, Ambrosio M, Ambrosone G, Carillo V, Coscia U, Maddalena P, Perillo E, and Raulo A 2008 *Appl. Phys. Lett* **93** 051911
[5] Ambrosio A, Ambrosio M, Ambrosone G, Carillo V, Coscia U, Gesuele F, Grossi V, Maddalena P, Passacantando M, Perillo E, Raulo A, Santucci S, and Ugolino U 2008 *NIM A* **589** 398

Aluminum Process Integration in Copper Metallization Multi Stack for 90 nm Technology Node CMOS Image Sensor Applications

S. Guerrieri, G. Testa, G. Mattioli,
S. Sellitto, A. Stilo, A. D'Anna

Micron Technology Italia – R&D Technology and Pixel Development Group
via A. Pacinotti, 5/7, 67051 Avezzano (AQ), Italy

The metal interconnect size for CMOS sensor image applications could be considered as one of the most important requirements for lighting a photo-diode while minimizing the obstacle on the light path. It has been possible to shrink the interconnect size by replacing aluminum with copper but an aluminum pad layer is still used in the IC industry for chip bonding. Two different advanced integration schemes were developed introducing aluminum into a copper back-end-of-line (BEOL), for both *signal routing* and *bonding* avoiding reliability issues related to a high solubility of aluminum in copper.

Characterization of PVD Ta and Ti Copper Diffusion Barriers

S. Guerrieri, G. Testa, A. D'Anna

Micron Technology Italia – R&D Technology and Pixel Development Group
via A. Pacinotti, 5/7, 67051 Avezzano (AQ), Italy

Advanced technology nodes for CMOS applications use copper multilevel metallization in order to shrink the signal routing size and improve the device RC delay. Copper integration in semiconductor devices could impact the product reliability due to a high diffusion property of copper in materials used for micro-chip applications such as silicon, silicon dioxide or aluminum.

In this study, copper diffusion through metallic PVD sputtered Ta and Ti based barriers was characterized by the XPS and SIMS analysis.

Polymer Material Characterization with High Refractive Index for 90 nm Technology Node CMOS Imager Sensor Applications

R. Marinelli[1], S. Guerrieri[2], G. De Amicis[2], A. Del Monte[2], M. Faccio[1], E. Palange[1], A. D'Anna[2]

[1] *Università degli Studi Dell'Aquila – Ingegneria Elettronica*
Piazzale Pontieri 1, 67040 Monteluco di Roio, L'Aquila, Italy

[2] *Micron Technology Italia – R&D Technology and Pixel Development Group*
via A. Pacinotti 5/7, 67051 Avezzano (AQ), Italy

A polymer material with a high refractive index was implemented on advanced CMOS image sensors at a 90 nm technology node. The polymer was spun into light pipe modules on top of each photodiode in order to improve the light channeling toward each single pixel improving thus the device performance. Refractive index variations of the polymer under different thermal treatments were studied with ellipsometric techniques. The experimental data of spectroscopic techniques were also compared with a 1-D simulation tool in Matlab. The material characterization was completed with optic microscopy, AFM, SEM, TEM to study the thermal stress and viscoelasticity while the chemical characterization (TGA) was studied for thermal stability.

Influence of Magnetic Agglomerates on EPR Spectrum of Free Radicals in Organic Matrix

N. Guskos[1a,2], G. Żołnierkiewicz[2], J. Typek[2], A. Guskos[2], D. Petridis[3]

[1] *Solid State Section, Department of Physics, University of Athens Panepistimiopolis, 15 784 Zografos, Athens, Greece*

[a] *ngouskos@phys.uoa.gr*

[2] *Institute of Physics, West Pomeranian University of Technology Al. Piastów 48, 70-311 Szczecin, Poland*

[3] *NCSR "Demokritos" Aghia Paraskevi, Attikis, Athens, Greece*

Two samples containing an extended free radical network derived from a condensation of cyanuric chloride and *p*-phenylenediamine were prepared. Both samples contained free radicals and the second sample additionally had a very small amount of magnetic centers in form of agglomerate nanoparticles. The temperature dependence of magnetic resonance spectra (EPR/FMR) was measured in the 4–290 K temperature range. At room temperature the magnetic resonance measurements showed that the EPR spectrum was the sum of two lines attributed to two different magnetic centers for the second sample: a narrow line at $H_r = 3373.46(3)$ Gs ($g_{eff} = 2.0031(1)$) with linewidth $\Delta H_{pp} = 8.63(2)$ Gs (due to free radicals) and a broad line centered at $H_r = 3053(5)$ Gs ($g_{eff} = 2.240(1)$) with linewidth $\Delta H_{pp} = 1010(5)$ Gs (arising from magnetic iron oxide agglomerates). The first sample showed only a single resonance line centered at $H_r = 3371.64(3)$ Gs ($g_{eff} = 2.0043(1)$) with linewidth $\Delta H_{pp} = 7.02(2)$ Gs. The sample was prepared in such a way that the narrow line was more intense. The integrated intensities decreased with decreasing temperatures in both spectra in the high temperature range. This type of behavior was similar to that of magnetic nanoparticles in nonmagnetic matrixes. The resonance field of the broad line shifted to smaller magnetic fields upon lowering the temperature with gradient $\Delta H_r/\Delta T = 2.3(1)$ Gs/K, while the narrow line shifted towards higher magnetic fields with $\Delta H_r/\Delta T = 4.8(1)\cdot 10^{-3}$ Gs/K for the first sample and $\Delta H_r/\Delta T = 5.8(1)\cdot 10^{-3}$ Gs/K for the second sample. The linewidth of the broader line increased with the decreasing temperature while this change was only minor for the narrow line (especially at higher temperatures) in both samples. The magnetic iron oxide clusters produced an internal magnetic field which could act on free radicals and its strength depended essentially on the relative concentration of clusters. The resonance field position at different temperatures essentially depends on the presence of magnetic cluster and thus a stronger dependence was observed for the second sample. This could indicate that the reorientation process was more intense for the sample without magnetic clusters.

Photoacoustic Response of Common Starfish Tissue

N. Guskos[1a,2], J. Majszczyk[2], J. Typek[2], J. Rybicki[3], I. Kruk[2], A. Guskos[2], G. Żołnierkiewicz[2], C. Adinis[4]

[1] *Solid State Section, Department of Physics, University of Athens Panepistimiopolis, 15 784 Zografos, Athens, Greece*

[a] *ngouskos@phys.uoa.gr*

[2] *Institute of Physics, West Pomeranian University of Technology Al. Piastów 48, 70-311 Szczecin, Poland*

[3] *Department of Solid State Physics, Faculty of Technical Physics and Applied Mathematics Gdansk University of Technology Narutowicza 11/12, 80-233 Gdansk, Poland*

[4] *Applied Physics Section, Department of Physics, University of Athens Panepistimiopolis, 15 784 Zografos, Athens, Greece*

Samples of common starfish (*Asterias Rubens*) tissue were prepared in a thick film form to study the photoacoustic (PA) response. A broad absorption band in the visible range (a peak at about 570 nm) of the electromagnetic PA spectrum was registered while absorption bands from the $\pi \rightarrow \pi^*$, $\pi \rightarrow n$ charge transitions were detected in the ultraviolet range. The visible PA spectra strongly depended on the sample decomposition processes in air. The measured PA spectrum was very similar to the earlier obtained spectrum of another living organism, *Trunculariopis trunculus*. The absorption band near 570 nm was also similar to that obtained for spermidine which was important in the information transfer to DNA. The obtained results are significant as they confirm experimentally that very old living organisms absorb particularly intensely that part of the solar radiation for which water is transparent [1]. Solar radiation could also play an important role as an ignition agent in metabolic processes in the human body. The effect of solar specific radiation ranges filtered by the Earth atmosphere on diabetes patients is discussed and a possible role of transition metal complexes present in blood is considered.

References

[1] N. Guskos, J. Majszczyk, J. Typek, J. Rybicki, A. Guskos, I. Kruk, C. Aidinis, and G. Żołnierkiewicz, "Photoacoustic response of Sea Urchin tissue" (L08), *5th International Workshop on Functional and Nanostructured Materials*, 31 August – 6 September 2008, L'viv, Ukraine

Chemical Surface Deposition of CdS Thin Films from Aqueous Solutions

G. Il'chuk, V. Kusnezh, P. Shapowal, R. Petrus'

Physics department, L'viv Polytechnic National University
Bandera 12, 79013 L'viv, Ukraine

Cadmium sulfide (CdS) grown by chemical bath deposition (CBD) has been used extensively as a window layer in CdS/CdTe solar cells. To optimize the current density in heterojunction solar cells using CdS window layers it is required to minimize the CdS film thickness to reduce optical absorptive losses for photons at $\lambda \, ¡ \, 500$ nm. To ensure spatially uniform device operation, the CdS film must be continuous, dense, and robust to subsequent device processing.

The goal of our work was to obtain the best CdS thin film window material for CdTe based solar cells by the Chemical Surface Deposition (CSD). CDS of CdS large area thin films (from 30 to 100 nm) from aqueous solutions of $CdCl_2$, $CdSO_4$, CdI_2 salts at 70°C is described in this paper. The CSD technique overcomes the limitations of the classic CBD, using the sample surface as the heat source and utilizing the solution surface tension to minimize the applied liquid volume. Heterogeneous nucleation is favored over homogeneous precipitation by thermally-enhanced reactivity at the warmer growth surface, resulting in a high fraction of the cadmium product in the film and, depending on the substrate, the heteroepitaxial film growth. A combination of heat delivery at the surface with a low solution volume results in a high cadmium species utilization.

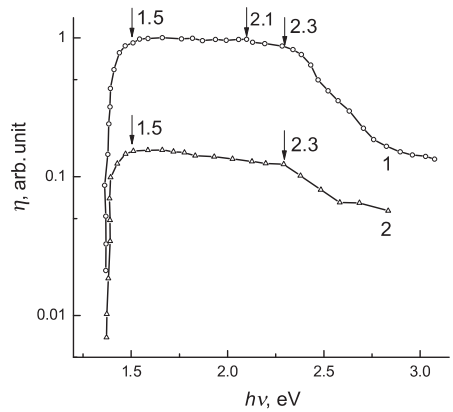

Figure 1: CdS thin films (100 nm) CSD from a $CdCl_2$ aqueous solution on a CdTe monocrystalline substrate

The CSD CdS thin films were amorphous, continuous, dense, and robust. Our results show that the use of CSD is an option to reduce the density of a pinhole and the adherent particulates. The surface morphology investigations show that CSD CdS films contain less than 10^7 adherent particulates per cm^2, compared to 10^9 for conventional CBD CdS films. Using the optical transmission data the band gap energy was calculated. The CdS film thickness was determined by ellipsometric measurements.

NdS/CdTe devices were fabricated using CSD NdS (100 nm) applied to pretreated monocrystalline p-CdTe. The high value of n-NdS/p-CdTe heterojunction photoconversion, in a region limited by NdS and CdTe band gaps, was provided, in our opinion, by the NdS deposition method. Thus, a possibility of fabricating n-NdS/p-CdTe high quality solar cells by CSD of NdS thin film is demonstrated.

Structure and Hyperfine Interactions of $Bi_9Ti_3Fe_5O_{27}$ Multiferroic Ceramic Prepared by Sintering and Mechanical Alloying Methods

M. Mazurek[1], E. Jartych[1], A. Lisińska-Czekaj[2], D. Czekaj[2], D. Oleszak[3]

[1] *Department of Experimental Physics, Institute of Physics, Technical University of Lublin Nadbystrzycka str. 38, 20-618 Lublin, Poland*

[2] *Department of Materials Science, University of Silesia Śnieżna str. 2, 41-200 Sosnowiec, Poland*

[3] *Faculty of Materials Science and Engineering, Warsaw University of Technology Wołoska str. 141, 02-507 Warsaw, Poland*

The $Bi_9Ti_3Fe_5O_{27}$ compound is one of the Aurivillius phase compounds from the $Bi_4Ti_3O_{12}$–$BiFeO_3$ system. Ferroelectric and antiferromagnetic properties in this material are combined, which makes this ceramic very attractive for applications in data processing and storage [1]. The structure, macroscopic magnetic and electric properties of the $Bi_9Ti_3Fe_5O_{27}$ compound are not well known. Moreover, the hyperfine interactions in this ceramic material have not been studied in sufficient detail yet.

In this work, X-ray diffraction (XRD) and Mössbauer spectroscopy (MS) were applied as complementary methods to investigate the $Bi_9Ti_3Fe_5O_{27}$ compound prepared by a solid-state sintering route and mechanical alloying. The crystalline structure of the sintered samples was examined using the Philips PW 3710 diffractometer with CoK_α radiation, while the mechanosynthesized samples were analyzed by the Philips PW 1830 diffractometer with CuK_α radiation. The MS studies were carried out at room temperature in standard transmission geometry using a source of ^{57}Co in a rhodium or chromium matrix. A 25-μm-thick metallic iron foil was taken as a standard for the spectrometer calibration.

As the XRD analysis proved, the compound formed a single phase at a sintering temperature above 993 K. In the case of mechanical alloying, after 50 hours of milling, the XRD patterns revealed an amorphous state with a small amount of a crystalline phase. The MS studies confirmed the diffraction measurements. The compound burnt at 993 K contained residual hematite, however, sintered at elevated temperatures was a single-phased material. The Mössbauer spectrum of a sintered $Bi_9Ti_3Fe_5O_{27}$ ceramic was a paramagnetic doublet suggesting that the Néel temperature, T_N, for this compound was smaller than room temperature, contrary to the estimation of $T_N > 300$ K in [2]. In the case of the mechanically alloyed sample, the MS spectrum consisted of a paramagnetic doublet originating from the desired $Bi_9Ti_3Fe_5O_{27}$ compound and a small amount of residual hematite. In both the sintered and mechanosynthesized samples, the paramagnetic component in the MS spectra was computer-fitted considering two ^{57}Fe – positions to be present. One of them was a tetrahedral site, i.e. in

the centre of the oxygen octahedron, where iron may substitute Ti atoms. The second one was an octahedral site, where iron may substitute Bi atoms in the corner of the cube.

References

[1] N. A. Lomanova, M. I. Morozov, V. L. Ugolkov, V. V. Gusarov, Inorganic Materials, 42(2) (2006) 189–195
[2] A. Srinivas, D. W. Kim, K. S. Hong, S. V. Suryanarayana, Mat. Res. Bull. 39 (2004) 55–61

EPR and IR Studies of Some Praseodymium(III) Tungstates

S. M. Kaczmarek[1], E. Tomaszewicz[2], A. Jasik[1]

[1] *Institute of Physics*
West Pomeranian University of Technology
Al. Piastów 17, 70-310 Szczecin, Poland

[2] *Department of Inorganic and Analytical Chemistry*
West Pomeranian University of Technology
Al. Piastów 42, 71-065 Szczecin, Poland

Trivalent metal molybdates and tungstates include a number of materials with interesting fluorescent, laser, piezoelectric, ferroelectric and ferroelastic properties. A special group are molybdates and tungstates of rare-earth metals for which a negative thermal expansion phenomenon of their network is observed.

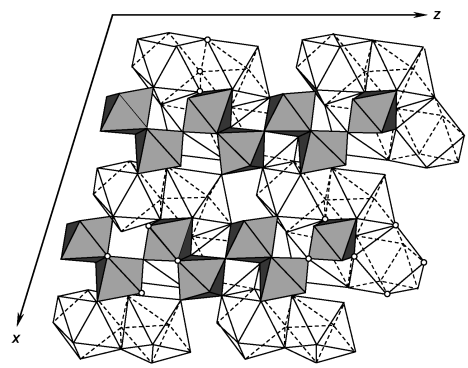

Figure 1: Structure of II-$Pr_2W_2O_9$: PrO_8 (ditrigonal prism) and PrO_9 (tritrigonal prism) were observed in the structure of II-$Pr_2W_2O_9$. The WO_6 octahedra connected by one common edge formed an endless, zigzag chain $[(W_2O_9)^{6-}]_\infty$

Praseodymium(III) tungstates $Pr_2W_2O_9$ and Pr_2WO_6 were synthesized by high-temperature solid-state reaction according to the following equations:

$$Pr_6O_{11(s)} + 6\ WO_{3(s)} = 3\ Pr_2W_2O_{9(s)} + O_{2(g)} \tag{1}$$

$$Pr_6O_{11(s)} + 3\ WO_{3(s)} = 3\ Pr_2WO_{6(s)} + O_{2(g)} \tag{2}$$

$Pr_2W_2O_9$ showed polymorphism. The low-temperature polymorphic modification (II-$Pr_2W_2O_9$) crystallized in the monoclinic system (S. G. $P2_1/c$; the lattice parameters were: $a = 0.770$ nm; $b = 0.984$ nm; $c = 0.927$ nm; $\beta = 106.5°$). The

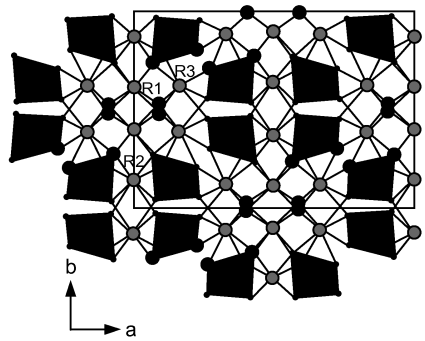

Figure 2: Structure of Pr_2WO_6: Pr_2WO_6 crystallized in the monoclinic system (S. G. $C2/c$). Deformed, isolated bipyramides WO_5 and deformed, nonequivalent PrO_8 cubes were observed in the structure of Pr_2WO_6

high-temperature modification (I-$Pr_2W_2O_9$) crystallized in the cubic system (a = 0.7105 nm).

The obtained compounds were characterized by EPR as well as by IR and DTA-TG methods.

Formation of Near-surface Inhomogeneity of Electromechanical Fields and Size Effect in Thin Dielectric Films

V. Kondrat, O. Hrytsyna

Center of Mathematical Modeling Institute of Apply Mathematic and Mechanics NAS of Ukraine, Dudajev str. 15, 79005, L'viv, Ukraine

A brief review of non-local theories of dielectrics which, in a model description, take into account the dependence of the body state on: the strain gradients [1]; the polarization gradient [2]; the electric field gradients or higher electric moments (quadrupoles, octupoles and so on) [3,4]; as well as the theories which predict constitutive relations of an integral type [5] are given in [6–9].

Recently, another non-local theory of nonferromagnetic dielectric bodies which takes into account the effect of local mass displacement has been proposed. The equations of such a non-local model with an account of the reversible process of the local displacement of mass are obtained in [10,11]. An irreversibility of the process of local mass displacement has been taken into account in [12] This allows us to study the process of formation of near-surface inhomogeneity of electromechanical fields due to the formation of new surfaces. The equations obtained above are used for studying the peculiarities of formation of near-surface inhomogeneity of mechanic and electric fields in a thin dielectric layer of constant thickness with traction-free surfaces. In particular, the dynamics of formation of the near-surface inhomogeneity of mechanical stresses, strains, polarization, electric potential as well as the surface electric charge is analyzed. The size effect of these quantities is studied. The value of the mechanical force acting along the layer of heterogeneous thickness (lateral force) is evaluated. The effect of the coupled mechanical and electric fields in the near-surface regions is analyzed.

References

[1] Kohan Sh 1963 *Phys. of Solids* **5** (10) 2829
[2] Mindlin R D 1968 *Int. J. Solids and Struct.* **4** 637
[3] Kafadar C B 1971 *Int. J. Engng. Sci.* **9** 831
[4] Yang X M, Hu Y T and Yang J S 2004 *Int. J. Solids and Struct.* **41** 6801
[5] Eringen A C 1984 *J. Math. Phys.* **25** (3) 717
[6] Maugin G A 1988 *Continuum Mechanics of Electromagnetic Solids*, Elsevier, 620
[7] Eringen A C 2002 *Nonlocal Continuum Field Theories*, Springer-Verlag, 376 p.
[8] Yang J 2006 *Appl. Mech. Rev.* **59** 335
[9] Kondrat V and Hrytsyna O 2009 *Phys.-Math. Model. and Inf. Technol.* **9** 7
[10] Burak Ya, Kondrat V and Hrytsyna O 2007 *Materials Science* **43** (4) 449
[11] Burak Ya, Kondrat V and Hrytsyna O 2008 *J. Mech. Mat. Struc.* **3** (6) 1037
[12] Hrytsyna O and Kondrat V 2007 *Phys.-Math. Model. and Inf. Technol.* **5** 42

Structure and Superconductivity of VN–SiO_2 Films Obtained by Thermal Nitridation of Sol-gel Derived Coatings

B. Kościelska[1], A. Winiarski[2], W. Jurga[3]

[1] *Faculty of Applied Physics and Mathematics, Gdansk University of Technology Narutowicza 11/12, 80-233 Gdansk, Poland*

[2] *A. Chełkowski Institute of Physics, University of Silesia Uniwersytecka 4, 40-007 Katowice, Poland*

[3] *Institute of Molecular Physics, Polish Academy of Science Smoluchowskiego 17, 60-179 Poznan, Poland*

Thin films of transition metal nitrides have attracted much attention as superconducting materials. The critical temperature (above 5 K) allows them to be used in several superconducting microelectronics applications. In this work, studies of structure and superconducting properties of xVN–$(100-x)SiO_2$ (where x = 90, 80, 70 and 6 mol %) are reported. The films were obtained through thermal nitridation (ammonolysis) of sol-gel derived V_2O_3–SiO_2 coatings at 1200°C. This process leads to a formation of a disordered structure with VN metallic grains dispersed in the insulating SiO_2 matrix. The structural transformations occurring in the films as a result of ammonolysis were studied using the X-ray diffraction (XRD) and X-ray photoelectron spectroscopy (XPS). The superconducting properties of the samples were examined with magnetically modulated microwave absorption (MMMA). All the samples exhibited a superconducting transition above 6 K.

Dynamics of Ethylene Glycol and Propylene Glycol Molecular Clusters Embedded in Carbon Nanotubes: Computer Simulation Study

M. Kośmider[1], S. Żurek[1], Z. Dendzik[2], K. Górny[2]

[1] *Institute of Physics, University of Zielona Góra*
Prof. Szafrana 4a, 65-516 Zielona Góra, Poland

[2] *Institute of Physics, University of Silesia*
Uniwersytecka 4, 40-007 Katowice, Poland

The dynamics of molecular clusters and molecular nanostructures has been widely studied during the last decades by theoretical, experimental and computer simulation techniques. The influence of finite size effects, surface effects and restricted geometry on the structure and dynamics of nanostructured systems is important in the scope of its potential applications and interesting from the fundamental point of view – for example glassy dynamics in nanoporous materials [1–3].

Molecules embedded in carbon nanotubes reveal interesting properties [4,5] and their potential importance in practical applications (chemical biosensors, nanoelectronic devices, field emission displays or energy storage) have been studied by many authors [6–8].

We performed fully atomistic molecular dynamics simulations of ethylene glycol and propylene glycol molecular clusters embedded in single-walled carbon nanotubes to study the confinement size effect on the dipolar relaxation of the clusters.

References

[1] Swenson J, Schwartz G A, Bergman R and Howells W S 2003 *Eur. Phys. J. E* **12** 179
[2] Schönhals A, Goering H, Schick Ch, Frick B ans Zorn R 2003 *Eur. Phys. J. E* **12** 173
[3] Erdem Ö F, Tsuwi J, Hong S B, Michel D 2006 *Microporous and Mesoporous Materials* **94** 261
[4] Kolesnikov I A, Zanotti J M, Loong C K, Thiyagarajan P, Moravsky A P, Loutfy R O and Burnham C J 2006 *Phys. Rev. Lett.* **93** 035503
[5] Zhao J, Buldum A, Han J and Lu J P 2002 *Nanotechnology* **13** 195
[6] Dillon A, Jones K, Bekkadahl T, Kiang C, Bethune D and Heben M 1997 *Nature* **386** 377
[7] Chen P, Wu X, Lin J and Tan K *Science* **285** 91
[8] Lu J and Han J 1998 *Int. J. High Speed Electron. Syst.* **9** 101

Numerical Approach to Cooling and Crystallization in Melt-spinning Process of $Fe_{40}Ni_{40}P_{14}B_6$ Alloy

S. A. Kostyrya[1], V. I. Tkatch[1], S. G. Rassolov[1],
K. W. Wojciechowski[2], B. Idzikowski[3a]

[1] *Donetsk Physics and Engineering Institute*
National Academy of Sciences of Ukraine
R. Luxemburg 72, 83114 Donetsk, Ukraine

[2] *PWSZ im. Prezydenta Stanisława Wojciechowskiego*
Nowy Świat 4, 62-800 Kalisz, Poland

[3] *Institute of Molecular Physics, Polish Academy of Sciences*
M. Smoluchowskiego 17, 60-179 Poznan, Poland

[a] *idzi@ifmpan.poznan.pl*

For applications, physical properties of metastable structures are often superior with respect to stable ones. Melt quenching techniques, among which the melt-spinning procedure is the most common one, are well developed laboratory and industry techniques producing materials with metastable structures. As the properties of metastable phases crucially depend on their structure, precise control of structure formation during rapid cooling is of prime importance. Unfortunately, rapid solidification occurs in very short periods of time and small volumes, what makes direct experimental studies very difficult. For this reason, numerical solutions of proper physical models constitute a very useful tool for prediction of the microstructure as a function of the melt composition and processing conditions.

The aim of this paper is to present a modified version of the model described earlier [1]. The computations were carried out for the well-known glass forming the $Fe_{40}Ni_{40}P_{14}B_6$ alloy, which was the subject of numerous studies, e.g. [2–5]. By using the experimentally determined input parameters controlling both the heat transfer and glass crystallization the model correctly predicted the conditions of the melt amorphization for the case of homogeneous nucleation.

References

[1] V. I. Tkatch, S. N. Denisenko, B. I. Selyakov (1995) *Acta Metallurg. Mater* **43** 2485–2491
[2] H. Miura, S. Isa (1984) *J. Non-Cryst. Sol.* 68 255–260
[3] V. I. Tkatch, S. N. Denisenko, O. N. Beloshov (1997) *Acta Mater.* 45 2821–2826
[4] V. I. Tkatch, A. I. Limanovskii, V. Y. Kameneva (1997) *J. Mater. Sci.* 32 5669–5677
[5] T. D. Shen, R. B. Schwartz (2001) *Acta Mater.* 49 837–847

Free Energy of Hard Multisphere Crystals

M. Kowalik, K. W. Wojciechowski

Institute of Molecular Physics, Polish Academy of Sciences
M. Smoluchowskiego 17, 60-179 Poznań, Poland

Free energy plays a very significant role in physics. It is sufficient to determine the stability and physical properties of any system. A simple [1,2] and precise [3,4] method for determining the free energy of model molecular solids has been proposed by Frenkel and Ladd. This method is used here to estimate free energies of a few selected structures of hard multispheres. The aim of the work is to search for thermodynamically stable phases, i.e. those of the lowest free energy, for simple multisphere molecular models.

The choice of hard-body systems deserves a comment since any hard interaction (zero when no overlaps occur in the system and infinity otherwise) seems, at least at the first look, to be a completely unphysical approximation of real interactions. However, hard-body systems are widely used in condensed matter physics. They serve as reference systems for liquids; allow for studying packing effects and short range correlations in condensed matter phases; and provide good insight into internal mechanisms of various physical phenomena. They prove that even complex phenomena such as phase transitions can have a purely *geometrical* origin [5–8].

References

[1] D. Frenkel and A. J. C. Ladd, *J. Chem. Phys. 81*, 3188 (1984)
[2] D. Frenkel and B. Smit, *Understanding molecular simulations*, Academic Press (1996)
[3] K. V. Tretiakov and K. W. Wojciechowski, *Phys. Rev. E 60*, 7626 (1999)
[4] J. M. Polson, E. Trizac, S. Pronk, and D. Frenkel, *J. Chem. Phys. 112*, 5339 (2000)
[5] B. J. Alder and T. E. Wainwright, *J. Chem. Phys. 27*, 1208 (1957)
[6] D. Frenkel, B. M. Mulder, and J. P. McTague, *Phys. Rev. Lett. 52*, 287 (1984)
[7] K. W. Wojciechowski, D. Frenkel and A. C. Brańka, *Phys. Rev. Lett. 66*, 3168 (1991)
[8] J. A. van Meel, D. Frenkel, and P. Charbonneau, *Phys. Rev. E 79*, 030201 (2009)

Band Structure for Fe-based and Ruthenate Superconductors

S. P. Kruchinin[1], A. Zolotovsky[2], J. Dow[3]

[1] *Bogolyubov Institute for Theoretical Physics, NASU*
Kiev, 03143, Ukraine

[2] *Lashkaryov Institute of Semiconductor Physics*
Kiev, Ukraine

[3] *Department of Physics, Arizona State University*
USA

We investigated the band structure of Fe-based and ruthenate superconductors using the first-principle methods. The ferrugate of LaOFeAs and doped Sr_2YRuO_6 showed superconductivity at the temperatures as high as 45 K and 49 K, respectively.

Both superconductors have a complicated multiband structure.

We underline the importance of the zone structure near the Fermi level. The band structure and density of states around the Fermi level suggest the LaOFeAS superconductors have semimetal-like characteristics. We discuss the many-band effect in these superconductors.

Photoluminescence of Nanostructured $Pb_{1-x}Cd_xSe$ ($x = 0$–0.20) Layers

D. B. Chesnokova, V. A. Moshnikov[b], A. E. Gamarts, O. A. Aleksandrova, V. V. Kuznetsov[a]

St. Petersburg State Electrotechnical University, Russia

[a] *vvkuznetsov@inbox.ru,* [b] *vamoshnikov@mail.ru*

The $Pb_{1-x}Cd_xSe$ ($x = 0$–0.20) alloys are perspective semiconductor materials for fabrication of 3–5 μm spectral range IR-emitters and photodetectors operating at room temperature.

The models of photoconductivity and methods of $Pb_{1-x}Cd_xSe$ layers formation including deposition and thermal activation have been discussed by many authors. Nevertheless, the physics of $Pb_{1-x}Cd_xSe$ layers photoluminescence at room temperature and the mechanisms of radiative recombination remain studied insufficiently. The purpose of this work is to determine the correlation between the fabrication conditions and elemental chemical and phase composition, microstructure and photoluminescence properties of $Pb_{1-x}Cd_xSe$ layers ($x = 0$–0.20).

Polycrystalline layers were deposited by thermal vacuum evaporation of preliminary synthesized charge $Pb_{1-x}Cd_xSe$ alloys on glass substrates. In order to obtain photoluminescence the samples were thermally activated by annealing in the temperature range of 523–873 K in an oxygen-containing atmosphere in the presence of iodine vapors. The annealing temperature and the vapor atmosphere composition were precisely controlled. The microstructure, elemental chemical and phase composition of the fabricated layers were investigated with use of local physical methods, e.g. scanning electron microscopy (SEM), atomic force microscopy (AFM), scanning tunneling microscopy (STM), X-ray diffraction analysis, optical microscopy and Auger-spectroscopy The electrophysical properties of the samples were investigated by Hall-measurements, the thermal probe method and IR- spectroscopy methods. The photoluminescence properties were studied under the optical excitation by a GaAs light-emitting diode. A PbSe-based photoresistor was used as a photodetector.

The layers had a polycrystalline column structure after deposition. The crystalline grains of [100] orientation had a mean transverse size of 300 nm. The layers were monophase, their composition corresponded to the composition of the preliminary synthesized charge. During heat treatment in the presence of iodine vapors and oxygen a fast recrystallization of the layers and formation of heterophase samples were observed. After annealing, new phases of Pb and Cd oxides and iodides were formed on the layer surface and on the side walls of grains. The $Pb_{1-x}Cd_xSe$ alloy nanocrystals had a round form. The size of nanocrystals did not exceed 50–100 nm. The structure reorganization occurred in the presence of a liquid phase containing Pb and Cd iodides. Such conditions of recrystallization led to a reduction in the concentration of radiationless recombination centers and to oxygen saturation of $Pb_{1-x}Cd_xSe$ grains.

It was noticed that composition x of the $Pb_{1-x}Cd_xSe$ layers after thermal treatment decreased in comparison to the initial value. The photoluminescence spectrum shifted in the direction of longer wavelengths. This corresponded to the $Pb_{1-x}Cd_xSe$ alloys with a lower Cd content in comparison to the initial composition x. The decreasing Cd content in the $Pb_{1-x}Cd_xSe$ alloys ($x = 0.4$–0.20) during the heat treatment may be explained by a decomposition of the supersaturated solid solution and a retrograde **solidus** curve on the T-x diagram PbSe–CdSe. The influence of the heat treatment conditions (temperature, time, iodine vapors pressure, cooling rate) on the decomposition of the supersaturated solid solution was also studied. It was discovered that the decomposition of a solid solution inside grains led to a formation of graded-gap structures which were characterized by a gradient of composition x, and accordingly a band gap gradient. The formation of a graded-gap structure was confirmed by the AFM data and by the expansion of photoluminescence spectra and X-ray diffraction lines.

A numerical simulation of the photoluminescence spectrum with respect to various mechanisms of radiative recombination showed that radiative recombination in samples was mostly determined by the direct band-to-band transitions and transitions to a deep acceptor (oxygen) level. The significant increase in the photoluminescence intensity may be explained by the formation of a graded-gap structure in the nanocrystalline grains.

Electronic Structure of Defects in $Sr_2MgSi_2O_7:Eu^{2+},R^{3+}$ Persistent Luminescence Materials

J. Hassinen[1], J. Hölsä[1,2], T. Laamanen[1a,3], M. Lastusaari[1,2], P. Novák[4]

[1] *University of Turku, Department of Chemistry FI-20014 Turku, Finland*

[a] *taanla@utu.fi*

[2] *Turku University Centre for Materials and Surfaces (MatSurf) Turku, Finland*

[3] *Graduate School of Materials Research (GSMR) Turku, Finland*

[4] *Academy of Sciences of the Czech Republic, Institute of Physics CZ-16253 Prague 6, Czech Republic*

Eu^{2+} doped alkaline earth magnesium disilicates ($M_2MgSi_2O_7:Eu^{2+},R^{3+}$; M = Ca, Sr, Ba; R = Nd, Dy, Tm) show persistent luminescence for up to 24 hours [1,2]. The proposed persistent luminescence mechanisms (*e.g.* [3,4]) have not yet been thoroughly proven since essential experimental data is missing or contradictory. The connection between the host electronic band structure as well as the energy levels of intrinsic lattice defects (vacancies, interstitials *etc.*) and the rare earth (co-)dopants need to be clarified.

The energy positions of the strontium and oxygen vacancies in the host band structure of distrontium magnesium disilicate ($Sr_2MgSi_2O_7$) were studied with density functional theory (DFT) calculations employing the WIEN2k package [5]. The trap level structure of $Sr_2MgSi_2O_7:Eu^{2+},R^{3+}$ (R = none, Y, La–Lu excl. Pm) was also investigated with thermoluminescence (TL) measurements.

The Sr vacancy states were located very close to the top of the valence band corresponding to shallow hole traps. Oxygen vacancy states were located close to the bottom of the conduction band (CB) with the lowest-lying states at *ca.* 1.4 eV below CB. The O vacancy states correspond to electron traps which can be quenched by thermal energy. Additional O vacancy states were found deep in the energy gap (*ca.* 5 eV below CB) of the host. However, electrons in the deep traps cannot participate in creating persistent luminescence due to the high amount of energy required to bleach the traps.

The TL glow curves of $Sr_2MgSi_2O_7:Eu^{2+},R^{3+}$ are characterized by a strong band centered at 80–90° (corresponding trap depths 0.6–0.8 eV). This band is in the range ideal for persistent luminescence and can be considered intrinsic, common for the $Sr_2MgSi_2O_7:Eu^{2+}$ host. Extrinsic high temperature bands at 100–200° (trap depths

0.9–1.3 eV) appear with the introduction of the R^{3+} co-dopant. The requirement of strong luminescence combined with good energy storage properties at room temperature due to shallow and deep traps, respectively, is very well met with *e.g.* the Eu^{2+}, Dy^{3+} co-doping. The modification of the trap structure due to the defect aggregates has to be studied in detail experimentally and using DFT calculations since the thermally controlled mechanism is sensitive even to slight changes in the defect structure.

References

[1] Jiang L, Chang C, Mao D 2003 *J. Alloys Compd.* **360** 193
[2] Lin Y, Tang Z, Zhang Z, Wang X, Zhang J 2001 *J. Mater. Sci. Lett.* **20** 1505
[3] Dorenbos P 2005 *J. Electrochem. Soc.* **152** H107
[4] Aitasalo T, Hölsä J, Jungner H, Lastusaari M, Niittykoski J 2006 *J. Phys. Chem. B* **110** 4589
[5] Blaha P, Schwarz K, Madsen G K H, Kvasnicka D, Luitz J, In: Schwarz K (Ed.) 2001 *WIEN2k, An Augmented Plane Wave + Local Orbitals Program for Calculating Crystal Properties, User's Guide*, Vienna University of Technology, Austria

Effect of Promotors on Structure and Thermostability of Nanocrystalline Cobalt Catalyst for Ammonia Synthesis

Z. Lendzion-Bieluń[a], W. Arabczyk, U. Narkiewicz

West Pomeranian University of Technology
Institute of Chemical and Environment Engineering
Pulaskiego 10, 70-322 Szczecin, Poland

[a] *zosi@ps.pl*

Nanocrystalline cobalt was prepared by wet hydroxide precipitation followed by calcination (200°C/2 h, air) and reduction. $Co(OH)_2$ was precipitated using an ammonia aqueous solution at pH = 8. Promotors were introduced into the Co_3O_4 during precipitation. The samples were characterized by the TPR, XRD, OES-ICP and MDC methods.

In this work the effects of NH_4OH dosing, the stirring rate and additions of promotors (aluminum and manganese oxides) were determined for:

– the Co_3O_4 reduction rate;

– the average size of crystallites and the cobalt specific surface area;

– the cobalt thermostability in reduction atmosphere.

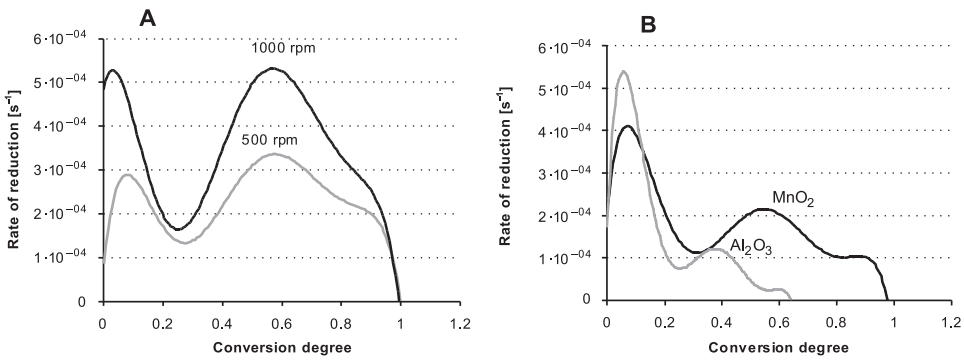

Figure 1: **A** – Influence of the stirring rate on the Co_3O_4 reduction; **B** – the effect of promotors on the Co_3O_4 reduction process. Reduction conditions: temperature 240°C, flow rate 20 dm^3H_2/min

The dosing rate of the precipitation agent, at 500 rpm, did not affect the crystallite size and the specific area of cobalt which was obtained by the cobalt oxide reduction. The average size of cobalt crystallites after isothermal reduction at 240°C was 38 nm and the specific surface area was 5 m^2/g. It was observed that an increase in the stirring rate to 1000 rpm with an increase in the NH_4OH dosing rate caused an increase in the average size of the cobalt crystallites and a decrease in the specific surface area. The reduction rate of the cobalt oxide obtained at 500 rpm was slower than that for the cobalt oxide obtained at 1000 rpm, Figure 1A. It suggested a greater crystallite size of Co_3O_4. The reduction in the cobalt oxide proceeded in two stages. At the first CoO was formed then it was reduced to metallic cobalt. There were the characteristic minima observed on the reduction rate curves which could be ascribed to the end of the first stage of reduction. The slowest stage was the reaction on the surface of cobalt(II) oxide crystallites.

The reduction process of an aluminum promoted cobalt catalyst was significantly slower, Figure 1B. The reduction at 240°C was not completed. The molar ratio of the unreduced cobalt oxide and aluminium oxide (CoO/Al_2O_3) was 15. The manganese addition resulted in a slower second stage of the Co_3O_4 reduction. The alumina increased the thermostability of the cobalt catalyst.

Re-investigations of Thermal Decomposition of Gadolinium Sulfate Octahydrate

E. Tomaszewicz[1], S. M. Kaczmarek[2a], G. Leniec[2]

[1] *Department of Inorganic and Analytical Chemistry, Pomerania University of Technology Al. Piastów 42, 71-065 Szczecin, Poland*

[2] *Institute of Physics, Pomerania University of Technology, Al. Piastów 17, 70-310 Szczecin, Poland*

[a] *skaczmarek@ps.pl*

Gadolinium sulfate octahydrate crystallizes in a monoclinic system with space group C2/c and the lattice constants: $a = 1.3531(7)$, $b = 0.6739(2)$, $c = 1.8294(7)$ nm, $\beta = 102.20(8)^\circ$ [1]. In the structure of this compound, Gd ions are coordinated by 4 oxygen ions of crystal water and 4 oxygen ions of sulfate groups giving rise to distorted square antyprisms [1]. The luminescence of Pr^{3+} doped gadolinium sulfate hydrates and both polymorphic modifications of anhydrous $Gd_2(SO_4)_3$ was reported under 195 nm laser excitation [2].

In our studies the crystals of $Gd_2(SO_4)_3 \cdot 8H_2O$ were obtained by slow crystallization from a saturated solution previously received by dissolving Gd_2O_3 in an aqueous solution of sulfuric acid. The obtained gadolinium sulfate octahydrate crystals were dried in acetone, grounded and tested by the DTA-TG (air and nitrogen atmosphere) and XRD methods. On the base of the DTA-TG tests a mechanism of $Gd_2(SO_4)_3 \cdot 8H_2O$ dehydration and a mechanism of decomposition of anhydrous gadolinium sulfate were confirmed [1,3]. During the heating of gadolinium sulfate octahydrate in 500°C and 800°C for 8 hrs both polymorphic modification of $Gd_2(SO_4)_3$ were obtained. It was found that the number and positions of the diffraction lines recorded on the diffraction patterns of low- and high-temperature polymorphic modification of $Gd_2(SO_4)_3$ were very different in comparison to the data reported by other authors [1,3]. The products of $Gd_2(SO_4)_3 \cdot 8H_2O$ dehydration, amorphous gadolinium sulfate, both polymorphs of $Gd_2(SO_4)_3$ as well as the intermediate and final solid product of the anhydrous gadolinium sulfate thermal decomposition were examined by the XRD, IR and EPR methods.

References

[1] H. U. Hummel, E. Fischer, T. Fischer, P. Joerg, G. Pezzei, *Z. Anorg. Allg. Chem.*, 619 (1993) 805
[2] E. Bayer, J. Leppert, B. C.Grabmaier, G. Blasse, *App. Phys. A*, 61 (1995) 177
[3] A. Saito, *Thermochim. Acta*, 124 (1988) 217

Epitaxial Growth of GaSb-based Nanoheterostructures by MOCVD

D. A. Kudryashov[1], R. V. Levin[1a], V. I. Ratushnyi[2], L. S. Lunin[2], V. V. Kuznetsov[3], B. V. Pushnyi[1], V. M. Andreev[1]

[1] *Ioffe Physical Technical Institute*
St Petersburg 194021, Russian Federation

[a] *Lev@vpegroup.ioffe.ru*

[2] *South-Russian State Technical University*
Novocherkassk, 346400, Russian Federation

[3] *Saint Petersburg Electrotechnical University*
St Petersburg, 197376, Russian Federation

$A^{III}B^{V}$ compounds containing Sb, lattice matched with GaSb or InAs, are of great interest for the manufacture of a wide range of optoelectronic devices. The GaSb-based devices can be used in thermophotoelectric converters and highly efficient mechanical photovoltaic stack solar cells (as a high-performance infrared spectrum converter). Today, the primary production method of devices based on $A^{III}B^{V}$ structures on an industrial scale is the MOCVD epitaxy.

In this paper, growth processes were performed at a AIX200 low pressure horizontal MOCVD reactor. The growth temperature was 600°C. Triethylgallium (TEGa), trimethylaluminum (TMAl), trimethylantimony (TMSb) and arsine (AsH_3) were used as precursor materials.

The growth regime was discovered and optimized (growth temperature, V/III ratio and reactor pressure); the charge carrier concentrations, the base and emitter layers thickness were fitted; the technological growing process of multilayer structures with a pn-junction was developed; the composition of quaternary solid solutions was proved and developed the growth process of thin (up to 0.1 microns) quaternary solid solutions $Al_{1-x}Ga_{1-x}As_ySb_{1-y}$. The latter are used as restriction and barrier layers in the photocell.

As a result, the laboratory GaSb-based heat photoconverters were made with the following characteristics: open-circuit voltage $U_{oc} = 0.4$–0.49 V, fill factor FF = 0.66–0.71 with photocurrent density $J = 1$–10 A/cm^2 for samples 3.5×3.5 mm in size.

Adding an upper 100 nm wide band-gap $Al_{1-x}Ga_{1-x}As_ySb_{1-y}$ nanolayer in thermophotovoltaic structures (depending on the composition of 5 to 10%) resulted in increasing the spectral photoresponse.

Transport Properties of $M_2InV_3O_{11}$ (M(II) = Zn(II) and Co(II)) Compounds

N. Guskos[1,2], V. Likodimos[3], S. Glenis[1], K. Karkas[1], G. Żołnierkiewicz[2], M. Bosacka[4]

[1] *Department of Physics, University of Athens Panepistimiopolis, 15 784 Zografos, Athens, Greece*

[2] *Institute of Physics, Szczecin University of Technology Al. Piastów 17, 70-310 Szczecin, Poland*

[3] *NCSR "Demokritos", Inst. Phys. Chem, Athens 15310, Greece*

[4] *Department of Inorganic and Analytical Chemistry, Szczecin University of Technology, Al. Piastów 17, 70 -310 Szczecin, Poland*

The transport properties of a new (M(II) = Zn(II) and Co(II)) vanadate oxide were investigated by electrical conductivity measurements. Both compounds exhibited semiconducting behavior. The replacement of non-magnetic Zn(II) cations with

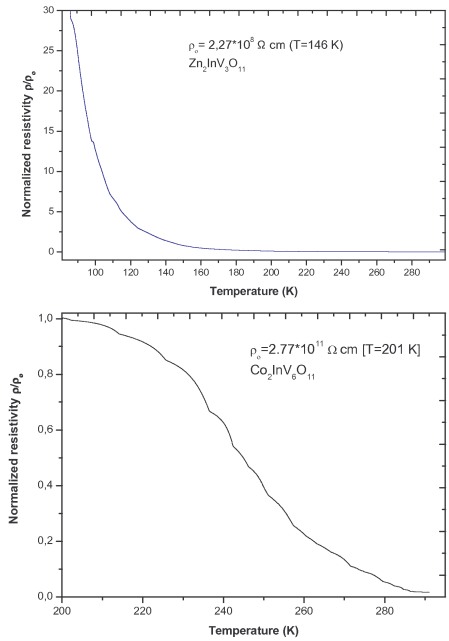

Figure 1: Normalized temperature dependence of resistivity for vanadate oxides, top: $Zn_2InV_3O_{11}$ and bottom: $Co_2InV_3O_{11}$

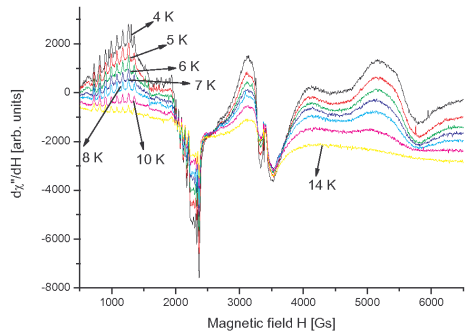

Figure 2: EPR spectra of the $Co_2InV_3O_{11}$ compound

magnetic Co(II) ions resulted in a significant drop in the electrical conductivity by over four times and a variation in the activation energy (Figure 1). The activation energies were determined to be $E_g = 0.43(3)$ eV at $T < 180$ K and $E_g = 0.18$ eV at $T > 200$ K for $Zn_2InV_3O_{11}$, in contrast to $E_g = 0.35$ eV derived at high temperatures for $Co_2InV_3O_{11}$. The EPR spectroscopy showed the presence of trivalent vanadate ions for both compounds, while the presence of divalent cobalt ions was identified at low temperatures for the $Co_2InV_3O_{11}$ oxide (Figure 2).

XAFS Study of Ru 4*d* Orbital Occupation in Ruddlesden-Popper Strontium Ruthenates $Sr_{n+1}Ru_nO_{3n+1}$ ($n = 1, 2, 3$): Influence of Lattice Distortions on Electronic Structure

M. Malvestuto

Sincrotrone Trieste
Strada Statale 14 - km 163,5 in AREA Science Park, 34149 Trieste, Italy

The polarization-dependent XANES study results of the electronic and local atomic structures of the Ruddelsden-Popper (RP) layered strontium ruthenate series, $Sr_{n+1}Ru_nO_{3n+1}$ are reported.

Ruthenium oxides are a particularly interesting class of materials exhibiting fascinating physical properties like unconventional superconductivity, ferromagnetism and metamagnetism, antiferromagnetic insulating behavior, and orbital ordering, resulting from the intimate interplay between charge, spin, orbital, and lattice degrees of freedom.

In particular, the $Sr_{n+1}Ru_nO_{3n+1}$ layered system has become a prototype for exploring intriguing physical phenomena due to a subtle interplay between structural anisotropy and distortions, multi-band effects and magnetic fluctuations. In fact, despite the fact that $Sr_{n+1}Ru_nO_{3n+1}$ compounds are all based on Ru^{4+} ions, octahedrally coordinated by oxygen atoms, with electronically inactive Sr-site counter-ions, they show a rich variety of magnetic and electronic states with experimental signatures of strong coupling to the lattice distortions driven by the number n of perovskite RuO_6 layers in the unit cell.

Oxygen K-edge XAS spectroscopy has a proven ability to shed light on the site symmetry and the occupation of empty states hybridized with O 2*p* orbitals and has been successfully employed in 3*d* correlated transition metal oxides such as cuprates, manganites and cobaltates.

By comparing the polarization-dependent O K-edge XANES data with the complementary structural information provided by the X-ray diffraction study, it is shown how the unoccupied DOS resulting from the hybridization of O 2*p* – Ru 3*d* and O 2*p* – Sr 3*d* are affected by the rotations and tilting of the RuO_6 octahedra. The results on the O K-edge XANES spectra and partial density of states simulated by means of the Full Multiple Scattering theory and directly compared with the experimental data are also presented.

Hierarchical Nanostructured Porous Semiconductors for Gas Sensors

V. A. Moshnikov[a], I. E. Gracheva, V. V. Kuznetsov, A. I. Maximov, S. S. Karpova, A. A. Ponamoreva

Saint-Petersburg State Electrotechnical University "LETI"

[a] *vamoshnikov@mail.ru*

In recent years, nanotechnology has emerged as an attractive field for the development of novel materials with unusual properties and has provided different pathways to make issues in various fields. Nanostructured materials attract attention of many researches because of the possibility to apply them for near future devices and sensors. The gas sensitive composites based on tin dioxide are a perspective for sensors. This kind of sensors may be used in ecological monitoring of the environment, for indicators of gas discovery in mines; for poisonous gas leakage control, etc.

The sol-gel method ("bottom-up" chemical technique) is used in the sensor semiconductor technology, due to a possible formation of composites containing a certain morphology and nanoparticles. The sol-gel technology [1,2] is applied to nanotechnology, ensuring a formation of functional nanostructures beginning from the molecular level. The sol-gel transition is a phenomenon which strongly depends on the network connectivity. In the case of a virtually irreversible chemical sol-gel transition in a solution, a constant increase in the degree of polymerization of individual clusters contributes to an increase in the solution viscosity only gradually in an earlier stage of polymerization. The continued growth of clusters, however, reaches a point where the first single connection across the system dimension is formed. Around this point, typically denoted as the sol–gel transition point, a steep increase in and a divergence of viscosity is observed, and, in parallel, the system turns from a viscous fluid to an elastic solid. Due to continued polymerization reactions within a loosely connected network, the network density gradually increases to arrest motions of constituents in increasingly finer dimensions [3].

The sol-gel process is complicated because each stage of the synthesis depends on the previous one and many parameters are involved. The variation of parameters such as the alkoxide molar ratio, pH, temperature, solvent leads to a formation of different polymeric structures. It is shown that atomic force microscopy (AFM) can be used as an effective method for analysis of the formation and evolution of a fractal system, preparing by the sol-gel method, and also for research of the structure transition from fractal aggregates to percolating clusters. The advantage of AFM is a direct observation of fractal structures in contrast to the indirect small angle X-ray scattering method [4]. It was shown that the evolution of fractal aggregates based on tin dioxide could be controlled by thermodynamic and kinetic conditions of the sol-gel synthesis. It was found that fundamental steps of evolution of this fractal system based on tin

dioxide were as follows: diffusion-limit aggregation, cluster-cluster aggregation, formation of percolating transition and formation of a nanostructured network. A model of the formation mechanism for nanostructured semiconductor networks with a hierarchical structure (several levels of pores the sizes of which were determined by evolution of fractal aggregates in sol-gel processes and the spinodal conditions) was proposed. Two mechanisms of phase-separation (nucleational and spinodal) were revealed.

In this paper, the gas-sensitivity of hierarchical nanostructured compositions based on tin dioxide, synthesized by sol-gel method was investigated. A laboratory bench was used for the gas-sensitivity measuring. Short-term (several seconds) anomalous changes in the resistances of semiconductor films (at the moments when the gas–reagent impulse is supplied and terminates) were put on the basis of new diagnostic methods, analyzing the homogeneity of percolating nanobranches. In addition, this diagnostic principle can be used for tree-dimensional nanostructures synthesized by the sol-gel method. These tree-dimensional nanostructures are of interest for creation of new generation sensors, which selectively determine the gas environment compound.

Sensor nanostructures were investigated by impedance spectroscopy at 300–400°C and at various gas environment and gas-reagents detection temperatures. The presence of one or two maximums was detected at the frequency dependences of an imaginary part versus the effective dielectric permittivity in air and in the presence of gas-reagents, respectively. Possibilities management of the admittance of a nanosensor system were shown, and these possibilities open new perspectives for developing of sensitivity and selectivity for such multisensor systems as the «electron nose».

References

[1] Brinker C. J., Scherer G. W. Sol-Gel Science. The Physics and Chemistry of Sol-Gel Processing. San Diego: Academic Press, 1990, p. 908
[2] Maximov A. I., Moshnikov V. A., Tairov Yu. M., Shilova O. A. Basics of sol-gel technology of nanocomposites. Second issue. "Tehnomedia". SPb.: "Elmor", 2008, p. 255
[3] Nakaishi K. Sol-gel process of oxides accompanied by phase separation. Bull. Chem. Soc. Jpn. V. 79, N. 5 (2006), pp. 673–691
[4] Hyeon-Lee J., Beaucage G, Pratsinis S. E., Vemury S. Fractal analysis of flame-synthesized nanostructured silica and titania powders using small-angle x-ray scattering. Landmuir. V. 14, N 20 (1998), pp. 5751–5756
[5] A Computer-Aided Setup for Gas-Sensing Measurements of Sensors Based on Semiconductor Nanocomposites. Instruments and Experimental Techniques. V. 51, N. 3 (2008), pp. 462–465

Self-Organized Porous Structure with Several Levels of Pores in Electrochemical Anodized Silicon

Y. M. Spivak, V. A. Moshnikov[a], V. V. Kuznetsov, A. Yu. Savenko, N. E. Preobrajensky, P. G. Travkin

Saint-Petersburg State Electrotechnical University «LETI»
Russian Federation

[a] *vamoshnikov@mail.ru*

Nowadays nanostructured materials are in focus of extremely high interest because of wide possibilities of receiving materials with brand new properties. Porous materials today form an independent line of inquiry of functional materials for modern solid state electronics. Porous silicon is very important as a functional material for alternative energy (solar cells, various types of sensors, photonics, medicine) applications, etc. [1,2]. Nanotechnology today includes not only advanced sintering techniques for nanomaterials, but also well known technologies such as the electrochemical group of methods. Electrochemical deposition could be classified as a "bottom-up" nanotechnology, and electrochemical etching as a "top-down" nanotechnology. The advantages of these methods are low cost, room temperatures of processes, a possibility of integration with the silicon microelectronics technology, a wide variety of structures for the same materials.

Porous silicon is a unique material with a 3D-porous structure. Two different concepts to produce porous silicon with the desired structures may be highlighted. The first way is used mostly to obtain a highly ordered porous structure which may be classified as macroporous silicon (by IUPAC). In this step of surface preparation – the template creation (by photolithography, microstamping, etc.) has to be included before electrochemical anodization of silicon. This type of por-Si is employed in photonics, optics, microcavity structures, microreactors, membranes, as templates, etc. Another way is based on self-organised processes taking place during the electrochemical treatment of the silicon surface. By this way meso-, nanoporous silicon and por-Si with a complicated hierarchical structure (several types of pores) could be obtained [3]. These types of por-Si are very important for sensors, photoemitters, waveguides, in catalysis, MEMS, medicine, etc. It is also porous silicon and pitted silicon that should be distinguished. The following may be used as a criterion for porous silicon: porous silicon should contain two continued systems: a system of a silicon skeleton and a system of connected pores.

Samples of porous silicon were obtained by electrochemical anodization of monocrystalline silicon in HF solutions with the Unno-Imai approach. Monocrystalline silicon of different types (n- and p-type electroconductivity with a various doping level, various crystallographic orientations) was used as a substrate. It should be noted that por-Si n-type electroconductivity in this work were obtained without UV-illumination.

Electrochemical treatment was provided in several steps by varying technological parameters to receive porous silicon with a special structure. The por-Si samples obtained in such a way were characterized by different porosity, pore sizes (from 15 nm to 400 nm in different conditions) and shapes, porous structure type, surface morphology.

The surface morphology peculiarities were studied by atomic force microscopy (Ntegra Terma, NT-MDT) and FIB-imaging (STRATA FIB 205, FEI) [4]. The chemical composition was studied by IR spectroscopy. The XPS and USXES methods were used to investigate the distribution of the chemical phases depth profile. It was shown by Raman spectroscopy that the porous silicon was stressed. Different types of porous silicon structures were observed. One type (both for n-por-Si and p-por-Si with a low dopant level) showed a strong dependence on the crystallographic orientation, the pores were shaped according to the direction of propagation in crystal. In this case the silicon skeleton maintained a crystalline structure. An intricate porous structure with two types of pores was also formed in p-por-Si (100) [5]: the main pore channels propagated normally to the sample surface (with pore sizes of 130–400 nm in various conditions of treatment); and also smaller, secondary pores were directed perpendicular to main pores. Secondary pores could be characterized by a 15–40 nm diameter and formed an interconnected system. The fractal self-similar structure of a porous material could be presumed. Self-organized ordered por-Si obtained in certain conditions were also observed and showed a very narrow distribution of pore sizes on the surface. It is likely that the skeleton branches in this type of por-Si consist of recrystallized silicon and products of chemical reactions.

References

[1] Foll H., Christophersen M., Carstensen J., Hasse G. Formation and application of porous silicon / Materials Science and Engineering R 39 (2002) 93–141

[2] Starkov V., Gavrilin E., Vyatkin A., etc. Transition from quasi-hexagonal to quasi-one dimensional pores distribution during deep anodic etching of uniaxialle stressed silicon plate / Proc. SPIE Micro- and Nanoelectronics 2003; Vol. 5401, pp. 225–234, Eds. May 2004

[3] Zimin S. P., Gorlachev E. S., Kanageeva Yu. M., Savenko A. Yu., Luchinin V. V., Moshnikov V. A. Structural and Electrical Parameters of Porous Silicon with Intricate Morphology / V International Conference «Amorphous and microcrystalline semiconductors», Saint-Petersburg, 19–21 of June 2006, Saint-Petersburg, 2006, pp. 226–227

[4] Канагеева Ю. М., Савенко А. Ю., Лучинин В. В., Мошников В. А., Зимин С. П., Бучин Э. Ю. Изучение структурно-морфологических особенностей макропористого кремния при препарировании образцов остросфокусированным ионным пучком / Петербургский журнал электроники, № 1, 2007, с. 35

[5] Канагеева Ю. М., Бучин Э. Ю., Зимин С. П., Лучинин В. В., Максимов А. И., Мошников В. А., Савенко А. Ю. Изучение особенностей образования структуры пористого кремния / XXI Российская конференция по электронной микроскопии, г.Черноголовка, 6–9 июня 2006 г., Москва, 2006

Low Temperature Liquid Phase Epitaxy of Zn-Cd-Te System

P. Moskvin[1a], E. Avramchuk[1], L. Rashkovetskyi[2], G. Olchowik[3], J. M. Olchowik[4b], A. Zdyb[4], W. Sadowski[5]

[1] *Zhytomyr State Technological University*
103 Chernyakhovsky str., Zhytomyr, 10005, Ukraine

[a] *moskvin@us.ztu.edu.ua*

[2] *V. Lashkaryov Institute of Semiconductor Physics*
41 Prospect Nauki, Kiev, 03028, Ukraine

[3] *Medical University of Lublin*
Jaczewskiego 4, 20-090 Lublin, Poland

[4] *Institute of Physics, Lublin University of Technology*
Nadbystrzycka 38D, Lublin 20-618, Poland

[b] *j.olchowik@pollub.pl*

[5] *Technical University of Gdansk*
G. Narutowicza 11/12, 80-233 Gdansk, Poland

$Zn_xCd_{1-x}Te$ solid solutions can be applied as buffer layers when producing highly effective heterostructures with a $Cd_xHg_{1-x}Te$ active layer by LPE for IR techniques. $Zn_xCd_{1-x}Te$ layers can be independently applied as ionizing and X-ray radiation detectors.

The creation process of multilayer structures of such type becomes easier if every subsequent layer of the solid solution is formed at the same temperature. This kind of a low temperature process of a buffer layer forming from a $Zn_xCd_{1-x}Te$ solution demands that the synthesis conditions are set in a precise way. It is difficult to determine those conditions without a thermodynamic analysis.

The performance of an epitaxial process at low temperatures and a low solubility of components in a liquid phase together with a high growth rate of layers demands obtaining high mass stream values in the growth boundary direction. In case of significant differences in the solubility of each liquid phase component, the solution becomes saturated enough for one component and the forming of the other component flux becomes possible when its relative partial saturation is also important. This kind of situation is observed in a Zn-Cd-Te system for a synthesis at temperatures below 650°C.

In this work a kinetic-diffusive model is proposed to describe the presented issue. The kinetic-diffusive model of system crystallization is based on the assumption that the layer growth rate is determined by mass transport in the interfacial boundary direction when the concentrations of components correspond to interfacial equilibrium conditions on the growth surface. The solution of the isothermic diffusion equation

together with phase equilibrium equations makes it possible to describe the crystallization process fully [1]. The thermodynamic parameters necessary to solve phase equilibrium equations were determined on the basis of the data from the phase diagrams of the binary systems forming the $Zn_xCd_{1-x}Te$ solid solution.

The kinetic analysis results were the data on a mutual relation of the growth temperature, the final liquid phase composition, the system super-cooling values and the layers growth rate. The experiments connected with forming $Zn_xCd_{1-x}Te$ solid solution layers on a CdTe surface were carried out at temperatures in the range of 50–550°C from a liquid phase the composition of which corresponded to the calculated data. The thickness of the obtained layers with Zn in the solid phase at 0.05–0.2 p/mol was in the range of 5–10 μm. The surfaces of the layers obtained in this way were planar and mirror-like and they were very good to be used in the next step of the layers growth. The calculation results correlate with the experiment very well.

Liquid-Solid Interaction at Formation of Nanocomposite Systems

S. Mudry, I. Shtablavyi[a]

Ivan Franko National University of L'viv, Physics of Metal Department
Kyrylo and Mephodiy str., 8, Ua-79005 L'viv, Ukraine

[a] *sihor@ukr.net*

Composite systems with a liquid matrix have attracted the attention of researchers during last years due to the promising practical use. Unfortunately, the fundamental knowledge is still too poor to find a new sphere of application. In this work we present the results on structure studies of a metallic melt consisting of micro- and nanoscale powder. For example, such mixtures include ferrocolloid suspensions and various kinds of nanocrystals present in liquids. In most cases it is important to avoid particle-particle and particle-matrix interactions.

In this work we present the results where this interaction is used in order to obtain new phases of a nanoscale size.

Small particles of Ni and Cu (3 m) were mixed with molten Pb–Sn and Bi-Pb eutectic alloys. Upon some definite time interval of a diffusive process the alloys were quenched and studied by the X-ray diffraction and electron scanning microscopy methods.

It was found that a nanocrystalline structure could be formed in such a way. After cooling, the alloy under investigation revealed a shift in the eutectic point and a reduction in the Ni and Cu powder size and the powder was covered with intermetallics.

Influence of Antimony on Structure and Physical Properties of Tin

S. Mudry[1,a], Yu. Plevachuk[1], V. Sklyarchuk[1], A. Yakymovych[1], V. Sidorov[2]

[1] *Ivan Franko National University, Department of Metal Physics*
8 Kyrylo and Mephodiy Str. 79005 L'viv, Ukraine

[a] *mudry@physics.wups.lviv.ua*

[2] *Ural State Pedagogical University*
26 Cosmonavtov Av. 620017 Ekaterinburg, Russia

Tin and antimony are neighbours in the periodic table which suggests a regular dependence of the structure and physical properties in terms of temperature and concentration. However, the Sn–Sb system phase diagram differs significantly from a diagram expected for a system with an unlimited solution of components in solid and liquid states. Thus, it should be expected that the structure and properties in liquid state will be different than in case of random atomic distribution.

The above mentioned facts motivate a study of the Sb addition influence on the structure and physical properties of tin in the liquid state. The Sn–Sb alloys are considered as favorable lead-free solders.

Liquid Sn–Sb alloys containing various content of antimony were studied by means of X-ray diffraction and viscosity measurements. The structure factors and pair correlation functions were analysed and interpreted using simple models – a random atomic distribution model and a "quasieutectic" model. The results of diffraction studies showed that the structure changes upon addition of Sb atoms to Sn were more significant than expected in case of random atomic distribution, only at higher content of antimony (> 20 at. %). When the content of Sb was lower, the main structure parameters were in fact the same as for liquid pure Sn. This allowed us to suppose that Sb atoms substituted Sn ones, forming a typical atomic solution revealing a chemical and topologic short range order. The tin-like structure persisted within some temperature interval upon melting and became more density packed with further heating. In other words the chemical ordering showed a higher stability to heating than the topologic one.

Effects of Heating Atmospheres on Surface Conductivity in Cu_2O–Al_2O_3–SiO_2 Glass

L. Murawski[a], R. J. Barczyński, K. Trzebiatowski, L. Wicikowski

Faculty of Applied Physics and Mathematics, Gdansk University of Technology
Narutowicza 11/12, 80-233 Gdansk, Poland

[a] *lemur@mif.pg.gda.pl*

Cu_2O–Al_2O_3–SiO_2 glasses show very interesting physical properties. The thermal expansion coefficient of these glasses is comparable with those of silica glass [1]. In addition copper ions exist in both Cu^+ and Cu^{2+} states. This glass exhibits mixed electronic-ionic conductivity [2]. Electronic conduction occurs by small polaron hopping between Cu^+ and Cu^{2+} ions. On the other hand, Cu^+ ion diffusion is responsible for ionic conductivity. In this paper we present the results of surface conductivity investigation in $12.5Cu_2O$–$12.5Al_2O_3$–$75SiO_2$ (in mol %) glass, that was heated in various atmospheres. Before heat treatments, DC conductivity up to 350°C showed Arrhenius behavior with a single activation energy of 0.85 eV. The effects of electrode polarization were visible at 400°C where a drop of conductivity was observed which led to the conductivity hysteresis. The behavior of copper ions on the surface of Cu_2O–Al_2O_3–SiO_2 glass depended strongly on the annealing temperature and the atmosphere. When the glass, in which about 80% of Cu exist as Cu^+ ions, was heated in air at 350°C a CuO layer was formed on the surface. The conductivity of the layer was typical as for CuO with the activation energy of 0.36 eV. This value corresponded to the half of the band gap of crystalline CuO. The opposite behavior was observed when the glass was heated in hydrogen. A large jump of conductivity from 10^{-4} [S cm^{-1}] to 0.05 [S cm^{-1}] took place at 417°C. The X-ray diffraction pattern of the glass surface showed that the copper ions were reduced to the metallic states. The reduced glass exhibited typical metallic behavior with a linear increase in resistivity with temperature.

References

[1] K. Matusita, J. D. Mackenzie *J. Non-Cryst. Solids* 30 (1979) 285
[2] R. J. Barczyński, L. Murawski *J. Non-Cryst. Solids* 307–310 (2002) 1055

FMR Study of Temperature Dependence of Magnetic Anisotropy of Nanocrystalline Fe_2O_3 Doped with ZnO

N. Guskos[1,2], G. Żołnierkiewicz[2], J. Typek[2], D. Sibera[3], U. Narkiewicz[3]

[1] *Solid State Section, Department of Physics, University of Athens Panepistimiopolis, 15 784 Zografos, Athens, Greece*

[2] *Institute of Physics, Pomeranian University of Technology Al. Piastów 48, 70-311 Szczecin, Poland*

[3] *Institute of Chemical and Environmental Engineering Pomeranian University of Technology Al. Piastów 17, 70-310 Szczecin, Poland*

Nanocrystalline Fe_2O_3 samples doped with two different concentrations of ZnO (10 and 20 wt. %) were prepared by coprecipitation and calcination processes [1]. The phase composition of samples was determined by X-ray diffraction. The crystalline phases of Fe_2O_3 and $ZnFe_2O_4$ were identified for nanocrystalline samples of Fe_2O_3 doped with ZnO. The ferromagnetic resonance (FMR) investigations of the obtained samples were carried out in the temperature range from liquid helium to room temperature (RT) (Figure 1). An asymmetrical and very intense magnetic resonance line was recorded at all temperatures. A significant shift of the spectra towards lower magnetic fields with the decreasing temperature was observed. A very good fitting by two Lorentzian functions was obtained suggesting the existence of a strong anisotropic magnetic interaction. An analysis of the resonance line showed that the

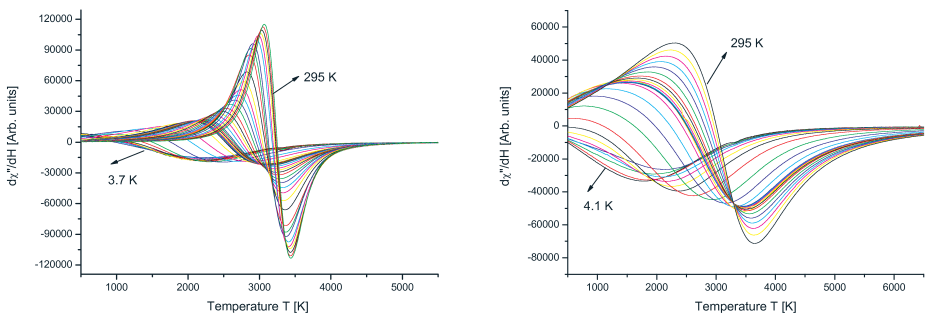

Figure 1: Temperature dependence of FMR spectra of fine particles of ferrite $ZnFe_2O_4$ with 20 % (left) and 10 % of ZnO (right)

blocking process was dominating for the investigated spin system inducing ordering in the z-axis direction at ~ 100 K and thus exerting the magnetic anisotropy of the studied samples.

References

[1] D. Sibera, U. Narkiewicz, N. Guskos, and G. Żołnierkiewicz, J. Phys.: Conference Series **146**, 012014 (2009)

Influence of Annealing Temperature on Light Emission Efficiency of ZrO_2 Doped with Tb^{3+} Ions

U. Narkiewicz[1], J. Kaszewski[1a], M. Godlewski[2,3], S. Yatsunenko[2], W. Łojkowski[4]

[1] *Institute of Chemical and Environment Engineering*
West Pomeranian University of Technology
ul. Pułaskiego 10, 70-322 Szczecin

[a] *jaroslavuss@wp.pl*

[2] *Institute of Physics, Polish Academy of Sciences*
Al. Lotników 32/46, 02-668, Warsaw, Poland

[3] *Department of Mathematics and Natural Sciences College of Science*
Cardinal S. Wyszyński University, Warsaw, Poland

[4] *Institute of High Pressure Physics, Polish Academy of Sciences*
Sokołowska 29/37, 01-142, Warszawa, Poland

Terbium is one of the most attractive rare earth (RE) dopants to achieve efficient (mostly green color) light emission. Several Tb^{3+} doped wide band-gap materials have been commercialized for use as light conversion phosphors in e.g. fluorescence lamps.

Recently, interest has shifted to the properties of RE doped nanoparticles. For example, displays, displaying matrices, e-ink displays etc. have been made for information visualization in modern electronic devices based on doped nanoparticles. The main motivation for these new applications has been the high quantum yield of dopants (intra-shell emission in case of RE ions) photoluminescence (PL).

One of main obstacles for a wider application of RE doped materials has been the difficulty with the $4f$–$4f$ excitation upon host excitation. This is why $4f$–$5d$ or charge transfer excitation has been used, limiting the selection of host materials. This problem can be often solved by using RE doped nanoparticles. For example, we have demonstrated recently that emission in ZnS:Tb nanoparticles co-doped with Mn ions Tb^{3+} $4f$–$4f$ can be efficiently excited upon host (ZnS) excitation which makes this system very attractive for different applications.

In the present work the results of optical investigations of ZrO_2 nanocrystals obtained by solvothermal reaction, doped with Tb ions are discussed. A very efficient $4f$–$4f$ luminescence of Tb^{3+} was observed at room temperature. The properties of this emission (intensity, PL excitation conditions) were followed in the annealing temperature function. Strong influence of annealing temperature on luminescence efficiency was observed, as will be reported.

Elastic Properties of Three-dimensional System of Soft Dimmers at Zero Temperature

J. Narojczyk, K. W. Wojciechowski

Institute of Molecular Physics, Polish Academy of Sciences
M. Smoluchowskiego 17, 60-179 Poznań, Poland

Studies of elastic properties of simple models help understand the elasticity of real materials. Soft dimmers are very simple model molecules, each formed by two interaction sites ('atoms') remaining at a fixed distance. In the present numerical simulations, the dimmers interacted through the site-site inverse power interaction potential. The influence of the exponent of the potential on the elastic properties of the system was studied in the zero temperature limit. It was assumed that it was only the nearest neighbouring atoms that interacted and that the atomic centres formed an f.c.c. lattice. Various structures of dimmers were studied. The results were compared with those obtained for soft sphere systems interacting through the same potentials. Special attention was paid to the Poisson's ratio of the system.

Modification of Bone Structure After Cortycotherapy by Microwave Irradiation

G. Olchowik[1a], M. Tomaszewska[2], M. Tomaszewski[3]

[1] *Department of Biophysics, Medical University of Lublin*
ul. Jaczewskiego 4, 20-090 Lublin

[a] *grazyna.olchowik@am.lublin.pl*

[2] *I Department of Radiology, Medical University of Lublin*
ul. Jaczewskiego 8, 20-954 Lublin

[3] *Department of Human Anatomy, Medical University of Lublin*
ul. Jaczewskiego 4, 20-950 Lublin

The formation of bone mass is a result of a dynamic balance between active bone resorption by osteoclasts and the ossific function of osteoblasts. This balance allows for regular self-regeneration of the osseous tissue and it is a fundamental mechanism which is connected with the supporting constant bone mass. Disorders of homeostasis in the bone tissue induct a loss of the bone mass which is a result of a predominance process of resorption over the ossific process.

One of the pathogens are exogenous glucocorticosteroids which are administered in concentrations higher than physiological. The mechanism of their action on the osseous tissue has not yet been fully explained. Nowadays, it is assumed that adrenal steroids inhibit the synthesis of the intracellular substance of bone by osteoblasts and stimulate resorbtion by osteoclasts. Inhibition of the ossific action depends on a decrease in the activity of subperiosteal area osteoblasts and a decrease in the proliferation degree of periosteum cells – precursors of osteoblasts. They suppress the differentiation during the development of osteogenetic cells and also the inhibit collagen synthesis or other components of the organic matrix of the bone.

Glucocorticosteroids depress also the active intestinal absorbtion of calcium, as a result of their direct activity on the mucous cells. They cause a suppressing effect on the reuptake of calcium in the renal tubule which may cause additional secondary hyperparathyroidism. A reduced absorption of calcium from the alimentary tract leads to a decrease in calcemia, which stimulates the secretion of parathormone (PTH) which in turn increases the desorption of the bone. Long-term taking of glucocorticosteroids leads to the development of osteoporosis.

The stimulation of a coetaneous synthesis of vitamin D – using the optimal exposure to the sunlight, physical exercises depending on the age and individual capabilities and elimination of risk factors from the "life style" group are the protective factors in the development of osteoporosis. However, the applied pharmacological drugs may not give the expected results.

In this work we present the results of the research of usage of monochromatic microwave radiation as a protective factor for the bone tissue of animals during a long-term administration of hydrocortisone. The correlation between the bone composition, the biomechanical parameters, the bone tissue structure ands the microwave irradiation treatment during steroid medicaments application was examined.

The results show that long-term steroidotherapy gives rise to the development of osteoporosis but microwave radiation at a frequency of 53.57 GHz used during the glucocorticosteroid treatment is a protective factor for the bone tissue and prevents the development of posteroidal osteoporosis.

Synthesis and Spectroscopy of Lithium and Potassium–Lithium Tetraborate Glasses Doped with Copper

B. Padlyak[1, 2a], W. Ryba-Romanowski[3], R. Lisiecki[3], Ya. Burak[1], V. Adamiv[1], I. Teslyuk[1]

[1] *Institute of Physical Optics*
23 Dragomanov Str., 79-005 L'viv, Ukraine

[2] *Institute of Physics, University of Zielona Góra*
4a Szafrana Str., 65-516 Zielona Góra, Poland

[a] *B.Padlyak@proton.if.uz.zgora.pl*

[3] *Institute of Low Temperatures and Structure Research, Polish Academy of Sciences*
2 Okólna Str., 50-422 Wroclaw, Poland

Borate crystals and glasses, doped with transition and rare-earth elements are very promising materials for thermoluminescent dosimetry, quantum electronics and non-linear optics as well as neutron and gamma detectors. Cu-doped lithium and potassium-lithium tetraborate ($Li_2B_4O_7$ and $KLiB_4O_7$) glasses of high optical quality were obtained from polycrystalline compounds by fast cooling of the corresponding melts. The melts were heated to a temperature more than 100 K higher that their melting temperatures (T_{melt} = 1190 and 1080 K for the $Li_2B_4O_7$ and $KLiB_4O_7$ compounds, respectively) to exceed the glass transition point. Lithium and potassium carbonates (Li_2CO_3 and K_2CO_3) and boric acid (H_3BO_3) of high chemical purity were used for a solid state synthesis of the $Li_2B_4O_7$ and $KLiB_4O_7$ compounds. Cu impurity was added to $Li_2B_4O_7$ compounds in the form of CuO oxide in the amount of 0.4 mol %.

Electron paramagnetic resonance (EPR) spectra of Cu-doped glasses with lithium and potassium-lithium tetraborate compositions were investigated. On the basis of an analysis of the EPR spectra it was shown that the Cu impurity was incorporated into the tetraborate glass network as paramagnetic Cu^{2+} ($^2D_{5/2}$, $3d^9$) ions. The EPR spectra of Cu^{2+} centres were almost identical for glasses with $Li_2B_4O_7$ and $KLiB_4O_7$ compositions and were typical for glassy (or vitreous) compounds. The Cu^{2+} EPR spectra parameters (g-values, hyperfine constants and peak-to-peak linewidths) in glasses with $Li_2B_4O_7$ and $KLiB_4O_7$ compositions were measured at T = 300 K.

Optical absorption, luminescence excitation and emission spectra as well as luminescence kinetics of the Cu-doped glass with $Li_2B_4O_7$ composition were registered in the UV-VIS-NIR spectral range at room temperature. A characteristic broad absorption band, peaked near 750 nm, was assigned to the $^2B_{1g} \rightarrow {}^2B_{2g}$ transition of Cu^{2+} centres in the $Li_2B_4O_7$ glass network. An intense absorption in the UV region

($\lambda < 350$ nm) was assigned to the $Cu^{2+} \rightarrow O^{2-}$ charge-transfer band. In the photoluminescence spectra of the Cu-doped glass with $Li_2B_4O_7$ composition broad emission bands with the maxima near 420 and 470 nm were observed. The observed emission was characterised by single exponential decay with $\tau = 27.7$ μs at $T = 300$ K. The emission band, peaked near 420 nm was assigned to Cu^+ centres, which were related to parity- and spin-forbidden $3d^9 4s \rightarrow 3d^{10}$ transition from a triplet state of Cu^+ ions [1,2]. The emission band, peaked near 470 nm, can be related to recombination luminescence, induced in the $Li_2B_4O_7$:Cu glass by the UV excitation.

Peculiarities of the cooper impurity incorporation and the EPR and optical spectra of the Cu-doped lithium and potassium-lithium tetraborate glasses are discussed and analysed in comparison with the results obtained by different authors in the same and other borate glasses and corresponding single crystals.

References

[1] J. W. M. Verwey, J.M. Coronado, G. Blasse, J. Solid State Chem. **92** (1991) 531–536
[2] M. Ignatovych, V. Holovey, A. Watterich, T. Vidóczy, P. Baranyai, A. Kelemen, O. Chuiko, Radiat. Measur. **38** (2004) 567–570

Direct Synthesis of $L1_0$ FePt Nanoparticles within Carbon Nanotubes by Wet Chemical Procedure

A. Capobianchi[1], D. Fiorani[1], C. Veroli[1], M. V. Mansilla[1], S. Foglia[2], E. Palange[3]

[1] *Istituto di Struttura della Materia-CNR*
Via Salaria Km 29.300, Montelibretti, 00016 Roma, Italy

[2] *Istituto di Fotonica e Nanotecnologie-CNR*
Via Cineto Romano 42, Roma, Italy

[3] *Dipartimento di Ingegneria Elettrica e dell'Informazione*
Università degli Studi dell'Aquila
67040 Monteluco di Roio, L'Aquila, Italy

This paper reports on a synthesis of iron-platinum (FePt) alloy nanoparticles within Multi Wall Carbon Nanotubes using a novel wet chemical method that allows the nanotube cavity to be filled while keeping the external wall clear. In the discussed case, the procedure permits the nanotubes to be filled with precursor salts of Pt and Fe and magnetic hard, face-centered-tetragonal (fct) crystallographic ($L1_0$) phase FePt alloy nanoparticles are obtained by direct heating at 700°C of the Fe and Pt mixed salts without the need to pass through the formation of the magnetic soft, face-centered-cubic (fcc) FePt alloy phase. Nanoparticles of two different sizes inside nanotubes with magnetic blocked and super-paramagnetic states were obtained at room temperature by a suitable selection of the starting material solution concentration. Morphological, structural and magnetic properties of the filled nanotubes were defined by magnetic measurements, X-ray diffraction and transmission electron microscopy in normal and high resolution modes.

Frequency Filters in Terahertz Region Based on Induced Dipolar Response of 2-dimensional Array of Functional Metamaterials

C. Rizza[1], P. Carelli[1], E. Palange[1], S. Lupi[2], O. Limaj[2], A. Nucara[2], M. Ortolani[3]

[1] *Dipartimento di Ingegneria Elettrica e dell'Informazione, Università dell'Aquila 67040 Monteluco di Roio, L'Aquila, Italy*

[2] *CNR-INFM COHERENTIA and Dipartimento di Fisica Università di Roma "La Sapienza" Piazzale Aldo Moro 2, 00185 Roma, Italy*

[3] *Istituto di Fotonica e Nanotecnologie, IFN-CNR Via Cineto Romano 42, 00131 Roma, Italy*

The scientific research in the terahertz (THz) frequency region of the electromagnetic spectrum can get benefits from components based on metamaterials. Terahertz systems are expected to provide new applications in chemical and astronomic spectroscopy, material investigation, medical and biological analysis and imaging, communication networks and defence and security screening. In order to provide a widely usable THz technology, the research on the optical components is mainly oriented at developing frequency filters, advanced focusing systems, polarization controllers and rotators. In this communication we will report the possibility to fully control the properties of the transmission response of metamaterials in the THz region in terms of their frequency selectivity and scaling as well as the resulting quality factor. The tailoring properties are obtained by using functional metamaterials composed of a 2-dimensional array of planar metallic elements for which the electromagnetic response is mediated by the induced dipolar currents. These metamaterials are analogous in the THz region of those investigated in the visible region and based on metallic nanoparticles deposited on dielectric substrates. By exploiting the Maxwell equation properties, it is possible to find a scale factor related to the shape of the planar element that allows the metamaterial transmission resonance frequency to be selected while maintaining the quality factor unaltered. Basing on these studies, we designed, fabricated and tested metamaterial-based filters having a trasmittivity characterized by single resonance in the spectral region ranging from 1 to 5 THz with the Q-factors higher than 7. The overall properties of the investigated metamaterials that require only few steps of lithographic process for fabrication, represent an improvement in the development of inexpensive THz filters having the characteristics similar to those of the coloured optical filters in the visible range.

Tuning the Electromechanical Response of an Individual CNT by Selective Electron Beam Induced Deposition

M. Passacantando[1], F. Bussolotti[2], S. Santucci[1]

[1] *Dipartimento di Fisica, Università degli Studi dell'Aquila*
Via Vetoio, 67100 Coppito (AQ), Italy

[2] *Japan Advanced Institute of Science and Technology*
School of Materials Science and Research Center for Integrated Science
1-1, Asahidai, Nomi, Ishikawa 923-1292 Japan

Carbon nanotubes have been recognized as one of the most promising materials for developing nanoelectromechanical systems. In particular, the electron beam induced deposition (EBID) process of amorphous carbon under scanning electron microscopy (SEM) represents a very well known and suitable technique for the realisation of stable mechanical and electrical contact between CNTs and the supporting material. Within this context, the effect of the EBID process on the electromechanical response of an individual multiwalled CNT has been directly investigated using a piezoelectric nanomanipulation system operating inside a SEM chamber. The experimental system ensures a high control capability on the geometric parameters of the as fabricated cantilevered CNT based structure, thus allowing a precise modelisation of the electrostatic CNT deflection process. The a-C coating is found to produce a variation of the mechanical response of the CNT cantilevered system, suggesting the use of EBID under SEM as an effective method for tuning the electromechanical properties of single CNT based nanostructures.

Removal of Amorphous Carbon and Metal Particles from MWNTs Using Hydrogen and Acid Treatment

I. Pełech

Institute of Chemical and Environmental Engineering
West Pomeranian University of Technology
Pułaskiego 10, 70-310 Szczecin, Poland

Multi walled carbon nanotubes were obtained by chemical vapor deposition. Ethylene was applied as a carbon source and nanocrystalline iron was used as a catalyst. The samples were reduced under a hydrogen atmosphere to remove amorphous carbon. After that, cementite was decomposed to iron and carbon, and metal was separated from a fibrous structure. This phenomenon facilitated further purification of carbon nanotubes from iron particles. The prepared material was refluxed in 1 or 5 M nitric and in 1 or 5 M hydrochloric acid for 60 and 300 minutes. The metal amount was decreased to approximately 1 wt %. The phase composition of samples and the graphitization degree were determined using the X-ray diffraction method. The morphology was characterized by high resolution transmission electron microscopy. The relative fraction of impurities in the samples was estimated by Raman spectroscopy and a quantitative analysis of the metal impurity content was evaluated using a thermogravimetric analysis.

Magnetic Properties of Mn_6 Sub-monolayers on Au(111) Investigated by X-ray Magnetic Circular Dichroism

U. del Pennino[1], F. Moro[1], V. Corradini[1], M. Evangelisti[1], R. Biagi[1], V. De Renzi[1], U. del Pennino[1], J. C. Cezar[2], R. Inglis[3], C. J. Milios[3], E. K. Brechin[3]

[1] *INFM-CNR S3 National Research Centre and Dipartimento di Fisica Università di Modena e Reggio Emilia via G. Campi 213/A, 41100 Modena, Italy*

[2] *European Synchrotron Radiation Facility 220, F-38043 Grenoble Cèdex, France*

[3] *School of Chemistry, The University of Edinburgh EH9 3JJ Edinburgh, United Kingdom*

We report a comparative study of the electronic and magnetic properties of Mn_6 molecular nanomagnets grafted on gold surface. Two derivatives with spin-ground state 4 and 12 have been functionalized with 3tpc ligands and characterized as thick films (TF) as well as sub-monolayers deposited on Au(111) (sML) by synchrotron-based techniques. X-ray absorption spectroscopy (XAS) at the Mn-$L_{2,3}$ edges shows the modification of the spectral lineshape in the sML with respect to the TF suggesting that the local symmetry around the Mn ions changes once the molecules interact with the gold surface. The results show that the expected Mn(III) oxidation state is preserved after grafting. X-ray magnetic circular dichroism (XMCD) spectra show that the total magnetic moment is given only by spin part because of the quenched orbital moment. Moreover, XMCD spectra collected as function of the magnetic field and temperature show a net decrease of the Mn spin moment for both derivatives on gold. This can be explained in terms of the Mn triangles distortion associated to a change in the Mn–Mn exchange coupling.

EFM Imaging of Carbon Nanotubes Sequestrered into Polystyrene Domains of Poly(styrene-b-isoprene-b-styrene) Block Copolymer Matrix

L. Peponi[1], A. Tercjak[2], J. Gutierrez[2], M. Cardinali[1], I. Mondragon[2], L. Valentini[1], J. M. Kenny[1]

[1] *Dipartimento di Ingegneria Civile e Ambientale, Università di Perugia, INSTM UdR Perugia, 05100 Terni, Italy*

[2] *'Materials + Technologies' Group, Escuela Politecnica Universidad País Vasco/Euskal Herriko Unibertsitatea Pza. Europa 1, 20018 Donostia-San Sebastián, Spain*

Nanocomposites based on block copolymers and having the ability to self-assemble into well-ordered nanostructured morphology constitute a multidisciplinary area of great interest.

In this work, atomic and electrostatic force microscopes (AFM and EFM) were used to demonstrate the sequestering of octadecylamine functionalized single-walled carbon nanotubes (ODA-SWCNTs) in the polystyrene phase of a polystyrene-b-polyisoprene-b-polystyrene (SIS) block copolymer matrix. Dodecanethiol (DT) was used as the surfactant to disperse the ODA-SWCNTs in the SIS block copolymer matrix. A change from cylindrical self-assembled nanostructures of neat SIS to ordered lamellar domains was observed from the morphological point of view when 1 wt % of DT-ODA-SWCNTs was added to the SIS matrix. The confinement of the carbon nanotubes into the lamellar domains of the PS block was detected by the EFM due to their excellent electrical properties. Thus, when voltage was applied between the tip and the sample, an evident phase contrast was evidenced, due to the high different electrical behaviour between the non-conductive polymer and the conductive CNT.

The BISMUTH Project

S. Picozzi, G. Giovannetti, A. Stroppa,
T. Fukushima, K. Yamauchi

Consiglio Nazionale delle Ricerche – Istituto Nazionale per la Fisica della Materia (CNR-INFM) CASTI Regional Lab. 67100 L'Aquila

Electronic magnetic ferroelectrics, i.e. complex magnetic oxides in which ferroelectricity is driven by non-centrosymmetric spin- or charge- or orbital-arrangements, have recently attracted great interests and constitute the core of our research activity within the BISMUTH project (acronym of "Breaking Inversion Symmetry in Magnets: Understand via THeory"), sponsored as a Starting Grant for Independent Research 2007 by the European Research Council [1].

Our research activity is focused on the existence and efficiency of different mechanisms for multiferroicity (*i.e.* coexistence of long-range dipolar and magnetic orders), based on the interplay between electronic and structural degrees of freedom. Within this framework, the magnetically-induced electric polarization can be driven by symmetric (Heisenberg-like) and/or antisymmetric (Dzyaloshinskii-Moriya-like) exchange interactions. Examples of transition metal oxides in which the first mechanism is active will be presented. Indeed, our ab-initio calculations show that the polarization induced by the Heisenberg-like S·S exchange can reach substantial values (up to few μC/cm^2). We will present several test-cases, ranging from manganites (prototypical $HoMnO_3$ [2], but also half-doped manganites, $La_{0.5}Ca_{0.5}MnO_3$) [3] to nickelates ($LuNiO_3$, $HoNiO_3$).

The second part of our presentation will be devoted to the possibility of achieving ferroelectricity in ferrimagnetic Fe_3O_4 below the Verwey transition. In that case, the peculiar non-centrosymmetric charge-ordering pattern of Fe^{2+}/Fe^{3+} on the Fe B sites of the inverse spinel structure induces an electric polarization of few μC/cm^2. The excellent consistency of our predicted values with corresponding experimental data unambiguously prove magnetite to be the first multiferroic known to mankind [4].

References

[1] http://www.casti.aquila.infn.it/homepages/bismuth/index.html
[2] Picozzi S, Yamauchi K, Sergienko IA and Dagotto E 2008 *Phys. Rev. Lett.* **99** 227201
[3] Giovannetti G, Kumar S, van den Brink J and Picozzi S, cond-mat://arXiv:0812.4380
[4] Alexe M, Ziese M, Hesse D, Esquinazi P, Yamauchi K, Fukushima T, Picozzi S, Gösele *Adv. Mater.* (in press)

Influence of Fullerene Side Chain Functionalization on Open-Circuit-Voltage of Polymer: Fullerene Bulk Heterojunction Solar Cells

F. Piersimoni[1], K. Vandewal[1], S. Chambon[1], S. Filippone[2], N. Martin[2], J. Zhao[3], G. Van Assche[3], B. Van Mele[3], L. Lutsen[1], P. Adriaansens[1], D. Vanderzande[1], J. Manca[1]

[1] *IMEC-IMOMEC, vzw and Institute for Materials Research Hasselt University, Wetenschapspark 1, 3590 Diepenbeek, Belgium*

[2] *Department of Organic Chemestry, Universidad Complutense E-28040 Madrid, Spain*

[3] *Department of Polymer Science and Structural Chemistry Vrije Universiteit Brussel (VUB), Pleinlaan 2, B-1050 Brussels, Belgium*

Organic solar cells are a promising technology for low cost renewable energy. In particular organic bulk heterojunction solar cells consisting of blends of a conjugated polymer with a fullerene, nowadays show power conversion efficiencies of 5–6% [1,2]. This value needs to be improved in order to obtain a marketable product and depends crucially on the photocurrent and the photovoltage produced by the solar illumination.

The short-circuit current (J_{sc}) depends directly on the amount of absorbed photons and the subsequent transport of photogenerated electrons and holes through the nano-phases of the blend. The open-circuit voltage (V_{oc}) depends mainly on the energy E_{CT} of the interfacial charge-transfer (CT) state, a weakly bound electron-hole pair at the polymer: fullerene interface [3,4]. E_{CT} is mainly determined by the difference between the Highest Occupied Molecular Orbital (HOMO) of the polymer and the Lowest Unoccupied Molecular Orbital (LUMO) of the fullerene.

This work aims to better understand the influence of fullerene side chain functionalization on the V_{oc} of polymer: fullerene solar cells. Therefore, photovoltaic properties of material blends consisting of the conjugated polymer poly[2-methoxy-5-(3',7'-dimethyloctyloxy)-1,4-phenylene vinylene] (MDMO-PPV) with several fullerene molecules with different side chains [5] (Figure 1) were investigated. The morphology and crystallization behavior of the blends were determined by using Transmission Electron Microscopy (TEM), X-ray Diffraction (XRD), Nuclear Magnetic Resonance (NMR) and Differential Scanning Calorimetry (DSC). It was found that the acceptors with the shorter sidechains formed crystalline nano-phases in the blend, while the other acceptors did not. It is shown that this has a profound effect, not only on J_{sc} but also on V_{oc}.

In order to clarify the mechanism for the observed differences in V_{oc}, a highly sensitive technique called Fourier-transform photocurrent spectroscopy (FTPS) is used to detect the photocurrent produced by very weak optical transitions into the CT

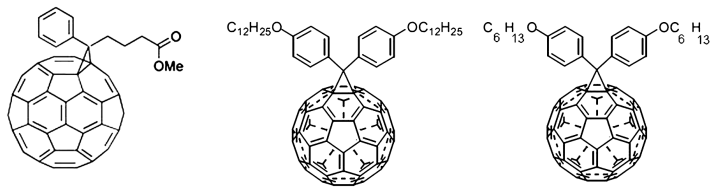

Figure 1: Chemical structure of the fullerenic acceptors: 1-[3-(methoxycarbonyl)propyl]-1-phenyl-[6.6]C61 (PCBM); 1,1-Bis-(Dodecyloxyphenyl)-(5,6)C61,Diphenylmethanofullerenes (DPM-12); 1,1-Bis-(Hexyloxyphenyl)-(5,6)C61,Diphenylmethanofullerenes (DPM-6)

state. This enables us to measure the value of E_{CT} accurately and directly on the photovoltaic devices. We find that fullerene crystallization lowers the value of E_{CT} by 0.2 eV, caused by a shift in the LUMO level of the fullerene crystal as compared to the isolated fullerene molecule. This causes V_{oc} to drop upon increased fullerene crystallization. The improved mobility of the crystalline phase however, causes J_{sc} to increase, causing a net positive effect on the overall power conversion efficiency, upon increased fullerene crystallization.

References

[1] Park SH, Roy A, Beaupré S, Cho S, Coates N, Moon JS, Moses D, Leclerc M, Lee K, Heeger AJ, 2009. *Nature Photonics* **3** 297
[2] Thompson BC, Fréchet JMJ, 2008. *Angew. Chem. Int. Ed.* **47** 58
[3] Vandewal K, Gadisa A, Oosterbaan WD, Bertho S, Banishoeib F, Severen IV, Lutsen L, Cleij TJ, Vanderzande D, Manca JV, 2008. *Adv. Funct. Mater.* **18** 2064
[4] Veldman D, Meskers SCJ, Janssen RAJ, 2009. *Adv. Funct. Mater.* **19** 1
[5] Riedel I, von Hauff E, Dyakonov V, 2005. *Adv. Funct. Mater* **15** 1979

Interactions and Potential Cytotoxicity of TiO_2 Nanoparticles and Thin Films on Murine Macrophages RAW 264.7 Cell Line

A. Poma[1a], S. Di Bucchianico[1], A. Galano[1], S. Santucci[2]

[1] *Department of Basic and Applied Biology, University of L'Aquila, Italy*

[a] *annamaria.poma@univaq.it*

[2] *Department of Physics, University of L'Aquila, Italy*

Few studies suggest that ultrafine (P-25) TiO_2 particles produce greater pulmonary inflammation when compared with fine-sized TiO_2 particles. The results of recent studies comparing the effects of nano- vs. fine-sized particles have indicated that pulmonary exposures in rats to uncoated TiO_2 nanoscale rods (200 nm lengths $\times$ 30 nm diameters) and TiO_2 nanoscale dots (particle size $<$ 30 nm) did not produce enhanced lung inflammation in rats when compared to fine-sized TiO_2 particle exposures (particle size $\sim$ 270 nm). In this work thin films (TiO_2, TiO_2:In, TiO_2:WO_3, TiO_2:Fe_2O_3) and nanoparticles (TiO_2, TiO_2:In, TiO_2:WO_3, TiO_2:Fe_2O_3) were prepared and characterized by SEM, XRD, AFM. A cytotoxicity analysis by the Trypan blue method and the MTS assay, a morfological analysis by SEM and mTNF-α ELISA determination were performed on cells incubated on thin films and particles (25 μg/ml). Cell proliferation and mitochondrial activity data did not show the average reduction compared with a check after 12, 24 and 48 hours of incubation on thin films and with particles. The SEM analysis confirmed the presence of an agglomerate of 100–150 nm particles that interacted with cells. The degree to which engineered nanoparticles aggregate *in vitro* or in aerosol or in an occupational environment and subsequently do or do not disaggregate following the particle deposition in the lung, should strongly influence the particle deposition rates as well as interactions. We also present data showing macrophage activation connected with the contact with nanoparticles. The TNF-α release of RAW 264.7 cells was determined after 5 and 24 h of incubation with nanoparticles (25 μg/ml). The TNF-α production was higher after 5 hours of treatment, in particular with TiO_2 and TiO_2:In nanoparticles. The average TNF-α release decreased after 24 hours of treatment except for TiO_2:In nanoparticles confirming their potential cytotoxicity.

Development of Compact Ka-Band MEMS Phase Shifter for Electronic Beam Scanning Antennas

M. Dispenza[1], P. Farinelli[2], I. Pomona[3]

Team CONFIRM [reCONFIrable circuits by Rf Mems]
FINMECCANICA CORPORATE PROJECT
ADVANCED MATERIALS & ENABLING TECHNOLOGIES
– MINDSH@RE COMMUNITY

[1] *Selex Sistemi Integrati Spa*
Via Tiburtina, Km 12, 400-00131 Rome, Italy
mdispenza@selex-si.com

[2] *RF Microtech, a spin-off of the University of Perugia*
Via G.Duranti, 93, 06125, Perugia, Italy
paola.farinelli@rfmicrotech.com

[3] *Selex Communications Spa*
Via Sidney Sonnino, 6-95045 Misterbianco (CT), Italy
ignazio.pomona@selex-comms.com

Microwave phase shifters are basic components used in a variety of communication and radar systems, microwave instrumentation, and industrial applications. As commercial and military systems increasingly move towards smaller and high performance antenna systems, the MEMS technology can be applied to develop electronically reprogrammable phase shifters with low-power consumption, low loss, and excellent linearity [1–5].

In this paper the development of a compact 5-bit Ka-band MEMS phase shifter is presented. The device was designed to be fabricated on a high resistivity silicon substrate at Fondazione Bruno Kessler Laboratories (Trento, Italy), employing the well-established eight-mask surface micro-machining process outlined in Figure 1 [6].

The process consists of about 120 process steps and allows the electrodeposition of two gold layers of different thicknesses for highly complex movable bridges and microstrip lines. It brings together the movable Au bridge structures integrated with high resistive poly-silicon actuation pads and optional high value resistors and DC blocking capacitors. The air-bridges and moveable bridges are realized without the need of any planarization step, utilizing two electrodeposited gold layers of different thickness which are also used for the realization of coplanar waveguides. A third gold layer is used for the realization of low resistance metal-to-metal electromechanic contacts for series ohmic switches and floating electrodes for shunt switches.

A high performance ohmic contact cantilever switch was employed as the basic block for the 5 bit MEMS phase shifter.

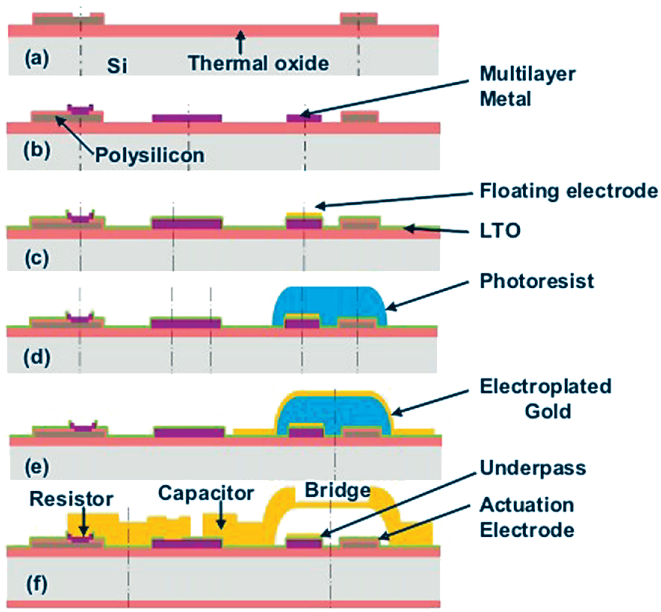

Figure 1: The eight masks fabrication process

The 5-bit MEMS phase shifter was developed with a hybrid architecture to operate in the Ka bandwidth. For the first three bits (180°, 90° and 45°) a switched line topology was chosen since in the frequency band of interest it turned out to be the best trade-off among the large phase shift, low loss and reduced space occupation. The fourth and fifth bits (22.5° and 11.25°) were based on a loaded line topology, which was convenient when a small phase shift was required. The device was monolithically designed on a 200 μm thick HR Silicon substrate in microstrip technology.

The single bits were designed using ADS Momentum [7], a full-wave electromagnetic tool capable of predicting and properly moving out the band off-path resonances not visible in circuital models. Afterwards the simulations were circuitally cascaded in order to predict the performance of the whole structure. The simulated results show a return loss and an insertion loss better than 15 dB and 3 dB, respectively, for all the phase shifter states.

The design activity is in progress and the most significant simulation results will be shown in the final paper.

References

[1] M. Kim, J. B. Hacker, R. E. Mihailovich, and J. F. DeNatale, "A DC-to-40 GHz four-bit RF MEMS true-time delay network," *IEEE Microwave and Wireless Components Lett.*, vol. 11, no. 2, pp. 56–58, Feb. 2001

[2] G. L. Tan, R. E. Mihailovich, J. B. Hacker, J. F. DeNatale, and G. M. Rebeiz, "A very-low-loss 2-bit X-band RF MEMS phase shifter," presented at the 2002 IEEE Int. Microwave Symp., Seattle, WA

[3] B. Pillans, S. Eshelman, A. Malczewski, J. Ehmke, and C. Goldsmith, "Ka-band RF MEMS phase shifters," IEEE Microwave Guided Wave Lett., vol. 9, pp. 520–522, Dec. 1999

[4] S. Bastioli, F. Di Maggio, P. Farinelli, F. Giacomozzi, B. Margesin, A. Ocera, I. Pomona, M. Russo, R. Sorrentino, "Design and Manufacturing of a 5-bit MEMS Phase Shifter at K-band", EuMW 2008, Amsterdam, 27–30 Oct 2008

[5] J. S. Hayden , A. Malczewski, J. Kleber, C. L. Goldsmith, G. M. Rebeiz "2 and 4-Bit DC-18 GHz Microstrip MEMS Distributed Phase Shifters" 2001 IEEE

[6] A. Ocera, P. Farinelli, F. Cherubini, P. Mezzanotte, R. Sorrentino, B. Margesin, F. Giacomozzi, "A MEMS-Reconfigurable Power Divider on High Resistivity Silicon Substrate", IEEE MTT-S International Microwave Symposium, Honolulu, 3–8 June 2007

[7] ADS Agilent Momentum, http://www.agilent.com/

On Electrical and Photoconductive Properties of Nb-doped TiO_2 Sol-gel Thin Films

D. Joskowska[1], K. Pomoni[2a], A. Vomvas[2], B. Kościelska[1], D. Anastassopoulos[2]

[1] *Faculty of Applied Physics and Mathematics, Gdansk University of Technology Narutowicza 11/12, 80-233 Gdansk, Poland*

[a] *pomoni@physics.upatras.gr*

[2] *Department of Physics, University of Patras 26 500 Patras, Greece*

Pure and Nb-doped TiO_2 thin films were prepared on silica glass substrates using the sol-gel technique. All the samples were heat treated at 800°C. The microstructure of the samples was studied using X-ray diffraction (XRD) and atomic force microscopy (AFM). With the exception of the 10% Nb-doped sample in which both the anatase and the rutile phase were present, it was only the anatase phase that was detected for the 20%, 30% and 40% Nb-doped samples. The electrical conductivities of films, heat-treated at 800°C, were studied in the temperature range of 300–380 K in vacuum and in air. The transient photoconductivities were examined in vacuum and in air as a function of temperature and light intensity.

The dark conductivities in air for all the studied samples were found to be higher than in vacuum. The Nb addition causes an increase in the value of the dark conductivities by several orders of magnitude. The transient photoconductivity of the undoped sample is sensitive to the environment (air or vacuum) and reaches very high values. On the other hand the addition of Nb sharply decreases the photoconductivity.

Anomalous Deformation of Constrained Auxetic Square Under Pressure

A. A. Poźniak[1], P. Kędziora[1], H. Kamiński[2], B. Maruszewski[2], T. Stręk[2], K. W. Wojciechowski[1,3]

[1] *Institute of Molecular Physics, Polish Academy of Sciences M. Smoluchowskiego 17, 60-179 Poznań, Poland*

[2] *Institute of Applied Mechanics, Poznań University of Technology Piotrowo 3, 60-965 Poznań, Poland*

[3] *PWSZ im. Prezydenta St. Wojciechowskiego Nowy Świat 4, 62-800 Kalisz, Poland*

Materials with a negative Poisson's ratio, known also as auxetics, behave in a counterintuitive way: in contrast to common materials which shrink laterally when stretched, auxetics *expand* laterally at stretching. Auxetics show also other anomalous behaviour. One of them is discussed in the present communication.

A uniform pressure is applied to one of the sides of a two-dimensional unit square with the remaining sides clamped. The deformation of a square made of an isotropic material is studied by the Finite Element Method for different values of the Poisson's ratio. The simulations show that the displacement vector near the vertices exhibits anomalous behavior for negative values of the Poisson's ratio – it shows oscillations near the vertices and can be even antiparallel to the direction of the loading force. The obtained results suggest that when the Poisson's ratio tends to -1, the number of oscillations on the side under pressure tends to infinity.

Morphology Investigation of Periodic Nano-patterns Produced by Large Area X-ray Interference Lithography

S. Prezioso[1a], D. Luciani[1], P. Tucceri[1], P. De Marco[1], A. Gaudieri[1], J. Kaiser[2], S. Santucci[1], L. Ottaviano[1], P. Zuppella[1]

[1] *Dipartimento di Fisica, Università dell'Aquila, gc-LNGS INFN Via Vetoio, 67100, L'Aquila, Italy*

[a] *stefano.prezioso@aquila.infn.it*

[2] *Institute of Physical Engineering, Brno University of Technology Technická 2, 61669 Brno, Czech Republic*

A prototype low cost tabletop soft X-ray laser source (1.5 ns pulse duration, $\lambda = 46.9$ nm) was successfully employed as an Interference Nano-Lithography tool (INL). The laser pulse was produced by a single pass amplification of a $3p$–$3s$ transition in Ne-like Ar in an elongated plasma column created by a fast capillary discharge. Interference patterns were obtained with a simple Lloyd's mirror setup. Periodic structures on PMMA/Si substrates were produced on large areas (0.1 mm^2) with resolutions from 400 nm to the 22.5 nm physical limit half pitch (Figure 1). A systematical investigation of the morphology of the produced structures was performed as a function of the period. The actual possibility of pushing the resolution down to the $\lambda/4$ physical limit was evaluated, considering a trade-off between the good mutual coherence degree of the source and the intrinsic mechanical instability of the experimental setup.

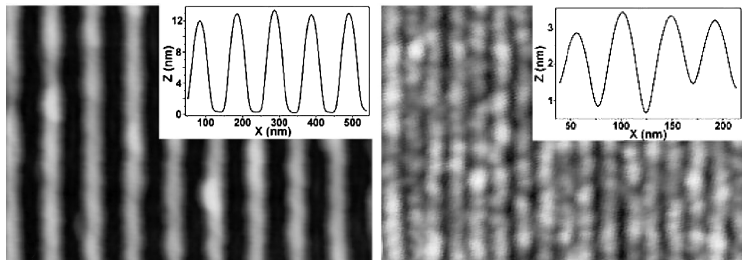

(a) (b)

Figure 1: AFM images of patterned PMMA/Si(100) with: (a) 50 nm and (b) 22.5 nm half-pitch; insets: average of 256 horizontal height line profiles taken from the corresponding AFM images

A Xe Based Plasma Source for EUV Nano-lithography Applications

S. Prezioso[1a], L. Ottaviano[1], A. Ritucci[1], P. Tucceri[1], F. Flora[2], L. Mezi[2], P. Dunne[3], P. Zuppella[1]

[1] *Dipartimento di Fisica, Università dell'Aquila gc-LNGS INFN, Via Vetoio, 67100, L'Aquila, Italy*

[a] *stefano.prezioso@aquila.infn.it*

[2] *ENEA, Dipartimento FIM-FIS-ACC, Centro Ricerche di Frascati Via E. Fermi 45 I-00044 Frascati, Italy*

[3] *UCD School of Physics, University College Dublin, Dublin 4, Ireland*

An Xe based capillary discharge plasma source was developed at the University of L'Aquila for EUV nano-lithography applications. The emission spectrum presented interesting features in the extreme ultraviolet (EUV) range between 10 and 18 nm, where high volume photolithography may amply benefit by the high reflectivity of molybdenum-silicon (MoSi) multilayer mirrors (67% at 13.5 nm) and by the properties of Kr gas at these wavelengths as a debris mitigator: features due to $4d$–$4f$ and $4d$–$5p$ transitions in a range of ions were observed, with the $4d$–$4f$ emission from ions Xe^{8+}–Xe^{12+} clearly identified in the spectrum. An addition of In_2O_3 powder inside the capillary, resulting in the participation of In ions to the discharge, was shown to increase the emission intensity of about the 30% in correspondence of the unresolved transition array around 14.3 nm, a spectral region where the Kr gas is quite transparent to radiation but not to debris. Despite this important improvement over the use of bare Xe, conversion efficiency from the electrical input energy to the in-band energy turned out to be still too low (about 0.1%) for any kind of nano-lithography application, be it by Mo/Be (around 11.3 nm) or by Mo/Si (around 13.4 nm) multilayer mirrors technology. A further enhancement of the optical power output may give, at least initially, the opportunity of using this source for metrology of EUV optics but, in the future, it may be a presupposition for a wider and wider employment in the nano-lithography technology, even as the main source of a photo-lithographic process.

Silicon Quantum-dots Based Solar Cells for Third Generation Photovoltaics

S. Prezioso[1a], S. M. Hossain[2,5], A. Anopchenko[2], L. Ferraioli[2], Zhizhong Yuan[2], M. Wang[3], G. Pucker[3], P. Bellutti[3], S. Binettir[4], M. Acciarri[4], L. Pavesi[1]

[1] *Dipartimento di Fisica, Università dell'Aquila, gc-LNGS INFN Via Vetoio, 67100, L'Aquila, Italy*

[a] *stefano.prezioso@aquila.infn.it*

[2] *Laboratorio di Nanoscienze, Dipartimento di Fisica, Università di Trento Via Sommarive 14, 38100 Povo (Trento), Italy*

[3] *Microtechnologies Laboratory, Fondazione Bruno Kessler Via Sommarive 18, 38100 Povo (Trento), Italy*

[4] *Dipartimento di Scienza dei Materiali, Università degli Studi Milano-Bicocca Via Cozzi 53, 20125 Milano, Italy*

[5] *Department of Physics, Bengal Engineering and Science University Sibpur, India*

An Si quantum-dots (Si-QD) based solar cell was developed in a joint effort at the University of Trento and FBK. The advantages of nano-structured materials opportunely modified by defect states were explored as a promising technology for third generation photovoltaics. A simple metal-insulator-semiconductor structure was used with the insulator layer consisting of silicon-rich oxy-nitride deposited by plasma-enhanced chemical vapor deposition. Si-QDs was formed by thermal annealing. A detailed study of both opto-electrical and spectral properties was performed revealing the presence of nitrogen related sub-bandgap trap states located at the Si-QD/dielectric interface. The role of these traps was accurately described: on one side, they promoted a rapid removal of photo-generated electrons from the Si-QDs, reducing the probability of electron-hole pair recombination in favor of a photocurrent increment; on the other side, they opened an absorption window in the near infrared range otherwise inaccessible to Si-based solar cells. A superlinear photovoltaic effect was observed and modeled on the base of an internal gain mechanism attributed to secondary carriers generation: electrons trapped in correspondence of the Si-QD's shell, be they directly photo-generated by infrared photons or prevented from recombining with holes inside the Si-QDs, were extracted as secondary carriers by impact ionization with hot photo-electrons. In the present work, new device concepts are suggested as possible strategies to fill the gap between the modern solar cell efficiency and the 93% thermodynamic limit, by harvesting a large part of the solar spectrum and improving the photo-carrier extraction.

Non-Polar GaN Films Prepared on Si Substrates Using Porous Al_2O_3 Anodic Oxide Masks

A. A. Donskov[1], L. I. D'yakonov[1], A. V. Govorkov[1], Y. P. Kozlova[1], V. V. Kuznetsov[3a], S. S. Malakhov[1], A. V. Markov[1], M. V. Mezhennyi[1], V. F. Pavlov[1], A. Y. Polyakov[1], V. I. Ratushnyi[2], N. B. Smirnov[1], T. G. Yugova[1]

[1] *Institute of Rare Metals*
Moscow, 119017, B. Tolmachevsky, 5, Russia

[2] *South-Russian State Technical University*
Novocherkassk, 346400, Russian Federation

[3] *Saint Petersburg Electrotechnical University*
St Petersburg, 197376, Russian Federation

[a] *analizbp@mail.ru*

Growth of non-polar GaN films with reasonable crystalline quality is an important scientific and practical problem of semiconductor electronics. In this talk we show that such films can be prepared by hydride vapour phase epitaxy (HVPE) on Si substrates masked by porous Al_2O_3 obtained by anodic oxidation of Al layers deposited on Si by vacuum evaporation. Such layers are known to have a self-organized porous structure with the pitch and diameter of open channels in the structure determined by applied voltage during anodic oxidation. When GaN was grown by HVPE at temperatures close to 1000°C on such Si substrates with porous Al_2O_3 the films orientation was found to be (11–20) (i.e. the films were non-polar a-GaN). The half-width of the X-ray rocking curves for the symmetric reflection was the function of characteristic dimensions of the pores and, particularly, the depth of the open channels. The optimal pores dimensions were close to 100 nm, the best crystalline quality was obtained for Al films oxidized practically through the entire thickness of Al (about 1 micron). Under these conditions the half-width of the (11–20) GaN rocking curve (double crystal diffraction) was quite low (450 arcseconds) and did not show a strong dependence on the diffraction plane rotation around the axis normal to the surface. The low width of the rocking curve and its small anisotropy point to the low density of stacking faults (SFs) which is also corroborated by the dominance in microcathodoluminescence (MCL) spectra of thus prepared a-GaN of the bandedge luminescence at 3.47 eV, with no strong contribution of the SF-related MCL bands at 3.42 eV and 3.3 eV. High magnification scanning electron microscope images of the cleaved surfaces of such GaN samples show that the open channels do not reach down to the Si surface and thus the growth is not selective epitaxial growth on masked Si substrates. Rather, the growth proceeds by deposition of GaN nuclei in the channels with further selection of the grains with the "right" orientation by preferential lateral growth. Decreasing the relative thickness of the open channels in oxide leads to

substantial deterioration of the crystalline quality of the films. X-ray analysis of the anodic oxide layers shows that they are amorphous in as-deposited state, but crystallize into sapphire with preferential crystalline orientation (11–23) upon heating of the films to temperatures characteristic of HVPE epitaxy. This process occurs irrespective of the Si substrate orientation (two orientations (111) and (100) were tried) and therefore the crystallization has a bulk character and is not driven by the processes at the interface with Si. The sapphire (11–23) orientation is reasonably close to the r-orientation (10–12) commonly used for growth of a-GaN. At this preliminary stage we argue that the a-GaN epitaxy in our case can be viewed as growth on patterned sapphire with orientation close to r-sapphire. An attractive feature of this process is that one expects it to be applicable to non-polar a-GaN deposition on any chosen substrate material, once this material is masked by properly prepared and crystallized anodic oxide of Al.

Stability of Dye-sensitized Solar Cells: Comparison of Sealing Strategies

E. Leonardi[1,2], S. Penna[1,2], A. Reale[1,2], T. M. Brown[1,2], A. Di Carlo[1,2]

[1] *CHOSE – Centre for Hybrid and Organic Solar Energy Via G. Peroni 400, 00197 Rome, Italy*

[2] *Electronic Eng. Dept., University of Rome Tor Vergata Via del Politecnico, 1, 00133 Rome, Italy*

Since the commercialization of dye-sensitized solar cells (DSC) is still around the corner, a stable definition of a set of testing conditions specific for the DSC technology is still on the way. The most commonly used set of reference tests is driven by the test methods for a-Si, such as IEC 68 or JIS C-8938.

Obviously, these tests are meaningful once the encapsulation and hermetic sealing of the cell is guaranteed. Tests on cells are useful to study the intrinsic mechanisms of the cell itself which degrade the performance. It has been assessed in a number of studies that DSCs do not significantly degrade under normal illumination [1,2].

A factor that limits the lifetime of cells is the exposure to UV light [3]. The degradation mechanism due to the UV light has been studied in detail and considerable improvements have been obtained by adding proper additives to the electrolyte.

In order to go beyond this figure it is possible to integrate a polymeric film in a cell structure [3] that filters the UV radiation. In this way it is possible to easily reach 20 years stability over the UV light. Another factor that limits the lifetime is the presence of oxygen or water. Accelerated lifetime tests have demonstrated a substantial invariance of performance for 27 500 hours at 55°C.

This leads to the conclusion that DSCs have a lifetime of 44 years under typical solar conditions of central Europe and 26 years in southern Europe [4]. These data let envisage a commercial use of this technology.

In the process of DSC fabrication, particular attention has been devoted to the sealing procedure, since the I-/I3-spilling may cause damage to the metallic contacts and grids. Encapsulation of glass substrates is obtained using a thermo sealing component such as Suryln and Bynel by Dupont.

In order to pass the aging tests at high temperatures it is necessary that the materials do not degrade. The thermo sealing resins alone are not sufficient to guarantee good hermetic properties since their fusion point is around 80°C.

In order to circumvent this problem it is possible to encapsulate the DSSC using high fusion temperature glass powders (glass frit) that are used today for plasma screen and LCD sealing [5–8].

The advantage of glass-frit is to be economic and it can be applied using screen printing techniques since it forms powders that are more or less viscous. It is also quite stable thermally and chemically.

The main disadvantage of this technique is that it requires high deposition temperatures (about 400°C), and both the dye and the electrolyte need to be injected afterwards. All the abovementioned methods will be compared in terms of the ageing behavior, and the main degradation mechanisms will be analyzed relating the performance of devices to material properties. This is a key aspect of the DSC technology, where material science, nanotechnology and device design and optimization are intimately correlated in the most exciting and challenging way among more modern photovoltaics technologies.

Acknowledgements
We acknowledge the support Regione Lazio. The helpful assistance of Tiziana Lo Pardo is greatfully acknowledged.

References

[1] A. Hinsch, J. M. Kroon, R. Kern, I. Hlendorf , Longterm stability of dye-sensitised solar cells 2001
[2] R. Sastrawan Photovoltaic modules of dye solar cells, Dissertation zur Erlangung des Doktorgrades der Fakultät für Mathematik und Physik der Albert-Ludwigs-Universität Freiburg im Breisgau, 2006
[3] H. Pettersson, T. Gruszecki, Long-term stability of low-power dyesensitised solar cells prepared by industrial methods 2001
[4] H. Desilvestro, Dyesol, 3rd DSC-IC Conference on the Industrialization of DSC technology, Nara, Japan
[5] M. Knupfer, Applied Physics A: Materials Science & Processing 77/5 (2003) 623
[6] R. Marks, J. Halls, D. Bradley, R. Friend, A. Holmes, Journal of Physics: Condensed Matter 6 (1994) 1379
[7] W. Huynh, J. Dittmer, A. Alivisatos, Science 295/5564 (2002) 2425
[8] C. Brabec, Solar energy materials and solar cells 83/2-3 (2004) 273

Well-Aligned Nanofibers Grown by Near-Field Electrospinning

M. Rinaldi[1], F. Ruggieri[2], L. Lozzi[1], S. Santucci[1]

[1] *Department of Physics*
University of L'Aquila, Italy

[2] *Department of Chemistry, Chemical Engineering and Material*
University of L'Aquila, Italy

It has been attempted to use the spatial orientation of electrospun fibers to obtain well aligned and highly ordered nanofibers due to their potential use as active components or interconnects in fabricating nanoscale electronic or electro-mechanical devices [1].

Recently a new technique, called near-field electrospinning (NFES), has been the subject of intensive research as an excellent system developed to deposit solid nanofibers in a direct, continuous and controllable manner [2,3]. This process is a simple yet powerful method for direct-write deposition of nanofibers with unprecedented controllability at resolutions comparable to those achieved with much more expensive and sophisticated tools and offers full control over the path of deposited nanofibers, allowing them to realize their engineering potential.

In this work attention is focused on the growth of TiO_2 nanofibers. TiO_2 is a semiconductor that has raised substantial interest in both industrial applications and scientific research, so that much work has been devoted to the synthesis of this material because of its potential applications in many areas including electronics, photonics, mechanics, and sensing. The performance of TiO_2 strongly depends on its crystallite phase, dimension, and morphology, since they give a decisive influence on their chemical and physical properties. In this work we will show our results on the possibility of producing low-dimensional nanostructured titanium oxide materials in a controllable and direct-write manner and investigate a synthesis and functionalization of TiO_2 nanofibers.

We have investigated the morphology, crystalline structure, chemical composition and electrical properties of these nanofibers using scanning Electron Micoprscope (SEM), X-ray diffraction (XRD), X-ray photoemission spectroscopy (XPS) and I-V characterization, both as deposited and after annealing processes. We will show that the annealing process determines the crystallization of TiO_2 nanofibers with a formation of small polycrystalline grains and solvent evaporation with the consequent reduction of the fiber diameter to less than 200 nm, without breaking the nanofibers which remain continuous and well aligned up to typical lengths of several millimiters.

Deposition of well aligned PANI nanofibers will be also reported. The chemical, optical, electrical and mechanical properties of polyaniline have attracted multidisciplinary research in the last decades due to the great possibility of application in

advanced technologies. In fact, for example, nanofibers of conductive polymers, such as polyaniline, have been extensively studied because of their high electrical conductivity and high mechanical flexibility, their ability to be electrochemically switched between electronically insulating and conducting states, and their potential applications in nanodevices. Among the methods that have been used to fabricate conducting polymers on a nanometer scale, NFES is an attractive technique to fabricate nanodevices based on conducting polymers due to its capacity to create a controlled assembly of parallel, periodic nanofiber arrays.

References

[1] W. E. Teo, S. Ramakrishna, Nanothecnology 17, R89 (2006)
[2] D. Sun, C. Chang, S. Li, L. Lin, Nano Lett. 6, 839 (2006)
[3] C. Chang, K. Limkrailassiri, L. Lin, Appl. Phys. Let. 93, 123111 (2008)

Local Order in Liquid Al-Cu, Al-Co and Al-Cu-Co Alloys

O. S. Roik[a], O. V. Samsonnikov, V. P. Kazimirov, S. M. Galushko, V. E. Sokol'skii

Chemical Department, National Taras Shevchenko University of Kyiv, 64 Volodymyrska str., Kyiv, UA-01033, Ukraine

[a] *e-mail: sasha78@univ.kiev.ua*

With an increasing number of research works devoted to the study of the atomic structure of liquid Al-based alloys, some features begin to attract more and more attention. The first feature is a prepeak in the $S(Q)$ function on the low-Q values side of the first peak [1]. The second feature is the dominance of the icosahedral short-range order (ISRO) in stable and undercooled liquid Al-TM and Al-TM_1-TM_2 alloys [2].

The present paper is devoted to examination of the local order of selected ternary alloys with compositions $Al_{60}Cu_{29}Co_{11}$, $Al_{63.9}Cu_{19.4}Co_{16.3}$ and $Al_{71}Co_6Ni_{23}$. The $Al_{60}Cu_{29}Co_{11}$ and $Al_{71}Co_6Ni_{23}$ melts were studied at 1413 K and 1483 K, respectively. A liquid $Al_{63.9}Cu_{19.4}Co_{16.3}$ alloy belonging to the field of the quasicrystalline (QC) phase formation was studied at 1373, 1443 and 1543 K. The study comprised the following steps: an X-ray diffraction experiment ($\lambda = 0.071069$ nm), calculations of the structure factor (SF) and the pair correlation function (PCF), reconstruction of the 3D-models of the liquid alloys from the SF experimental curves using the Reverse Monte Carlo (RMC) method, and an analysis of the local and medium-range atomic ordering by means of the Voronoi diagram and the Delaunay tessellation.

The local and medium-range atomic ordering in ternary Al-Cu-Co liquid alloys should be analyzed on a comparative basis taking in account the ordering in liquid binary Al-Co and Al-Cu alloys [3].

A prepeak in the $S(Q)$ functions at $11 < \mathrm{Q/nm^{-1}} < 21$ was found for the all ternary melts. The intensity of the prepeaks decreased considerably with an increase in temperature. The prepeak in the $S(Q)$ was interpreted as a correlation in the arrangement of transition metal (TM) atoms in the range of 0.43–0.45 nm.

The TM atoms in the RMC simulated model were located in the second coordination sphere of TM atoms, suggesting a repulsion of the TM-TM first neighbors. The localization of Al-atoms in the first coordination sphere of TM atoms indicates the chemical short-range order (CSRO) in the Al-Cu-Co, Al-Cu and Al-Co melts. On the other hand, the prepeak in the SFs indicates an ordering beyond the first few nearest neighbor distances between the TM atoms, corresponding to a medium range order (MRO).

In accordance with the results of the RMC simulation, the prepeak may be caused by MRO in dense packed polytetrahedral clusters. These clusters are presented by

aggregates of pentagons consisting of close to perfect tetrahedra which are adjacent by faces. Atomic centers in a pentagon form vertices of a pentagonal bipyramid (decahedron). An aggregation of several decahedrons leads to the formation of icosahedral-type clusters which determines the icosahedral short-range order (ISRO). Therefore, the ISRO is a particular case of a general atomic ordering in dense-packed polytetrahedral clusters.

The CSRO of liquid binary Al-Co and Al-Cu-Co alloys in the Al-rich region is reminiscent of that occurring in solid phases. For example, the structure of Al-Co and Al-Co-Cu decagonal and decagonal approximant phases has been described as being dense-packed tenfold or fivefold symmetry decagonal clusters. These clusters are characterized by a decagonal ring of alternating aluminum and cobalt atoms that correlates with our results. Thus, the presence of dense-packed polytetrahedral clusters with a specific chemical-short-order contributes to the appearance of QCs phases in liquid Al-Co and Al-Cu-Co alloys.

References

[1] Brillo J, Bytchkov A, Egry I et al. 2006 *J. Non-Cryst. Solids* **352** 4008
[2] Schenk T, Simonet V, Holland-MoritzEgry D et al. 2006 *Europhys. Lett.* **65** 34
[3] Roik O, Samsonnikov O, Kazimirov V, and Sokolskii V 2009 *J. Mol. Liquids* **145** 129

Phase Transformations in Nanocomposites with Ferroelectrics in Restricted Geometry: Phase Transitions and Macroscopic Properties

E. Rysiakiewicz-Pasek[1], A. Naberezhnov[2], A. Fokin[2], P. Jagus[1], E. Koroleva[2], Yu. Kumzerov[2], L. Korotkov[3], M. Tovar[4], S. Vakhrushev[2]

[1] *Institute of Physics, Wroclaw University of Technology W. Wyspiańskiego 27, 50-370 Wroclaw, Poland*

[2] *A.F.Ioffe Physico-Technical Institute 26 Polytechnicheskaya, S.-Petersburg 194021, Russia*

[3] *Voronezh State Technical University Moskovskii pr. 14, Voronezh, 394026 Russia*

[4] *Hahn-Meitner-Institut Glinicker Strasse 100, D-14 109 Berlin, Germany*

It is known that the size effect results in modification of macroscopic properties of substances, especially if the characteristic size is comparable with the correlation length of the order parameter critical fuctuations.

The embedding of substances into the pores of natural or artificial porous matrices permits to produce a large quantity of nanocomposite materials (NCM) and to use powerful additional experimental methods: neutron scattering, heat capacity measurements, etc. In this contribution the effect of the so-called restricted geometry on the structure evolution and on the ferroelectric phase transitions is considered for model ferroelectric sodium nitrite ($NaNO_2$) and its solid solutions $(1-x)NaNO_2$ – $(x)KNO_2$ at $x = 0.05$ and 0.1. Porous glasses (a 3D random dendrite pore network with the average pore diameter of 320, 20, 7 and 3 nm), artificial opals (a 3D regular pore network with the cavity size of 20 nm, 55 nm and 100 nm) and a chrysotile asbestos – quasy-1D system of parallel channels about 6 nm in diameter were used as host matrices. The NCMs were prepared by immersing preliminary annealed matrices in melted substances. The temperature evolution of the structure was studied by neutron diffraction in the temperature interval from room temperature (RT) up to melting. The macroscopic properties were studied by dielectric spectroscopy (at a frequency diapason of 1 Hz – 2.5 MHz), small-angular neutron scattering (SANS), measurements of heat capacity and NNR. The conductivity, internal friction and shear elastic modulus were studied for NCM containing embedded sodium nitrite in the ferroelectric and paraelectric phases. The principle results were the following:

– The temperature dependences of the order parameter for different average sizes of the NCMs were obtained and the crossover from the first order PT to the second order PT was observed for nanoparticles smaller than 50 nm.

– A decrease in the average nanoparticle size led to a suppression of the incommensurate PT observed in the bulk and a reduction of the TC.

– Formation of a volume premelting state manifesting itself in the growth of ion mobility and the unit cell volume was observed above the TC.

– It was shown that the wetting substances formed dendrite coherent nanoclusters with the "diffraction" (and gyration) radius essentially larger than the average pore diameter. The nanoclusters became more compact with the increasing pore diameter.

Acknowledgements
This work was supported by the Wroclaw University of Technology and the RFBR (09-02-00329).

Doping Effect at Grain Boundary of $YBa_2Cu_3O_{7-y}$: Fe Ceramic System

W. Sadowski[1], P. Fiertek[1], J. M. Olchowik[2]

[1] *Department of Solid State Physics, Gdansk University of Technology Narutowicza 11/12, 80-233 Gdansk, Poland*

[1] *Institute of Physics, Lublin University of Technology Nadbystrzycka 38D, Lublin 20-618, Poland*

Doping effect at grain boundary of $YBa_2Cu_3O_{7-y}$ (YBCO) was studied by Fe doping. It was observed that the dopants preferentially occupy the grain boundary region and have significant effects on the supercurrent transport through the grain boundary. The microstructure and composition were determined by scanning electron microscope (SEM), transmission electron microscope (TEM), energy dispersive X-ray (EDX) analysis, and electron probe microanalyses (EPMA). DC SQUID magnetometer was used to measure the magnetization loops. J_c was deduced from the M(H) loops (with H$\|$c) by the Bean's model.

The Influence of the Annealing Temperature on the NdCeCuO-214 Crystals Surface

W. Sadowski[1], T. Klimczuk[1], J. M. Olchowik[2]

[1] *Department of Solid State Physics, Gdansk University of Technology Narutowicza 11/12, 80-233 Gdansk, Poland*

[1] *Institute of Physics, Lublin University of Technology Nadbystrzycka 38D, Lublin 20-618, Poland*

Superconductivity in the $Nd_{2-x}Ce_xCuO_{4-y}$ system can be obtained in a narrow range of the cationic and anionic stoichiometry. One possibility to enlarge this range is lowering oxygen concentration with preservation of the T' structure. The surface morphology of $Nd_{1.94}Ce_{0.06}CuO_{4-y}$ after heat treatment in a reducing atmosphere (argon) in the wide temperature range from 890 to 1120°C was studied using atomic force and scanning electron microscopes. It was observed that the "as-grown" $Nd_{1.94}Ce_{0.06}CuO_{4-y}$ single crystals the surfaces are flat with steps about two lattices parameters while a high-temperature reduction process ($T > 1080$°C) leads to a considerable deviation from the flatness. Elongated, rectangular crystalline features of the height between 30 and 120 nm can be observed. EDAX investigations showed that the objects are $Nd_{2-x}Ce_xCu_{1-z}O_{4-y}$, with $z = 0.3$.

Modeling Structure of Liquid Al

O. V. Samsonnikov, O. S. Muratov,
O. S. Roik, V. P. Kazimirov

Chemical Department, National Taras Shevchenko University of Kyiv
64 Volodymyrska str., Kyiv, UA-01033, Ukraine

asa_lord@univ.kiev.ua

Alloys based on aluminum find wide practical application due to lightness, rust resistance and other useful properties. An X-ray diffraction study of a sample of $Al_{0.86}Mn_{0.14}$ received by rapid cooling from a liquid state in 1984, showed a 5-fold axis to exist which disagreed with classical crystallography and led to obtaining the first quasicrystalline material. The subsequent research has shown that the majority of them possess a unique spectrum of physical and chemical properties and quasi crystalline phases are received from binary and ternary melts of aluminum with 3d metals by means of quenching from the liquid state. Thus, research of structural and dynamic properties of melts of aluminum above and below the melting point has huge fundamental and applied value.

A simulation of a structure of liquid aluminum was made at the temperatures of 633 K, 733 K, 833 K, 883 K, and in the range from 933 K to 1173 K with a step of 20 K with a classical molecular dynamics (MD) method. The modeling was made for NVT-ensembles of particles containing 10648 atoms of metal. The potential of interatomic interaction $U(R)$ was calculated within the theory of pseudopotential using Ashcroft's form factor [1].

The received structural models were analyzed by means of the Voronoi-Delaunay method. A break in the range of 890–940 K was observed on curves of temperature dependences of metrical and topological characteristics testifying a difference between the temperature dependencies of the structure of aluminum melts from stable and undercooled states. It was also noticed that the so-called icosahedral short-range order (ISRO) was displayed in melts with the decreasing temperature [2]. ISRO is realized as a special case of a more general polytetrahedral ordering in the stable and undercooled melts. It is shown that splitting of the second maximum of the pair distribution function, $g(R)$, is characteristic to polytetrahedral order in melts.

References

[1] V. Heine, M. L. Cohen and D. Weaire 1973 *The Pseudopotential Theory*, Mir (in Russian) 557
[2] K. J. Dong, R. S. Liu, A. B. Yu, R. P. Zou and J. Y. Li 2003 *J. Phys.: Cond. Mat.* **15** 743

Selective Confinement of Proteins by AFM for Characterization Studies

B. Sanavio[1,2], C. Grunwald[3], G. Legname[1,4,5], L. Casalis[1,2,5], G. Scoles[1,2,5,6]

[1] *SISSA – ISAS, International School for Advanced Studies Via Beirut 2-4, 34151 Trieste, Italy*

[2] *SISSA ELETTRA Nano Innovation Laboratory, Sincrotrone Trieste S.C.p.A. S.S. 14 Km 163.5, 34149 Basovizza, Trieste, Italy*

[3] *Johann Wolfgang Goethe-Universität Frankfurt am Main, Institute of Biochemistry Biocenter Max-von-Laue-Straße 9 D-60438 Frankfurt, Germany*

[4] *ELETTRA Structural Biology Laboratory, Sincrotrone Trieste S.C.p.A. S.S. 14 Km 163.5, 34149 Basovizza, Trieste, Italy*

[5] *IIT – Italian Institute of Technology, SISSA-ISAS. Unit, Via Beirut 2-4, 34151, Trieste, Italy*

[6] *CBM Srl – Cluster in Molecular Biomedicine S.S. 14 Km 163.5, 34149 Basovizza, Trieste, Italy*

This study aims at providing an AFM based platform for protein and eventually for infectious polypeptide detection and characterization. Biochemical activity and ligand induced structural changes in a protein surface confined by AFM have already been successfully reported [1,2]. AFM permits direct fabrication and optimization of nanoscale molecular arrays with a fine tuned control over the molecule density and distribution in a spatially confined region by means of a technique called nanografting [3]. Briefly, a self assembled monolayer of HS–$(CH_2)_{11}$–EG_3 is used as a reference surface in which Nitrilotriacetate (NTA) modified thiols (HS–$(CH_2)_{16}$–EG_3–NTA) are patterned at a submicrometre scale permitting oriented immobilization of histidine tagged Fabs. Specifically, recombinant mouse prion protein residue 89 to 230 (recMoPrP(89–230)) was selectively oriented and anchored on submicrometer sized antibody arrays. Two monoclonal antibody fragments (Fab), namely cloneP and D18 can bind site-specifically recMoPrP(89–230) with sub nM affinity thus permitting its trapping on the surface in a controlled and oriented manner and therefore exposing it in a different orientation to the AFM tip. The molecular dimensions and the response to different environmental conditions were studied The device characterization as well as the effect of the fabrication parameters over MoPrP immobilization through density, concentration, and pH dependent studies will be presented.

References

[1] Staii C, Wood D W, Scoles G 2008 *JACS* **130** 640
[2] Staii C, Wood D W, Scoles G 2008 *Nano Letters* **8** 2503
[3] Liu M and Liu G-Yu 2005 *Langmuir* **21** 1972

Structural and Magnetic Properties of Fe and FePt Nanoparticles in MgO Synthesized by Ion Implantation

A. Shalimov[1], K. Potzger[1], D. Geiger[2], G. Talut[1], A. Misiuk[3], S. Zhou[1], C. Baehtz[1], J. Fassbender[1]

[1] *Forschungszentrum Dresden – Rossendorf*
Bautzner Landstr. 400, 01328 Dresden, Germany

[2] *Technical University, Institute of Structure Physics*
Zellescher Weg 16, 01069 Dresden, Germany

[3] *Institute of Electron Technology*
Al. Lotników 32/46, 02-668 Warsaw, Poland

Fe and FePt nanoparticles were synthesized in MgO (001) single crystals by Fe^+ and Pt^+ ion implantation using fluencies from $3 \cdot 10^{16}$ to $3 \cdot 10^{17}$ cm^{-2}. The magnetic and structural properties of Fe and FePt nanoparticles were studied using magnetometry in a temperature range from 2 K to 300 K, as well as by X-ray diffraction, transmission electron microscopy and Mössbauer spectroscopy. The experimental temperature and the isothermal field dependences of the magnetic moment were modeled using the theoretical Preisach approach of magnetization. The Theoretical computations allowed us to obtain an absolute concentration of ferromagnetic nanoparticles, their average spontaneous moment, mean coercive field and short-range interaction field, as well as a set of temperature-dependent characteristics. It was also found that Fe nanoparticles were presented by two structural phases – fcc (γ-Fe) and bcc (α-Fe). The content of ferromagnetic Fe and FePt phase increased at higher fluences of the implanted ions and after high temperature annealing. In the case of MgO implanted with Fe^+, we found a strong correlation between a fraction of the α-Fe phase and the strain state of nanoparticles, which depended on a temperature of implantation and the thermal expansion coefficient of the host crystal.

Acknowledgements
This work was supported by DFG under the Project No. PO1275/2-1 "SEMAN".

Photovoltaic Effect in Hybrid Heterojunction Formed from Cadmium Telluride and Zinc Perfluorophthalocyanine Layers

R. Signerski, G. Jarosz, B. Kościelska

Faculty of Applied Physics and Mathematics, Gdansk University of Technology
Narutowicza 11/12, 80-233 Gdansk, Poland

Hybrid organic-inorganic heterojunctions have recently attracted a lot of attention due to their potential application in optoelectronic devices, in particular, in heterojunction solar cells [1]. In our work the preliminary experimental results dealing with the photovoltaic effect in systems based on the cadmium telluride/zinc perfluorophthalocyanine ($CdTe/F_{16}ZnPc$) heterojunction will be presented. This type of a heterojunction has not been investigated yet. Cadmium telluride is a semiconductor widely applied in inorganic thin-film solar cells as an absorber of sunlight [2]. In our systems however the thin layers of CdTe with a thickness from the range of 60–600 nm are mainly applied as layer transporting holes. The other material forming heterojunction, $F_{16}ZnPc$, exhibits a high light absorption within the range of 550–900 nm and a relatively high mobility of electrons [3].

We investigated the photovoltaic effect in the following vacuum-evaporated systems: $ITO/CdTe/F_{16}ZnPc/BCP/Ag$ and $ITO/F_{16}ZnPc/CdTe/Au$. The layer of bathocuproine (BCP) was added in order to improve the electric properties of the Ag electrode. Measurements of the current-voltage curves of the systems without illumination and under illumination as well as of the dependence of the short-circuit current and open-circuit voltage on wavelength and light intensity were performed. In the dark, our systems exhibited a strong effect of current rectification. The illumination of the systems led to the photovoltaic effect resulting from exciton dissociation at the $CdTe/F_{16}ZnPc$ interface. The $ITO/CdTe/F_{16}ZnPc/BCP/Ag$ system exhibited higher values of short-circuit current and open-circuit voltage in comparison with the $ITO/F_{16}ZnPc/CdTe/Au$ system.

Acknowledgements
This work has been supported by Polish Ministry of Science and Higher Education with a grant for the years 2006–2009 under Program No. 3T11B06530.

References

[1] Sun S-S and Sariciftci N S (Eds) 2005 *Organic Photovoltaics*, Taylor&Francis
[2] Luque A and Hegedus S (Eds) 2003 *Handbook of Photovoltaic Science and Engineering*, Wiley
[3] Brinkmann H, Kelting C, Makarov S, Tsaryova O, Schnurpfeil G, Wöhrle D and Schlettwein D 2008 *Phys. Stat. Sol.* **205** 409

Structure of Condensed Films of Molecular Cryocrystals

A. A. Solodovnik, V. V. Danchuk

B.Verkin Institute for Low Temperature Physics and Engineering
National Academy of Sciences of Ukraine
47 Lenin Ave. Kharkov 61103, Ukraine

Electron diffraction studies of the structural characteristics of CO_2, N_2O deposits and their alloys are presented. Solid nitrous oxide and carbon dioxide belong to the class of molecular crystals consisting of linear molecules which is a convenient model system for investigating topical problems in the physics of solids: random systems, cluster phase transitions, structural-glass transformations, disordered media [1–3]. An N_2O (N–N–O) molecule differs from CO_2 (O–C–O) in terms of symmetry and the dipole moment. Both crystals are very similar physically and have a cubic (fcc) lattice in which the axes of molecules are directed along one of the four spatial diagonals of a cube (Pa3 space group) at the equilibrium vapor pressure. In the case of nitrous oxide, the molecules are "head-tail" disoriented because a long-range order is absent (the Pa3 symmetry is observed "on average"). A phase transition attributed to dipolar ordering may occur below 11 K according to the calculation [4]. The number of transformations can be still greater in case of small objects because the change in the structure of the deposited particles can also be caused by the size factor. Possible existence of icosahedral CO_2 clusters was considered in [5], however, according to the experimental data [6] the CO_2 free clusters had the Pa3 structure inherent to the bulk crystal. The interest towards a solid solution of CO_2–N_2O is mainly associated with the investigation of the phase transitions due to the molecule disorientation and the formation of an orientational glass state [7]. The effect of dilution on the orientational order was investigated in CO_2-based alloys and it was established that the rare gas doping lowered the potential barrier hampering the molecule rotation [8,9].

Investigations were carried out by transmission high-energy electron diffraction (THEED) using a helium cryostat. The specimens were prepared directly *in situ* by quench depositing room-temperature gas onto a composite substrate which consisted of amorphous carbon and polycrystalline aluminum films. Al substrate film served as the internal standard. The relative lattice parameter measurement error was usually about 0.1 percent. 99.99 percent pure gases were used in our investigations. The composition of the investigated mixtures was varied within the entire range of mutual concentrations from 0 to 1. Measurements were taken in the temperature range between 5 and 65 K. The size of the samples ranged from 2 to 45 nm. As the procedure permitted to detect a newly formed phase, the dimensions of its domains were of the order of several nm, diffraction patterns were recorded continuously during the condensation. Investigating the initial stage of sample preparation was important for understanding the crystalline phase formation mechanism in pure solids and solutions.

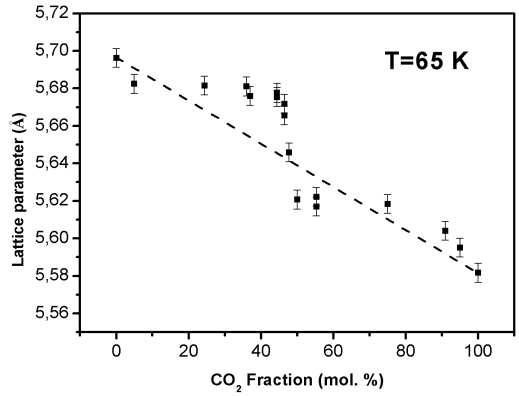

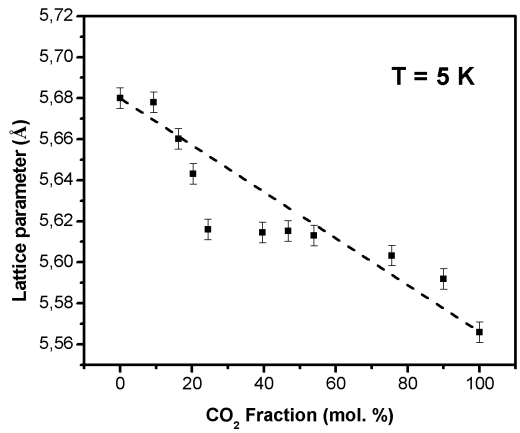

Pure nitrous oxide and carbon dioxide

During film deposition the size-dependent structure of the N_2O and CO_2 samples was investigated as a function of both the temperature and the dimensional factor. It was established that CO_2 condensates had a structure inherent to a bulk crystal in the temperature range of 5-60 K. However, the degree of orientational disordering of CO_2 molecules increased with a decrease in the dimension, this was reflected in a decrease in the relative intensity of "superstructural" diffraction peaks. The size effect influence on the orientational order was investigated in CO_2 and N_2O films. The unusual result were the structural transformations of N_2O deposits below 11 K. At the initial stage of quenching the condensates had a structure in which "superstructural" diffraction peaks were absent. The amount of the deposited N_2O gas having been increased further, the initial phase transformed into an amorphous modification and then a transition into the Pa3 phase occurred. It can be assumed that the distinctions of anisotropic interaction of both crystals determined the character of the evolution of the structures.

CO_2-N_2O mixed crystals

The crystallographic structure and the existence range of solid solutions of CO_2-N_2O alloys were determined using deposits 30 nm in thickness. It was established that CO_2 with N_2O formed homogeneous solid solutions in the temperature range of 5-65

K at any concentration and the molecules mutually replaced one another in lattice sites. The structure of solid solutions belongs to the ordered state Pa3 symmetry. Like pure components, solid solutions do not display any transition from an orientationally ordered to disordered phase. The lattice parameter concentration dependencies at $T =$ 5 K and $T = 65$ K have the same character and differ from Vegard's approximation (ee figures). The curves have a step in the lattice parameter which is observed at $T = 65$ K for an equimolar composition and shifts to 25 mol % CO_2 fraction at helium temperature. The presence of the step means that the range between N_2O-based and CO_2-based solutions is critically narrow. A possible explanation of this phenomenon is suggested. The solution lattice reconstruction is connected with conditions in which the non-equivalency of the ends of N_2O molecules and strong anisotropic interaction in the crystals facilitate the transition from an N_2O-based to CO_2-based solution. The influence of doping on the orientational order in CO_2 and N_2O lattices is studied. In cryocrystals formed from linear 3-atom molecules the direct anisotropic intermolecular interaction plays a decisive role in the solid state formation.

References

[1] V. G. Manzhelii, Yu. A. Freiman, M. I. Klein, and A. A. Maradudin (eds) 1997 *The Physics of Cryocrystals*, AIP Press. Woodbury

Direct Synthesis of Tetragonal $L1_0$ Ferromagnetic FePt Nanoparticles

M. Villani[1], G. Calestani[2], M. Solzi[3], C. Pernechele[3]

[1] *Istituto IMEM-CNR*
Parco Area delle Scienze 37/A, 43124 Parma, Italy

[2] *Dipartimento di Chimica GIAF, Università di Parma*
viale G. P. Usberti 17/A, 43100 Parma, Italy

[3] *Dipartimento di Fisica, Università di Parma – CNISM*
viale G. P. Usberti 7/A, 43100 Parma, Italy

Stoichiometric FePt nanoparticles in the tetragonal $L1_0$ phase, for which a very high uniaxial magnetocrystalline anisotropy ($K_u = 6.6 \cdot 10^7$ erg/cm^3) is associated to a theoretical thermal stability of magnetization for grains with a size as small as 3 nm, represent one of the leading candidates for the next generation high-density recording media [1]. Unfortunately as-synthesized FePt nanoparticles, usually obtained by a soft chemical route through the well-known polyol process, are arranged in a disordered fcc structure characterized by a low magneto-crystalline anisotropy and a superparamagnetic behaviour at room temperature. The transition to the tetragonal ferromagnetic structure is usually obtained by post-annealing of the as-synthesized FePt nanoparticles at temperatures ranging from 500 to 650°C in a reducing atmosphere. However, in these conditions, the protective agent surrounding the as-synthesized particles is thermally decomposed and the nanoparticles aggregate by sintering, so that both the average grain size and the dimensional polydispersity increase with increasing temperature or annealing time [2].

Since the dimensional control can be efficiently operated only during the synthesis, an alternative procedure to obtain monodisperse ferromagnetic FePt nanoparticles should take into account the possibility of carrying the synthesis at higher temperatures, sufficient to ensure the direct formation of the ordered $L1_0$ phase. In the present work the use of solvents and surfactants possessing an elevate thermal stability, that we considered as the key factor for a successful application of similar strategies, was explored. We demonstrated a possibility of obtaining monodispersed FePt nanoparticles ordered in an $L1_0$ phase without further annealing by using poly(N-vinyl-2-pyrrolidone) (PVP) and Triton X-100 as the protective agent and reaction solvent respectively. The synthesis was carried out in nitrogen atmosphere using $Fe(acac)_3$ and $Pt(acac)_2$ (acac = acetylacetonate) as metallic precursors: monodisperse nanoparticles, ranging from 5 to 7 nm depending on the synthesis conditions, were obtained. For reaction temperatures exceeding 280°C, the nanoparticles are ferromagnetic at RT. The coercive field at RT strongly depends on the reaction temperature, increasing from 405 Oe to 1 kOe (see the upper figure) when the temperature is raised from

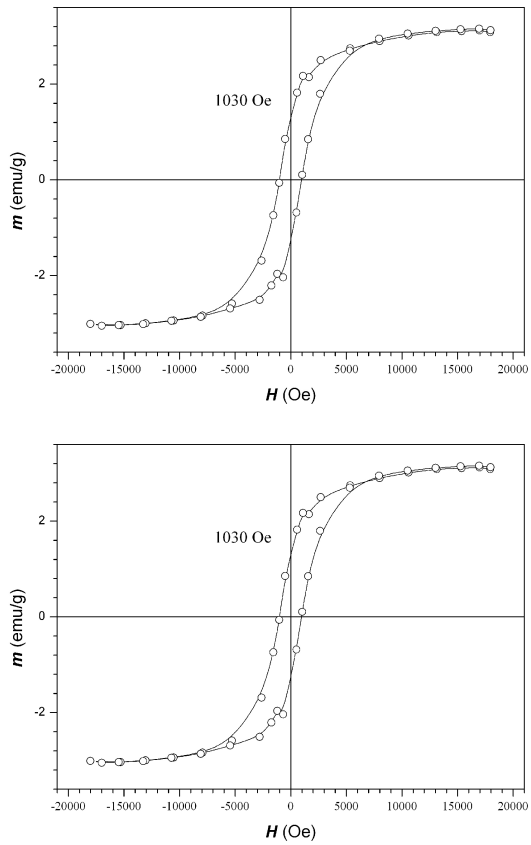

290 to 330°C. The increase of coercive field is strictly related to the increase in the structural order, revealed by X-ray (see the lower figure) and electron diffraction.

References

[1] S. Sun et al., Science 287 (2000) 1989
[2] S. Sun, Adv. Mater. 18 (2006) 393

Surface Superconductivity in Transverse Electric Field in Two-component Model

P. Konsin[a], B. Sorkin[b]

Institute of Physics, University of Tartu
Riia 142, 51014 Tartu, Estonia

[a] *konsin@fi.tartu.ee*
[b] *sorkin@fi.tartu.ee*

In [1,2] the influence of the transverse electric field $\boldsymbol{E}$ on the superconducting transition temperature T_c of cuprate films is studied. The theory [1,2] considers the bulk properties of the superconducting films caused by the external electric field. The surface superconductivity in cuprates in the electric field is investigated [3] on the basis of the one-band Ginzburg-Landau equations in the frames of the BCS theory. The shift of T_c in the electric field in [3] occurs through the DeGennes boundary conditions depending also on the correlation length ξ and $\boldsymbol{E}$. The mechanism of the high-T_c superconductivity in cuprates is a question of debate. In [4] the two-component theory of the superconductivity in cuprates is developed (for a two-band model of superconductivity in MgB_2 see for example [5]) the two-band model is characterized by the two correlation lengths of the Cooper pairs ξ_1 and ξ_2. These correlation lengths calculated on the basis of various microscopic two-band models [6–8] are real quantities (not imaginary) and $\xi_1 \gg \xi_2$. In our approach the surface superconductivity is considered on the basis of the two-band Ginzburg-Landau equations. The DeGennes boundary conditions in this case depend on ξ_1 , ξ_2, $\boldsymbol{E}$ and the thickness L of films. We have found that T_c lowers or increases in the field $\boldsymbol{E}$ (in dependence on the direction of $\boldsymbol{E}$) and can oscillate with thickness L through ξ_2 .

This work is supported by Estonian Science Foundation grant No. 7389.

References

[1] P. Konsin, B. Sorkin, Phys. Rev. B 58, (1998), 5795
[2] P. Konsin, B. Sorkin, J. Phys. Condens. Matter 13, (2001), 10031
[3] P. Lipavsky, K. Moravetz *et al.*, Phys. Rev. B 73, (2006), 052505
[4] N. Kristoffel, P. Konsin *et al.*, Riv. Nuovo Cimento 17, (1994), 1
[5] P. Konsin, B. Sorkin, Supercond. Sci. Technol. 17, (2004), 1472–1476
[6] Yu. M. Poluektov *et al.*, Fiz. Nizkih Temp. 15, (1989), 1259
[7] P. Konsin, B. Sorkin, Physica C, 435, (2006), 16
[8] A. E. Koshelev, A. A. Varlamov *et al.*, Phys. Rev. B 72, (2005), 064523

Synthesis, Crystal Structure and Characterization of a New Monohydrate NCS^- and a Schiff Base Copper(II) Complex

A. Makal[1], K. Woźniak[1], A. Szady-Chełmieniecka[2], E. Tomaszewicz[2], G. Leniec[3], S. M. Kaczmarek[3], E. Grech[2]

[1] *Department of Chemistry, University of Warsaw, Poland*

[2] *Department of Inorganic and Analytical Chemistry*
West Pomeranian University of Technology, Szczecin, Poland

[3] *Institute of Physics*
West Pomeranian University of Technology, Szczecin, Poland

Transition metal complexes containing Schiff base ligands are of great interest due to antibacterial activities. In this paper we present a synthesis of a new copper(II) monohydrate complex derived from NCS^- and Schiff base (condensation N,N-dimethyl-ethane-1,2-diamine with 2-hydroxy-4-methoxybenzoaldehyde) which was obtained using a similar procedure previously reported in [1]. The newly prepared compound was characterized by X-ray single crystal diffraction, DTA-TG and EPR techniques.

Using the X-ray pattern a structure is proposed for a compound and local symmetry of Cu^{2+} ions forming complexes with three nitrogen and one oxygen atoms.

Experimental data obtained from DTA-TG studies show the mass loss between 328 and 367 K for the analyzed complex. The observed mass loss was equal to 4.91% (the calculated value – 4.99%) and is attributed to the loss of one water molecule per molecule of complex. The final residue obtained after DTA-TG examinations was analyzed by the XRD method and was identified as CuO.

The magnetic resonance spectra of this sample in the powder form and as selected platelets of single crystal were registered in the 90–300 K temperature range and analysed using a computer program to extract anisotropic g_i-factors ($g_{xy} = 2.145$ and $g_z = 2.0139$). For powders, a typical powder pattern of an axially compressed copper complex with hyperfine structure was observed. These spectra obviously belong to Cu^{2+}, for which $S = 1/2$ and $I = 3/2$. Since the line width is broad, different kinds of cooper isotopes hyperfine lines are not clearly resolved. The integrated intensity of the spectra calculated for the nitrogen temperature range revealed the Curie-Weiss type behaviour with the Curie-Weiss constant $T_c = 18$ K evidencing the ferromagnetic interaction between copper ions.

References

[1] Y.-X. Sun, D.-S. Kong, G. Yang, Z.-L. You: Polish J. Chem. 80 (2006) 1457–1463

Solid-State Synthesis and Characterization of New Cadmium and Rare-earth Metal Molybdato-tungstates $Cd_{0.25}RE_{0.50}(MoO_4)_{0.25}(WO_4)_{0.75}$

E. Tomaszewicz[1], G. Dąbrowska[1], S. M. Kaczmarek[2], H. Fuks[2]

[1] *Department of Inorganic and Analytical Chemistry*
West Pomeranian University of Technology
Al. Piastów 42, 71-065 Szczecin, Poland

[2] *Institute of Physics*
West Pomeranian University of Technology
Al. Piastów 17, 70-310 Szczecin, Poland

White light-emitting diodes (WLEDs) find wide applications as backlights for portable electronics, architecture or medical lighting, and first of all, as a white light source to replace traditional incandescent and fluorescent lamps. Host candidates for luminescent applications are doped and undoped double rare-earth molybdates and tungstates with a scheelite type structure such as: $K_{1-x}Eu_x(MoO_4)_y(WO_4)_{2-y}$; $LiEu(MoO_4)_x(WO_4)_{2-x}$ and $NaM(MoO_4)_x(WO_4)_{2-x}$:Eu where M = Gd, Y.

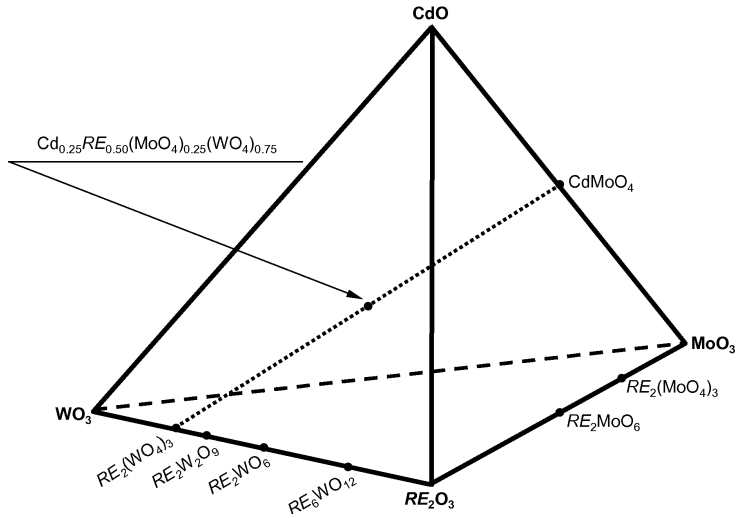

Figure 1: Concentration tetrahedron of the CdO-WO_3-RE_2O_3-MoO_3 system with a position of $Cd_{0.25}RE_{0.50}(MoO_4)_{0.25}(WO_4)_{0.75}$

In the present work, new cadmium and rare-earth metal molybdato-tungstates with the formula $Cd_{0.25}RE_{0.50}(MoO_4)_{0.25}(WO_4)_{0.75}$ where RE = Pr-Dy were prepared by the high-temperature solid-state reaction according to the following equation:

$$CdMoO_{4(s)} + RE_2(WO_4)_{3(s)} = 4\ Cd_{0.25}RE_{0.50}(MoO_4)_{0.25}(WO_4)_{0.75(s)}$$

The obtained compounds crystallized in the scheelite type structure. At the concentration range above 50.00 mol % of $CdMoO_4$ in initial $CdMoO_4/RE_2(WO_4)_3$ mixtures, new cadmium and rare-earth molybdato-tungstates formed, together with $CdMoO_4$, $Cd_xRE_{2-2x}(MoO_4)_x(WO_4)_{3-3x}$ solid solutions with a scheelite type structure. New cadmium and rare-earth molybdato-tungstates melted congruently at the temperatures above 1080° C. Their lattice parameters and cell volume decreased linearly with the increasing atomic number of a lanthanide. The melting point and lattice constants of the $Cd_xRE_{2-2x}(MoO_4)_x(WO_4)_{3-3x}$ solid solutions decreased with the $CdMoO_4$ content in an initial $CdMoO_4/RE_2(WO_4)_3$ mixture. The $Cd_{0.25}RE_{0.50}(MoO_4)_{0.25}(WO_4)_{0.75}$ compounds as well as the $Cd_xRE_{2-2x}(MoO_4)_x(WO_4)_{3-3x}$ solid solutions were studied also by the IR and EPR techniques.

Obtaining and Dielectric Properties of Ferroelectric Glassceramics on the Basis of $Sn_2P_2S_6$

V. M. Rubish[1], B. R. Tsizh[2a], S. M. Gasynets[1], O. G. Guranich[1], P. P. Guranich[3]

[1] *Uzhgorod Scientific-Technological Center of the Institute for Information Recording NASU 4 Zamkovi Skhody Str., 88000 Uzhgorod, Ukraine*

[2] *Kazimierz Wielki University in Bydgoszcz 30 Chodkiewicza, 85-064 Bydgoszcz, Poland*
[a] *tsizhb@ukw.edu.pl*

[3] *Uzhgorod National University 46 Pidhirna Str., 88000 Uzhgorod, Ukraine*

Chalcogenide vitreous materials on the basis of ferroelectric-semiconductor tin hipothiodiposphate ($Sn_2P_2S_6$) arouse considerable practical and scientific interest, for there is a possibility of forming crystalline inclusions of targeted morphology ferroelectric properties in a matrix of such glasses. Moreover, no data concerning the existence of glasses on the basis of $Sn_2P_2S_6$ are to be found in scientific papers. The peculiarities of obtaining and the dielectric properties of glassy alloys $(Sn_2P_2S_6)_{100-x}(As_2S_3)_x$ $(55 \leq x \leq 100)$ and the ferroelectric glassceramics formed on their basis are studied in the present paper.

$Sn_2P_2S_6$-As_2S_3 system glasses were obtained by vacuum melting of corresponding mixtures of components. The homogenization temperature for the system was 850–1100 K and the melting time was 36–48 hours. The melts were cooled in the air and in cold water (273 K).

The temperatures of the thermal effects, i.e., glass forming T_g, crystallization T_{c_0} and T_{c_m} (beginning and maximum) and melting T_m were determined by the DTA method at different rates (q).

It was established with regard to the studied glasses in the conditions of continuous heating that the prevailing mechanism crystallization with a stable phase separation of tin hipothiodiposphate was taking place in the temperature range of $T_g - T_c$. The formation of nanosized crystals $Sn_2P_2S_6$ in a glass matrix at heating and their growth were accompanied by anomalies in the temperature dependences of dielectrical permittivity (ε) and dielectric loss angle tangent ($\operatorname{tg}\delta$). The glass crystallization was accompanied by a sharp increase in ε and $\operatorname{tg}\delta$. A mechanism of forming $Sn_2P_2S_6$ nanocrystals in a glass matrix was suggested.

The effect of annealing regimes on the dielectric properties of the studied materials was studied. The maxima in a wide temperature range conditioned by smeared phase transitions in crystalline inclusions $Sn_2P_2S_6$ were revealed on $\varepsilon(T)$ and $\operatorname{tg}\delta(T)$ dependences of the crystallized samples.

Photoluminescence Characteristics of Green and Blue Emitting Alq_3 Organic Molecules in Crystals and Thin Films

T. Tsuboi[1], Y. Torii[2]

[1] *Faculty of Engineering, Kyoto Sangyo University*
Kamigamo, Kyoto 603-8555, Japan

[2] *Iwatani Chemical Engineering Ltd.*
Bodaiji, Konan, Shiga 520-3242, Japan

Organic molecule tris(8-hydroxyquinoline) aluminum (Alq_3) is widely used in organic light emitting diodes (OLEDs) as electron transport material and green emitting material. Its optical properties have been widely studied, but no detailed study has been performed for the solid solvation effect and for vibronic structure in the emission spectra. For example, it is not established whether the vibronic structure is present in thin films.

Alq_3 was synthesized by mixing 8-quinolinol and $Al(OH)_3$ (the mixing ratio is 2:1) in water at 95°C. The reaction time of 24 h gives yellow-color Alq_3 powder consisted of microcrystals with α-phase, while the reaction time of 100 h gives white-color Alq_3 powder consisted of microcrystals with γ-phase.

Crystals of Alq_3 with α- and γ-phases give green and blue emission bands, respectively. The photoluminescence quantum efficiency was estimated as 42% and 25% for the powders of α- and γ-phases, respectively. They exhibit vibronic structure clearly at the high-energy side at low temperatures below 30 K, while a structure-less broad band appears at the low-energy side. The vibronic structure is different between the two samples. The Huang-Rhys factor was estimated from the vibronic structure at 10 K, leading to clarification for different configuration between the ground and excited states. The photoluminescence (PL) spectra change with variation of excitation wavelength. Excitation with light of shorter wavelength of $\lambda < 400$ nm gives PL spectrum with vibronic structure, while excitation with light of longer wavelength gives PL spectrum with a symmetric broad band. From these results, it is suggested that several conformations are presented. The same results were also obtained for neat Alq_3 thin films which were evaporated thermally in vacuum or by spin-coating. Relationship between the presence of *mer*- and *fac*-Alq_3 isomers and formation of various crystal phases is discussed, together with the relation with α- and γ-phases.

EPR/FMR Study of Nanocrystalline Hematite–Ilmenite Solid Solutions

N. Guskos[1,2], G. Żołnierkiewicz[2], J. Typek[2], A. Guskos[2], D. Petridis[3]

[1] *Solid State Section, Department of Physics, University of Athens Panepistimiopolis, 15 784 Zografos, Athens, Greece*

[2] *Institute of Physics, West Pomeranian University of Technology Al. Piastów 48, 70-311 Szczecin, Poland*

[3] *NCSR "Demokritos" Aghia Paraskevi Attikis, Athens, Greece*

Nanocrystalline hematite-ilmenite (γ-Fe_2O_3, $FeTiO_3$) solid solutions with small concentration of hematite were prepared. The magnetic resonance spectra were investigated in different temperature regions. The magnetic resonance spectra were fitted by two Lorentzian lines at room temperature centered at $H_r = 300.4(1)$ mT ($g_{\text{eff}} = 2.224(1)$) and $H_r = 335.3(1)$ mT ($g_{\text{eff}} = 2.015(1)$) with linewidth $\Delta H_{pp} = 83.0(1)$ mT and $\Delta H_{pp} = 54.0(1)$ mT, respectively. The temperature dependence of the resonance lines suggested that the first line arose from the ferromagnetic agglomerates (ferromagnetic resonance (FMR)) [1] and the second line from the isolated high spin trivalent iron(III) ions (electron paramagnetic resonance, EPR). The position of the resonance line and the value of linewidth at room temperature was consistent with a small concentration of the γ-Fe_2O_3 in a non-magnetic matrix [1]. The temperature derivate $\Delta H_r/\Delta T$ was over two times greater than observed for other matrices. This indicates that the reorientation processes of the magnetic moments in nanocrystalline hematite-ilmenite solid solutions (γ-Fe_2O_3, $FeTiO_3$) are more intense.

References

[1] N. Guskos, V. Likodimos, S. Glenis, M. Maryniak, M. Baran, R. Szymczak, Z. Roslaniec, M. Kwiatkowska, and D. Petridis, *J. Nanosci. Nanotech.* 8, 2127 (2008)

Magnetic Resonance Study of $Sb_3V_2Mo_3O_{21}$

J. Typek[1], N. Guskos[1], G. Żołnierkiewicz[1], E. Filipek[2]

[1] *Institute of Physics,*
West Pomeranian University of Technology
Al. Piastów 48, 70-311 Szczecin, Poland

[2] *Department of Inorganic and Analytical Chemistry*
West Pomeranian University of Technology
Al. Piastów 42, 71-065 Szczecin, Poland

The $Sb_3V_2Mo_3O_{21}$ compound is formed in the three-component oxide system a-Sb_2O_4-V_2O_5-MoO_3 from an appropriate amount of these oxides using the solid-state reaction method [1]. It crystallizes in a rhombic system ($Z = 4$) with the following values of unit cell parameters: $a = 2.0241$ nm, $b = 0.8449$ nm, $c = 0.8169$ nm at room temperature. An electron paramagnetic resonance (EPR) study of $Sb_3V_2Mo_3O_{21}$ was carried out in the 4–290 K temperature range. A comparison with the $VOSO_4 \cdot 5H_2O$ intensity standard revealed that only 11.3% of all vanadium ions in $Sb_3V_2Mo_3O_{21}$ are paramagnetic V(IV) species. The temperature dependence of the calculated EPR parameters (g-factor, linewidth, integrated intensity) was studied and the obtained results are correlated with the proposed magnetic properties of V(IV) single ions and clusters.

References

[1] Filipek E 2001 *J. Therm. Anal. Calorim.* 64 1095 1

Magnetic Resonance Study of Poly(ether-block-ester) Copolymers with Ferrocene Units

J. Typek, N. Guskos, G. Żołnierkiewicz, A. Szymczyk

Institute of Physics, West Pomeranian University of Technology
Al. Piastów 48, 70-311 Szczecin, Poland

The poly(ether-block-ester)s (PEEs) based on poly(butylene terephthalate) (PBT) which form the hard phase, and poly(oxytetramethylene) (PTMO) as the soft phase are a widely known class of thermo-plastic elastomers. In this work the PEE was obtained using 1,1'-ferrocedimetoxy as the catalyst. A small amount (1–2 mol %) of ferrocene units incorporated into a polyester hard block of PEE enhanced the tensile properties and thermal stability of the PEE.

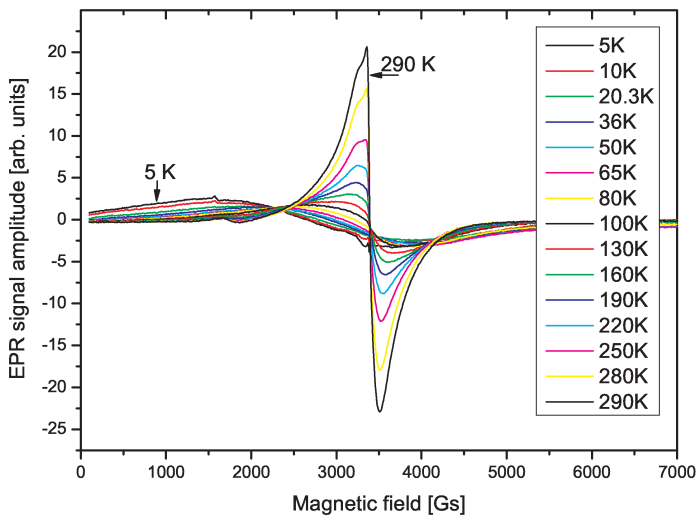

An electron paramagnetic resonance (EPR) study of the samples with different concentration of ferrocene units and different proportions of hard and soft segments (50/50 and 30/70) was carried out in the 4–290 K temperature range. The temperature dependence of the EPR parameters (linewidth, g-factors, integrated intensity) was investigated and the magnetic properties of copolymer were correlated with the electronic structure of the free radical.

Influence of Ni-intercalative Modification of Nanoporous Carbon on Structure and Properties of Electric Double-layer at Boundary with Electrolyte

B. Ya. Venhryn[1a], I. I. Grygorchak[1], S. Mudry[2b], Yu. O. Kulyk[2]

[1] *L'viv Polytechnic National University, 12 St. Bandera Str., 79013 L'viv, Ukraine*

[a] *venhryn_b@ukr.net*

[2] *Ivan Franko L'viv National University, 8 Kyrylo and Mefodiy Str., 79005 L'viv, Ukraine*

[b] *mudry@physics.wups.lviv.ua*

Nowadays it is obvious that a successful way to improve the working characteristics of capacitors with an electric double-layer is an effective combination of the optimal porous structure of activated carbon with its electronic structure which could be responsible for the unblocking of the Helmholtz capacity by the volume charge capacity in solid state. The chemical methods which are commonly used for modifying a porous structure are incapable at the same time of changing the electronic structure in a purposive way.

It is clear that this problem should be investigated in order to find a method for its practical realization. If to analyze the recent works, it can be concluded that in most of them the ways to improve the supercapacitors without motivation are related only to a modification of the porous structure or inoculation of the surface by some functional redox-groups. In this work we propose to use the Ni-intercalative technology which, while improving the porous structure with a simultaneous Ni injection into the structure of activated carbon, provides an increase in the free charge carriers concentration.

X-ray diffraction studies were carried out within a wide range of diffraction angles by means of a DRON-3 diffractometer. The Bragg-Brentano focusing geometry was used (Θ–2Θ scanning regime). A detail analysis of the principal diffusive maximum profile revealed its asymmetric shape and allowed us to conclude about the formation of carbon nanoclusters with a graphite-like short range order. The existence of nanopores was also established. The sizes of nanopores and their distribution were determined by means of the X-ray small angle scattering method.

Impedance measurements were carried out within frequency interval (10^{-3}–10^{6} Hz) at constant bias from interval $[-1, +1]$ V and used to obtain volt-farad dependencies. The De Levie equivalent electric circuit was modified by a structural chain, representing the volume charge capacity in activated carbon in order to model the obtained Nyquist diagrams. These data as well as the measured cyclic voltamperograms of electrochemical cells allowed us to determine the Fermi level change due to the modification and find the hierarchy in influences on the material's specific capacity and changes of the porous structure.

Structure vs Catalytic Activity in Carbon Supported Pt-based Catalysts

A. Witkowska[1], G. Greco[2], A. Moretti[3], G. Giuli[4], R. Marassi[3]

[1] *Department of Solid State Physics, Gdansk University of Technology Narutowicza 11/12, 80-233 Gdansk, Poland*

[2] *Department of Physics, University of Camerino via Madonna delle Carceri 9, Camerino (MC), Italy*

[3] *Chemistry Department, University of Camerino via S. Agostino 1, Camerino (MC), Italy*

[4] *Earth Science Department, University of Camerino via G. III da Varano, Camerino (MC), Italy*

The cathode polarization is the main source of electrical efficiency loss in low temperature polymer electrolyte membrane fuel cells (PEM FCs) and a lot of research efforts are directed to the development of more stable and cost- effective catalysts with increased activity toward oxygen reduction reaction (ORR). Recently PtCo nano-alloys have received much attention for use as cathode electrocatalysts due to their higher ORR activity and stability than pure Pt catalysts. Many attempts have been made to understand the relationship between the composition, structure, activity and stability of Pt-based alloy catalysts. Several hypotheses have been put forward in the literature to justify the reasons for enhancements of that activity (see e.g. the review presented in 1), but the matter is still under consideration.

In this contribution, using the X-ray absorption spectroscopy (XAS) performed at both Co K and Pt L_3 edges and X-ray diffraction (XRD) measurements combined with an electrochemical study (rotating disk electrode, RDE) we verify if and to what extent the activity enhancement of a PtCo nano-alloy is correlated with the geometric structure (i.e. with the mean particle size, the complexity of structural phases, the bond distances, the number of Pt nearest neighbors and the chemical disorder). We present a detailed structural analysis of carbon supported pure Pt and PtCo alloys composed of nanoparticles with various mean diameters and various structures at the atomic level. The relationship structure-activity leads us to the following conclusions:

- the mass ORR activity (A/mg_{Pt}) is correlated with the nano- particle size. A catalyst with a smaller mean particle size exhibits higher activity;
- a disordered multi-phase system offers more surface sites which are catalytic active sites and is a better catalyst material from the mass ORR activity point of view.

The presented results can be of fundamental and practical significance leading to the most effective catalyst for PEM FC. However, a good understanding of whole

correlations needs another detailed analysis performed on working catalysts, subjected to various operating conditions (e.g. cell potential, working time).

References

[1] Gasteiger H A, Kocha S S, Sompalli B and Wagner F T, Appl. Cat. B: Environmental 56, 9 (2005)

Ab initio Study on Ferroelectric Stability in Charge-ordered Multiferroic Iron Oxides

K. Yamauchi, S. Picozzi

CASTI Regional Laboratory, Consiglio Nazionale delle Ricerche – Istituto Nazionale di Fisica della Materia (CNR-INFM)

Exploring novel multiferroic materials [1] is an attractive challenge due to a great potential for applications as well as a high impact for fundamental physics. In this field, a new type of 'improper' ferroelectricity driven by charge order (CO), with significant cross coupling between charge, spin and lattice degrees of freedom, has been recently proposed in ferrite compounds, i.e. $LuFe_2O_4$ [2] and magnetite Fe_3O_4 [3]. In such systems, the stability of the ferroelectric polarization due to the non- centrosymmetric Fe^{2+}/Fe^{3+} charge-ordered pattern has been well analyzed by first principles simulations [4,5]: Fe_3O_4 shows a ferroelectric (FE) ground state in the base centered monoclinic Cc structure, whereas $LuFe_2O_4$ shows an antiferroelectric (AFE) ground state in the frustrated hexagonal layered structure. Via our newly developed GGA+U method, we can control the CO pattern, so as to find the ground state by comparing the total energy of different CO configurations. Here, we investigate the FE vs. AFE stability in such systems by changing the value of the effective on-site Coulomb interaction U as well as the lattice parameters, mimicking the pressure effects on the crystal structure. For Fe_3O_4, the experimentally observed centrosymmetric $P2/c$ structure was assigned to a paraelectric structure and a Cc structure to a ferroelectric one. By comparing these two structures, it was shown that the ferroelectric polarization arose only from two "shifts" of the charge between the selected octahedral Fe sites. Taking into account the related point-charge dipoles the calculated polarization showed good agreement with the experimental value. For $LuFe_2O_4$, both ferroelectric and antiferroelectric atomic structures were obtained, strongly depending on the CO pattern. The effect of the chemical substitution and structural layer intercalation is discussed (e.g. using $Lu_2Fe_3O_7$ instead of $LuFe_2O_4$) as an efficient approach to stabilize the FE ground state.

Acknowledgements
The research leading to these results has received funding from the European Research Council under the EU Seventh Framework Programme (FP7/2007-2013)/ERC Grant Agreement No. 203523.

References

[1] N. A. Spaldin and M. Fiebig, Science **309**, 391 (2005); S.-W. Cheong and M. Mostovoy, Nature Mater. **6** 13 (2007)
[2] N. Ikeda, et al., Nature **436** 1136 (2005)

[3] M. Alexe, M. Ziese, D. Hesse, P. Esquinazi, K. Yamauchi, T. Fukushima, S. Picozzi, and U. Gösele, Adv. Mater. (in press)
[4] M. Angst, et al., Phys. Rev. Lett. **101** 227601 (2008)
[5] K. Yamauchi, T. Fukushima, and S. Picozzi, Phys. Rev. B (in press)

Reading what Machines "Think": a Challenge for Nanotechnology

F. M. Zanzotto[1], D. Croce[1], S. Prezioso[2]

[1] *Dipartimento di Informatica, Sistemi e Produzione, Università di Roma "Tor Vergata" Viale del Politecnico 1, Rome, Italy*

[2] *Dipartimento di Fisica, Università dell'Aquila, gc-LNGS INFN Via Vetoio, 67100, L'Aquila, Italy*

Determining what machines "think" can be considered a well-set problem. Computational systems have became so complex to justify a parallelism with the human brain. Reading what machines "think" has henceforth become a potential field of interest, as fascinating as the field of neuro-imaging that studies the correlation of brain activations and thoughts. The parallelism between the brain and the computational systems may represent a reward for brain-imaging as brain interpretative models can be tested on a much simpler case. We performed a virtual observation of a computational machine: the machine activity was observed using a software program snapshotting the machine memory. Images of the memory activation states were produced with bit resolutions (Figure 1). Availing of these results, we are interested in what can be physically reading the machine's "thoughts" and what can be its technological implications. This is a peculiar challenging task for nanotechnology only, the elementary information unit 1/0 (the bit) corresponding on the chip to a physical elementary unit of nanometric dimensions. The capture of the activation states in the physical memory must be entrusted to devices that do not interfere with the internal electric fields of the chip and have imaging resolutions comparable with the minimum line separation typical of the modern processors. The present work has the purpose of stimulating the research activity in an unexplored field that can favor advances in neuro-sciences and, secondarily, in computer diagnostics.

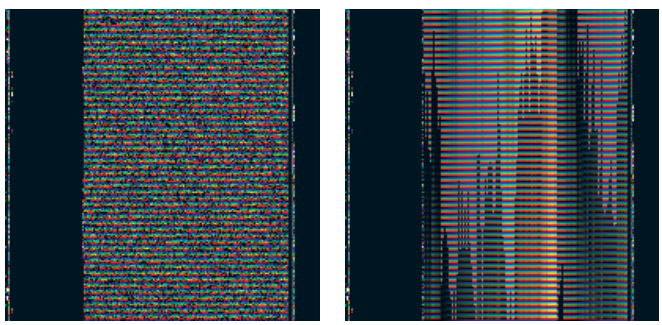

Figure 1: Visualization of two different activation states (left – initial; right – final)

Magnetic Resonance Study of ZnO–MnO System

N. Guskos[1,2], G. Żołnierkiewicz[2], J. Typek[2],
D. Sibera[3], U. Narkiewicz[3]

[1] *Solid State Section, Department of Physics, University of Athens Panepistimiopolis, 15 784, Greece*

[2] *Institute of Physics, West Pomeranian University of Technology Al. Piastów 48, 70-311 Szczecin, Poland*

[3] *Institute of Chemical and Environmental Engineering West Pomeranian University of Technology Al. Piastów 17, 70-310 Szczecin, Poland*

Fine particles composed of n(MnO)/$(1-n)$ZnO ($n = 0.05$ to 0.95) powders were prepared by the wet chemistry method. According to the XRD analysis the samples with $n = 0.95$, 0.90, 0.80, 0.70, 0.60 contained Mn_3O_4 and $ZnMn_2O_4$ phases, other samples contained $ZnMnO_3$ and ZnO phases. The mean crystalline size of $ZnMnO_3$ varied from 8 to 13 nm. The magnetic resonance investigations were carried out at room temperature. An almost symmetrical and very intense magnetic resonance line was recorded for all samples. The magnetic resonance spectra parameters showed a marked differences with increasing n (Table 1) which was mainly due to a variation in the magnetic susceptibility and a much slower evolution of spin relaxation associated with the interaction of crystal field and superexchange interactions. The relative intensity increased with the increasing n while the resonance field and linewidth were reaching a maximum for $n = 0.5$.

Sample composition (wt % of MnO)	H_r [Gs]	g_{eff}	Linewidth ΔH_{pp} [Gs]	Intensity ratio $I_{\%}/I_{5\%}$
0.05	3362(3)	2.000(2)	741(1)	1
0.20	3350(3)	2.007(2)	2480(2)	4034
0.30	3340(2)	2.011(2)	2600(2)	6038
0.40	3360(2)	2.001(2)	2700(2)	10669
0.50	3610(3)	1.863(2)	3500(3)	13225
0.60	3500(3)	1.921(2)	2200(2)	11200
0.70	3530(3)	1.905(2)	2350(2)	15201
0.80	3570(3)	1.883(2)	2350(2)	11700
0.90	3560(3)	1.889(2)	2330(2)	14300
0.95	3560(3)	1.889(2)	2410(2)	15483

Table 1: Values of magnetic resonance spectra parameters

Copper Doping Concentration Dependence of Structural and Electron Paramagnetic Resonance Properties of ZnO Nanorods

P. K. Sharma[1], A. C. Pandey[1], C. Rudowicz[2], N. Guskos[2,3], G. Żołnierkiewicz[2]

[1] *Nanophosphor Application Centre, University of Allahabad Allahabad 211002, India*

[2] *Institute of Physics, West Pomeranian University of Technology Al. Piastów 17, 70-310 Szczecin, Poland*

[3] *Solid State Section, Department of Physics, University of Athens 15 784 Zografou, Athens, Greece*

Copper doped ZnO nanoparticles were synthesized by a chemical technique based on a hydrothermal method. X-ray diffraction (XRD), small angle X-ray scattering (SAXS), and transmission electron microscopy (TEM) were employed to estimate the crystallite sizes. For different doping percentage of Cu^{2+} (1–10%), the crystallite sizes were found to be in the range of about 10–15 nanometers. The Rigaku, RINT2000/PC, Grain Size Analysis Program was used to calculate the size distribution of ZnO nanoparticles in the samples based on the Fankuchen method for the scattering intensity data obtained by the SAXS technique. The TEM images indicate formation of uniform nanorods, the aspect ratio of which varied with the Cu doping percentage. The electron paramagnetic resonance (EPR) studies at room temperature (300 K) indicate the presence of copper ions in these ZnO nanoparticles, indicating successful doping in the nanocrystals. These results are well supported by optical absorption and Fourier transform infrared (FTIR) studies.

Study of Magnetic Properties of $Co_3Fe_4V_6O_{24}$

N. Guskos[1,2], G. Żołnierkiewicz[2], J. Typek[2], R. Szymczak[3], C. Rudowicz[2], A. Błońska-Tabero[4], H. Ohta[5], S. Okubo[5]

[1] *Solid State Physics, Department of Physics, University of Athens Panepistimiopolis, 15 784 Zografos, Athens, Greece*

[2] *Institute of Physics, West Pomeranian University of Technology Al. Piastów 48, 70-311 Szczecin, Poland*

[3] *Institute of Physics, Polish Academy of Science Al. Lotników 36/42, Warszawa, Poland*

[4] *Department of Inorganic and Analytical Chemistry, West Pomeranian University of Technology Al. Piastów 17, 70 -310 Szczecin, Poland*

[5] *Molecular Photoscience Research Center, Kobe University 1-1 Rokkodai, Nada, Kobe 657-8501, Japan*

Multicomponent vanadate $Co_3Fe_4V_6O_{24}$ was synthesized using the solid state reaction method from an appropriate amount of Co_2O_3, V_2O_5, Fe_2O_3 metal oxides. The temperature dependence of the electron paramagnetic resonance (EPR) spectra and static magnetic susceptibility χ were investigated in the temperature range from liquid helium to RT. Both EPR spectra and magnetic susceptibility showed anomalous behavior (see figure). Preliminary considerations indicated that the magnetic competition process [1] may be responsible for this behavior. A comparison with the results of studies on related compounds $M_3Fe_4V_6O_{24}$ (M = Mg(II), Zn(II), and Cu(II)) revealed that the observed anomaly shifted to lower temperatures on replacing non-magnetic ions by magnetic Co(II) ions. The inverse susceptibility χ^{-1} showed antiferromagnetic interactions between Fe(III) and Co(II) spins with Curie-Weiss temperature $\Theta = -111(3)$ K, lower than for the system with Mn(II) at the cation position ($\Theta = -165(5)$ K) and comparable with Θ for systems containing diamagnetic

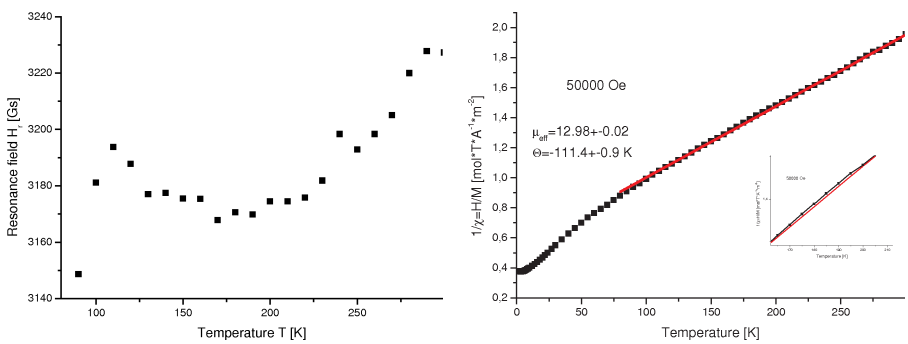

ions [2,3]. The introduction of cobalt cations intensified the magnetic frustration what reflected itself in the temperature dependence of the magnetic susceptibility at low temperatures. Preliminary HMF-EPR (high-magnetic field/high frequency EPR) results will be also briefly presented.

References

[1] G. Żołnierkiewicz, N. Guskos, J. Typek, E. A. Anagnostakis, A. Błońska-Tabero, M. Bosacka, *J. Alloys Comp.* **471** 28 (2009)

[2] N. Guskos, H. Ohta, G. Żołnierkiewicz, S. Okubo, W. Zhang, J. Typek, C. Rudowicz, R. Szymczak, M. Bosacka, T. Nakamura, *J. Non-Cryst. Solids* (2009); doi:10.1016/j.jnoncrysol.2009.05.031

[3] N. Guskos, V. Likodimos, S. Glenis, G. Żołnierkiewicz, J. Typek, R. Szymczak, A. Błońska-Tabero, *J. Appl. Phys.* **101** 103922 (2007)

INDEX OF AUTHORS